Norges miljø- og biovitenskapelige universitet

Master's Thesis 2020 60 ECTS
Faculty of Veterinary Medicine

Cloning, characterization and expression of three B22R genes from Salmon Gill Poxvirus

Kloning, karakterisering og uttrykk av tre B22R gener fra laksepoxviruset

Kathrine Andersen
Biotechnology

Acknowledgement

This master's thesis was funded by the Norwegian research council (NFR 267491) and was done at the Norwegian Veterinary Institute (NVI) in Oslo in the period from August 2019 to June 2020 and is the final part of the two years master's degree in biotechnology at NMBU.

This year has been a journey where I have learned and experienced a lot as well as gotten to know many new people. This thesis has been very exciting, and I have learned many new laboratory techniques that will be useful in my professional life.

Firstly, I would like to thank my main supervisor Maria Krudtaa Dahle at NVI who has been there for me during the whole process and helped me with both theory and practical laboratory work. I would like to thank my internal NMBU supervisor Turhan Markussen for helping me with theory and the bioinformatical part of the thesis, as well as my co-supervisor Mona Cecilie Gjessing at NVI for the theoretical help. Thank you all three for being so supportive, positive and motivational through the whole period and for your availability in helping or answering questions. I have been truly inspired and fascinated by all your knowledge and dedication to your work, which has been a huge motivation for me during this process.

I would also like to thank Marit Måsøy Amundsen for helping me with laboratory work, as well as sharing both the frustration and excitement of writing a master's thesis. I would like to thank Anita Solhaug for teaching me how to work with cell cultures and other useful laboratory methods. I would like to thank Hilde Sindre for helping me with transfection optimizations and Saima Nasrin Mohammad for helping me with the cloning procedures. I appreciate that you and everyone else I have met at the NVI have been so accommodating and helpful.

2020 will go down in the history books as the year when the COVID-19 pandemic shocked the whole world. I was lucky to have finished most of my work before the lockdown, but some things were not possible to complete, and these will be referred to in the text. I appreciate that my supervisors and me continued to have our meetings virtually, and I am looking forward to seeing you in real life again very soon.

Moss, May 2020.

Kathrine Andersen

Abstract

Salmon Gill Poxvirus Disease (SGPVD) is a severe viral disease that can cause acute mortality in farmed Atlantic salmon. The disease is caused by SGPV that is a large DNA virus. The virus infects gill epithelial cells and causes cell death and destruction of the gill respiratory surface in the acute phase. Due to the complex gill disease often seen associated with SGPV, it has been proposed that SGPV modulates the mucosal immune system, which then allows invasion of other pathogens.

The SGPV genome was characterized in 2015 and shown to encode over 200 genes. Among these are three paralogues of a large gene from the deadly human variola virus, called B22R. The B22R family of proteins are reported to inhibit T-lymphocyte function in the host and thereby promote viral virulence. The B22R-like genes in SGPV show a higher degree of sequence variation between isolates compared to the full genome. It is therefore hypothesized that these genes could play a role in the difference between severe and mild disease.

The three B22R-like SGPV genes (B22R1, B22R2 and B22R3) from two SGPV isolates; one originating from a severe disease outbreak in a Norwegian fish farm in 2019, and another isolated from wild Norwegian salmon without clinical disease, were cloned into expression vectors. A FLAG-tag encoding sequence was included in all constructs so that each B22R paralogue was expressed as a fusion protein with the tag fused to its C-terminal end. For B22R3, an N-terminal tagged variant was also constructed. Atlantic salmon gill epithelial cells (ASG-10) and *epithelioma papulosum cyprini* (EPC) cells (from carp) were transfected with the expression vectors. The presence and subcellular localization of the different proteins was explored using a fluorescent anti-FLAG antibody together with selected markers for intracellular compartments and structures. The B22R protein sequences were also investigated using several bioinformatics (*in silico*) tools to predict functional and structural properties. Expression of the B22R-like genes were also monitored by RT-qPCR in gill samples from an SGPV-infection experiment. This is the first step towards constructing targeted functional assays for SGPV B22R variants, and further explore their functional roles with potential links to virulence.

Sammendrag

Salmon Gill Poxvirus Disease (SGPVD), eller laksepox er en alvorlig virussykdom som kan føre til akutt dødelighet i lakseoppdrettsnæringen. Sykdommen forårsakes av laksepoxvirus eller SGPV er et stort DNA virus. Viruset infiserer de respiratoriske overflatecellene på gjellene og fører til at de dør og faller av under den akutte infeksjonsfasen. Laksepoxvirus blir noen ganger påvist i sammenheng med kompleks gjellesykdom og det har det blitt foreslått at SGPV modulerer slimhinneimmuniteten slik at barrierefunksjonen svekkes og lettere angripes av andre patogener.

Genomet til SGPV ble karakterisert i 2015, og viser seg å inneholde over 200 gener. Blant disse er det tre paraloger av et stort gen fra det dødelige, humanpatogene variolaviruset, kalt B22R. Det har blitt rapportert at proteinene i B22R-familien hemmer funksjoner hos T-lymfocytter i verten, og dermed fremmer virulens. De B22R-liknende genene i SGPV viser seg å ha en høyere sekvensvariasjon mellom isolater sammenliknet med resten av genomet. Hypotesen er at disse genene kan spille en rolle i forskjellen mellom alvorlig og mild sykdom.

De tre B22R-liknende genene (B22R1, B22R2 og B22R3) fra to SGPV isolater; et fra et alvorlig sykdomsutbrudd i et norsk fiskeoppdrettsanlegg i 2019, og et annet fra norsk villfisk uten klinisk sykdom, ble klonet inn i ekspresjonsvektorer. En FLAG-tag kodende sekvens ble inkludert i alle konstruktene, slik at hver B22R paralog var uttrykt som et fusjonsprotein med merking i proteinets C-terminale ende. En N-terminal merket variant ble også konstruert for B22R3. Gjelleepitelceller fra atlantisk laks (ASG-10) og epithelioma papulosum cyprini (EPC) celler (karpeceller) ble transfektert med ekspresjonsvektorene. Tilstedeværelse og subcellulær lokalisasjon av de tre ulike proteinene ble undersøkt ved å bruke et fluorescerende antistoff mot FLAG-taggen sammen med utvalgte markører for intracellulære strukturer. B22R proteinsekvensene ble også undersøkt ved å bruke ulike bioinformatiske (in silico) verktøy for å predikere funksjonelle og strukturelle egenskaper. Uttrykk av de tre B22R-liknende genene ble også undersøkt med RT-qPCR på gjelleprøver fra et oppdrettsanlegg og et smitteforsøk med SGPV-smitte. Dette er første steg mot å konstruere en målrettet funksjonell analyse av B22R varianter for SGPV, og videre utforske proteinenes funksjonelle roller og potensielle kobling til virulens.

Contents

1.0 Introduction

1.1 Atlantic salmon biology and aquaculture

Aquaculture is an important industry in Norway, and the production of Atlantic salmon (*Salmo salar*, hereafter salmon) accounts for most of the production. According to the Directorate of fisheries, about 350 million smolts were transferred to the sea and 269,5 million salmon, comprising more than 1,2 million tons, were slaughtered in 2019 (Fiskeridirektoratet, 2019, Fauske, 2019). Although aquaculture is an important resource for the Norwegian economy, the industry faces different challenges, including fish diseases and mortalities.

The salmon is an anadromous fish; they hatch in freshwater, develop to parr and 2-5 years after hatching a process known as smoltification starts. Smoltification is a physiological transformation allowing the fish to initiate their downstream migration and the successful transition from life in freshwater to seawater (Vøllestad, 2019). The smolt migrates to the sea from April to July, and about 1-4 years later when it has grown and reached sexual maturity, it migrates back to the same river where it was hatched (Wennevik and Hansen, 2019). Here, during the autumn, spawning takes place. The eggs hatch in late winter and the fry hide between small rocks until the yolk sac has been consumed. In the spring, the fry leave the bottom of the river and are then classified as parr (Vøllestad, 2019). Aquaculture mimics this life cycle. Roes are fertilized in incubator trays and when the yolk sac is consumed, they are fed with pellets and moved to tanks to grow. The salmon are transferred to sea as smolts of about 50-200 grams and kept in sea cages until they reach market size.

1.2 Diseases in salmon aquaculture

There are several health and welfare challenges in the Norwegian salmon farming. Sea lice infestations in addition to viral infections are responsible for large losses in the salmon farming industry. Most bacterial infections are well controlled by vaccinations in Norwegian aquaculture, and the use of antibiotics is low. Viral diseases, on the other hand, have proven more difficult to control. The dominating viral diseases in the Norwegian aquaculture are pancreas disease (PD), infectious salmon anemia (ISA), both of which are notifiable diseases and cardiomyopathy syndrome (CMS) and heart and skeletal muscle inflammation (HSMI) (NVI, 2019).

Gill disease is a major health and welfare issue in Norwegian salmon farming, and responsible for high losses. According to the Norwegian Veterinary Institute (NVI), the number of gill

disease cases have increased in recent years (NVI, 2019), but as gill diseases are not notifiable their prevalence is difficult to assess. The gills have a complex anatomy and a multifunctional physiology, as briefly outlined in chapter 1.3.1 below. Some of the main pathogens infecting the gills are listed in Table 1, and co-infections involving two or more of these agents are common, especially after sea transfer. Both infectious and non-infectious agents can cause problems in the gills and complex histopathological manifestations are common. The relative contribution of each pathogen in the clinical manifestation is therefore difficult to assess (Gjessing et al., 2019). Complex gill disease (CGD) is a term describing gill disease manifestations that are suspected to have a multifactorial causality (Herrero et al., 2018). However, two exceptions are Amoebic gill disease (AGD) caused by *Paramoeba perurans* and salmon gill poxvirus disease (SGPVD) caused by salmon gill poxvirus (SGPV). In these gill diseases, the lesions in the gills can be directly linked to the respective pathogens.

Table 1: List of the most important agents causing CGD.

Name	Type of agent
Candidatus Branchiomonas cysticola	Intracellular, cyst forming bacteria
Desmozoon lepeophtherii	Fungus
Paramoeba perurans	Amoeba
Atlantic salmon paramyxovirus	RNA virus
Salmon Gill Pox Virus	DNA Virus

1.3 Gills and epithelial cells

1.3.1 Gill structure and function

The gills are multifunctional organs with respiration as the main function. Salmonids have four pairs of gills, called holobranchs located on each sides of the cavity behind the mouth (pharynx). The gills are composed of a bony structure called the gill arch, and lining the whole outer side are two rows of regularly spaced filaments as shown in Figure 1. Gill rakers are in the front the gill arch (anterior) and contain taste buds and may function as a filter mechanism. Filaments are the functional units of the gill and are comprised of a type of connective tissue called cartilage in the core and with thin, closely stacked plate-like lamellae on both sides. With this structure, the gills have a large total surface area. The fish has muscles bound to the various parts of the gill, enabling control and regulation of the amount of water passing between the lamellae. It also has nerves for controlling the muscle movements and the blood flow through the gill (Olson, 2000). Because of the thin epithelial layer, the distance between water and blood

is short. The exposed surface of the gills enable numerous particulate and soluble substances, including several pathogens to penetrate this barrier (Koppang et al., 2015). The salmon's innate immune system plays an important part in the defense of these pathogens, and this will be explained in chapter 1.5.

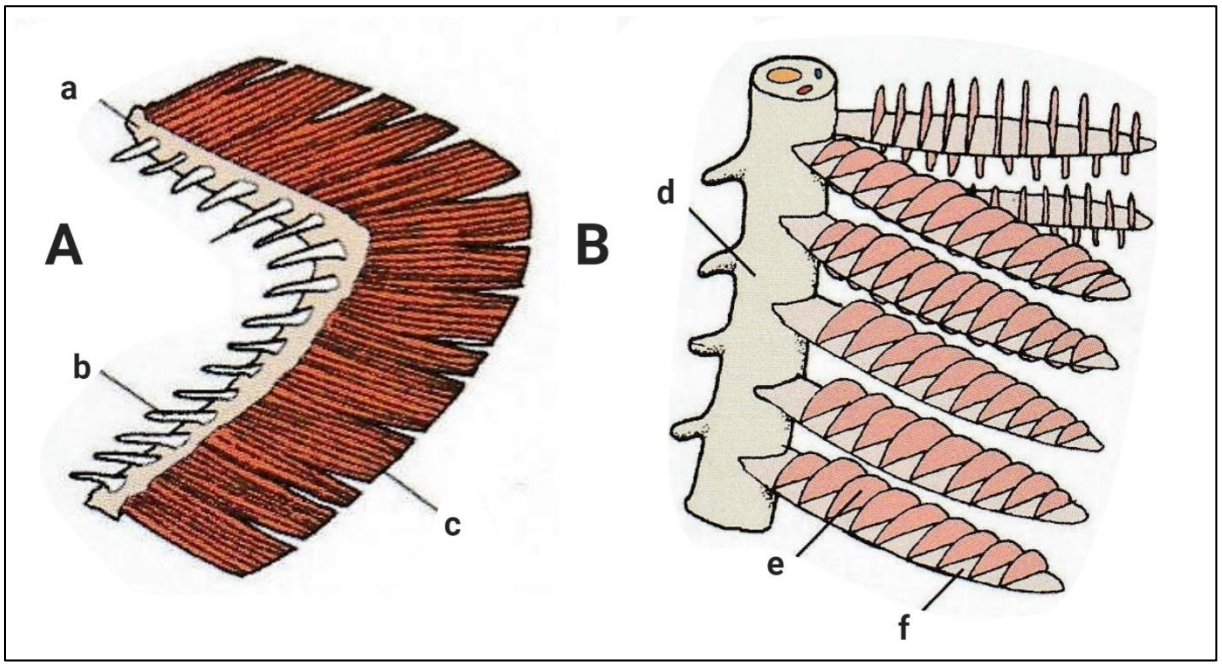

Figure 1: Gross gill anatomy. A) Gill holobranch and B) magnified section of a gill holobranch. a: gill arch, b; gill rakers, c; rows of gill filaments, d; gill arch, e; lamellae and f; filament. From Kryvi and Poppe (2016).

1.3.2 Epithelial cells

In complex organisms, there are different cell types that organize into four groups of tissues. The connective tissue provide structural strength, binds and protects the different parts of the body. The muscle cells are specialized for contraction and nerve cells generate and leads electrical pulses to transmit information between cells. Epithelial cells cover outer surfaces and the interior of hollow organs, such as lungs and gills. Epithelial tissue can be divided into surface epithelium and glandular epithelium. Surface epithelium covers the outer and inner surfaces of the body and physically protects the organism's organs and other tissues, regulate the transport of agents between the outer and inner environments and to record sensory stimuli. The cells are firmly attached to the underlying tissue and are also coupled together by tight junctions and desmosomes. The inner surfaces of the body, like the gills, are covered in one layer surface epithelium. (Sand et al., 2012) Gill epithelial cells are of special interest here, as they are the target cells for SGPV.

1.3.3 Epithelial cell lines from fish

Several epithelial cell lines have been developed and are useful in the study of responses to infectious agents and toxins. They are widely used to cultivate viruses. Cell cultures (monocultures) are convenient to work with in the laboratory where several features can be systematically investigated. Cell cultures are also an advantage when it comes to animal welfare as it can replace or reduce the number of experimental animals used in accordance with the three Rs perspective (reduce, refine, replace). In this thesis, two fish cell lines have been used. One of the cell lines are the *Epithelioma papulosum cyprini* (EPC) cells. EPC cells were established during experiments of carp pox etiology in 1969 and originate from carp epidermal herpes virus-induced hyperplasic lesions. The cell line is still widely used as it is a useful tool in diagnostics and in research on viral diseases in carp. The EPC cell line has a wide temperature range, a good splitting ratio and is susceptible to several fish viruses (Fijan et al., 1983). EPC cells have become one of the most widely used cell lines in diagnostics and in research on fish viruses. The cell line has for many years been passed on one laboratory to the next and has not been commercially available from a cell culture repository (Winton et al., 2010). Winton et al. (2010) describes that the current EPC cell lines in use appear to be contaminated by cells derived from *Pimephales promelas* (fathead minnow). Still, this cell line is favored because of its high susceptibility and relative ease of handling (Winton et al., 2010). The other cell line used here is the Atlantic salmon gill cell line. The two cell lines named ASG-10 and -13 were recently established and described by Gjessing et al. (2018). The ASG-10 cell line has morphological structures resembling epithelial cells, and the ASG-13 cells are suggested to be of a fibroblastic nature. The ASG-10 cell line could be a powerful tool in the research of host responses in the gills (Gjessing et al., 2018), and is now being developed as an Atlantic salmon gill model in the NRC-funded project GILLMODEL at NVI. In this thesis, the focus is on SGPV, a virus that infects the gill epithelial cells of salmon. Due to the origin and epithelial characteristics of ASG-10, this cell line is therefore very attractive for the experiments done in this thesis.

1.4 Cellular protein production

1.4.1 Transcription, translation and protein transport

Eukaryotic cells store most of their genome (the rest is in the mitochondria) inside an enveloped nucleus. A eukaryotic cell has several linear deoxyribonucleic acid (DNA) molecules, and each molecule is wrapped around histones to form a nucleosome. Chromatin is loosely packed DNA, and a chromosome is formed when the nucleosomes are densely packed. DNA stores genetic

information and directs the production of the functional biomolecules ribonucleic acid (RNA)s and proteins. These molecules define cellular identity and perform cellular functions. The process when an RNA molecule is synthesized from a DNA template is called transcription. This process has several similarities to replication, the process of copying DNA prior to cell division, since both mechanisms use DNA as a template and use multienzyme polymerase complexes to read DNA. However, in replication only one copy of the DNA is made, and the entire genome is synthesized. In transcription, only a part of the genome (a gene) is copied into RNA and multiple copies, called transcripts are formed. Transcriptional activation of a gene happens when the DNA molecule is unpacked in that specific region. The nucleosome properties are altered to make the promoter sequence accessible. Transcription can be split into three main phases: initiation, elongation and termination. At the initiation phase, the RNA-polymerase (RNAP) binds to the promoter upstream of the gene. DNA goes from a closed to an open structure because of structural changes made by the RNAP. A complex is formed between DNA, RNAP and RNA while nucleotides are added one by one. In the elongation phase, the RNAP escapes from the promoter and moves downstream on the DNA. The termination process occurs when sequence information tells the RNAP to stop (Watson et al., 2014).

In eukaryotic cells, it is important to stabilize the newly synthesized RNA and before it can exit the nucleus, it must be processed to mature messenger RNA (mRNA). Soon after the newly synthesized RNA emerges from the RNA-exit channel of the RNAP, a cap is added to the 5'-end of the RNA strand to protect it and increase its stability. The cap is also involved in nuclear export and binding to a ribosome in the cytoplasm. The product of eukaryotic transcription is called pre-mRNA and usually contains both exons (coding sequences) and introns (intervening non-coding sequences). The pre-mRNA undergoes RNA splicing inside the nucleus to remove introns and splice the exons together. The introns are degraded inside the nucleus. Polyadenylation is the final processing step of the mature RNA. About 200 adenyl bases are added to the 3'-end of the RNA. This protects the 3'-end from degradation and the poly-A tail is involved in nuclear export and binding to a ribosome in the cytoplasm. The RNA is now mature and can be transported through the nuclear membrane to the cytoplasm (Watson et al., 2014).

In the cytoplasm, the mRNA will associate with a ribosome and start translation of the nucleotide triplets (codons) into amino acids. This process is also called protein synthesis. Similar to transcription, translation can also be divided into three phases: initiation,

elongation/translocation and termination. In eukaryotic cells, the initiation starts when the small ribosomal unit recognizes and binds to the 5'-cap on the mRNA strand and then scans the strand until the AUG start codon is found. A tRNA carrying a methionine binds to the start codon, and then the large ribosomal unit is recruited. During the elongation/translocation step, the ribosome reads the codons on the mRNA strand one by one while the appropriate amino acid is added onto the growing peptide strand, thereby elongating it. This happens while the ribosome moves along the mRNA from the 5'-end to the 3'-end, the translocation. In the termination step, the ribosome encounters a stop codon and the translation stops. The polypeptide is released while the two ribosomal subunits and the mRNA strand separate. The ribosomal subunits are then recycled for a second round of translation (Watson et al., 2014). The flow of genetic information is illustrated in figure 2.

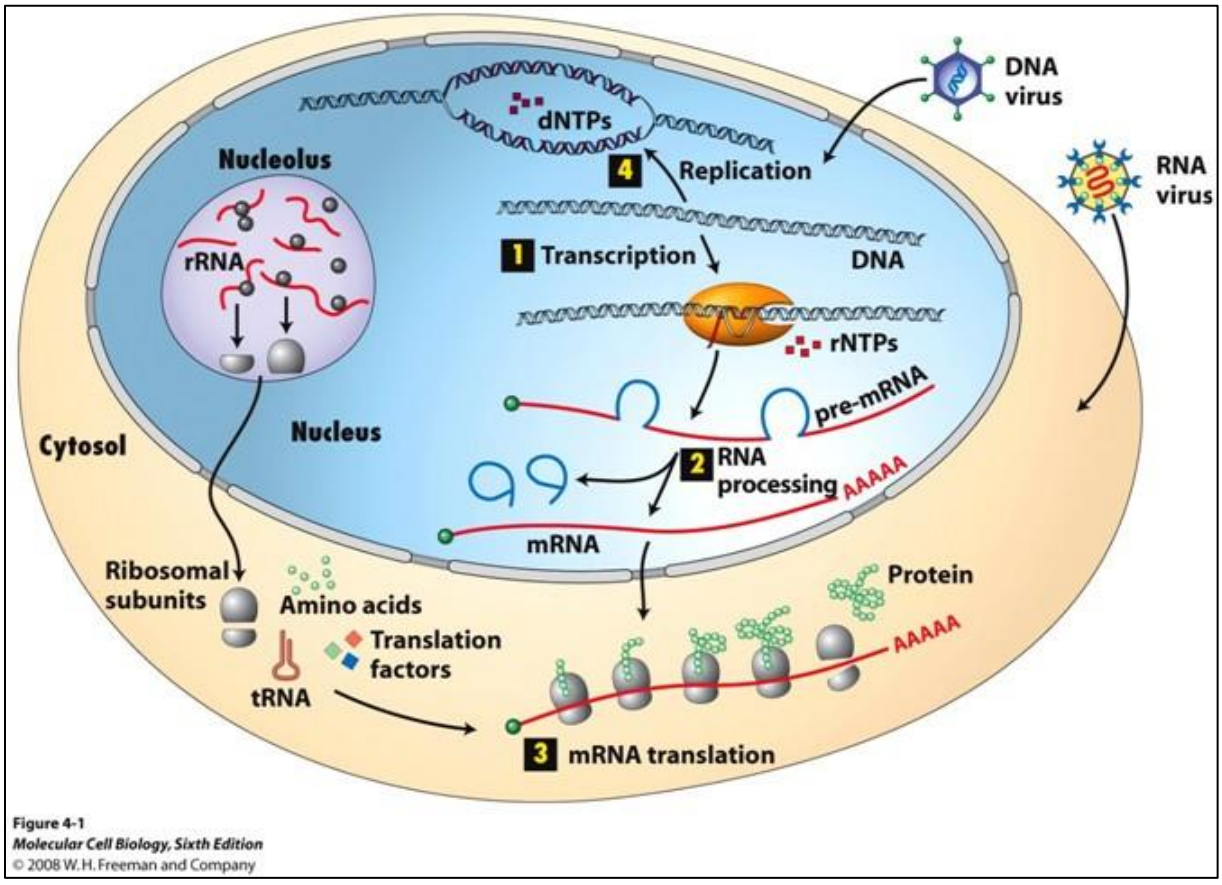

Figure 2: Illustration of the flow of genetic information inside a eukaryotic cell (Lodish et al., 2000). **1:** DNA is transcribed into RNA. **2:** RNA is processed by splicing, a cap is added to the 5'- end and polyA to the 3'- end. **3:** Ribosomes, tRNA, amino acids and translation factors together translate mRNA into an amino acid sequence ending up as a protein. **4:** DNA replication occurs upon cell division, and the whole genome is copied. Virus exploit these cellular mechanisms in their own replication. Most RNA viruses replicate in the cytoplasm and most DNA viruses enter the cell nucleus for transcription of the viral genome. The poxviruses are an exception as they encode their own polymerases and replicate entirely in the cytoplasm.

There are several paths the newly synthesized protein can be destined to follow. Proteins are primarily synthesized in the cytosol (except from a few in the mitochondria), but proteins with functions outside of the cell or transmembrane proteins carry a signal peptide (SP) directing their synthesis into the endoplasmic reticulum (ER). From here, they can be transported to the cellular membrane, to other organelles or secreted out of the cell. Proteins that are sorted out of the cytosol carry specific sorting signals for a particular destination in the cell. Signal sequences function as "address tags" after translation. These tags can be at different locations in the protein: N or C-terminus, internal, or structural. There are three different pathways of protein traffic: active transport through nuclear pore complexes (NPC) in the nuclear envelope is called gated transport. Specific protein transport through a membrane by transmembrane translocators is called transmembrane transport. Vesicular transport is when proteins are carried from one compartment to another by membrane enclosed transport vesicles (Alberts et al., 2015).

Proteins destined for the secretory pathway will first pass through the ER. The proteins are imported into the ER by co-translational transport, meaning that the ribosome is attached to the ER membrane when protein synthesis and translocation takes place. Some post-translational import of proteins into the ER can also occur, but this is rare. In the ER lumen, many of the proteins will be post-translationally modified, and a common modification here is N-glycosylation (Alberts et al., 2015). Here, a high mannose unit is attached to the side chain of the amino acid asparagine (Asn) within a Asn-X-Ser/Thr sequence, where X can be any amino acid except probably proline (Dell et al., 2010). N-glycosylation may be essential for proper protein folding and indicate whether the protein is ready to leave the ER. Not all proteins that go through the ER will be secreted. Proteins that are destined for lysosomes, endosomes, the Golgi apparatus and the plasma membrane are all initially sorted to the ER. There are two types of proteins imported to the ER. The first type are transmembrane proteins that will be embedded in the membrane. These will either stay in the ER membrane or undergo further transportation mediated through the budding of vesicles. Their destinations can be to the Golgi apparatus, lysosomes, endosomes or to the plasma membrane. The second type are soluble proteins that are fully translocated into the ER lumen. These can be ferried inside vesicles to lysosomes, endosomes or be secreted from the cell (Alberts et al., 2015).

1.4.2 Transfection and recombinant protein production

Foreign genetic material (e.g virus genes) can be introduced to a host cell for protein expression and to study their localizations and functions. Introduction of foreign nucleic acids into a cell is called transfection (usually referring to eukaryotic cells). There are two main ways to

introduce nucleic acids into a cell: transiently, where there is no integration of the nucleic acids into the host genome, or stably where the nucleic acids are integrated into the genome. In this project, the method of transient transfection has been used. A plasmid or mRNA will be transfected and then be degraded by the host cell after a period of time (Kim and Eberwine, 2010). Transfection can be performed using three types of methods: chemical, biological and physical (Kim and Eberwine, 2010, Kaestner et al., 2015). Listed below are examples of commonly used technologies of the three different transfection categories:

- Chemical: cationic polymer, cationic lipid and calcium phosphate
- Biological: virus-mediated/transduction.
- Physical: microinjection, electroporation, laser-irradiation, sonoporation, magnetic nanoparticle and biolistic particle delivery, µTool based thermoporation. (Kim and Eberwine, 2010, Kaestner et al., 2015).

The focus in this project will be on cationic lipids, cationic polymers and electroporation. The difference between plasmid and mRNA transfection will also be tested.

Lipofection is one of the most commonly used transfection methods. It is based on cationic lipids consisting of three parts: a hydrophobic body of either one or two hydrocarbon chains such as fatty acid chains of various lengths or cholesterol; a hydrophilic head group that is net positively charged at physiological conditions or at the lower pH that exists in endosomal environments; and a group that links the two functional groups together. These cationic lipids form vesicles and the positively charged head group binds to the negatively charged phosphate of the backbone of nucleic acids and forms unilamellar complexes as shown in figure 3. The positively charged head group in the exterior of the vesicle binds to the target cells negatively charged surface, and this allows for fusion of the complex with the membrane. (Kaestner et al., 2015). The exact mechanism of how the complex enters the cell is unknown but is thought to be entering by endocytosis. (Kim and Eberwine, 2010, ThermoFisher). Plasmids also have to enter the nucleus and must pass two membranes. Efficiency of transfection by this method can depend on many factors such as cell membrane conditions, pH of the solution and nucleic acid/reagent ratio (Kim and Eberwine, 2010). Different cell lines may react and behave differently so each new cell line to be used should be optimized for achieving the best transfection efficiency.

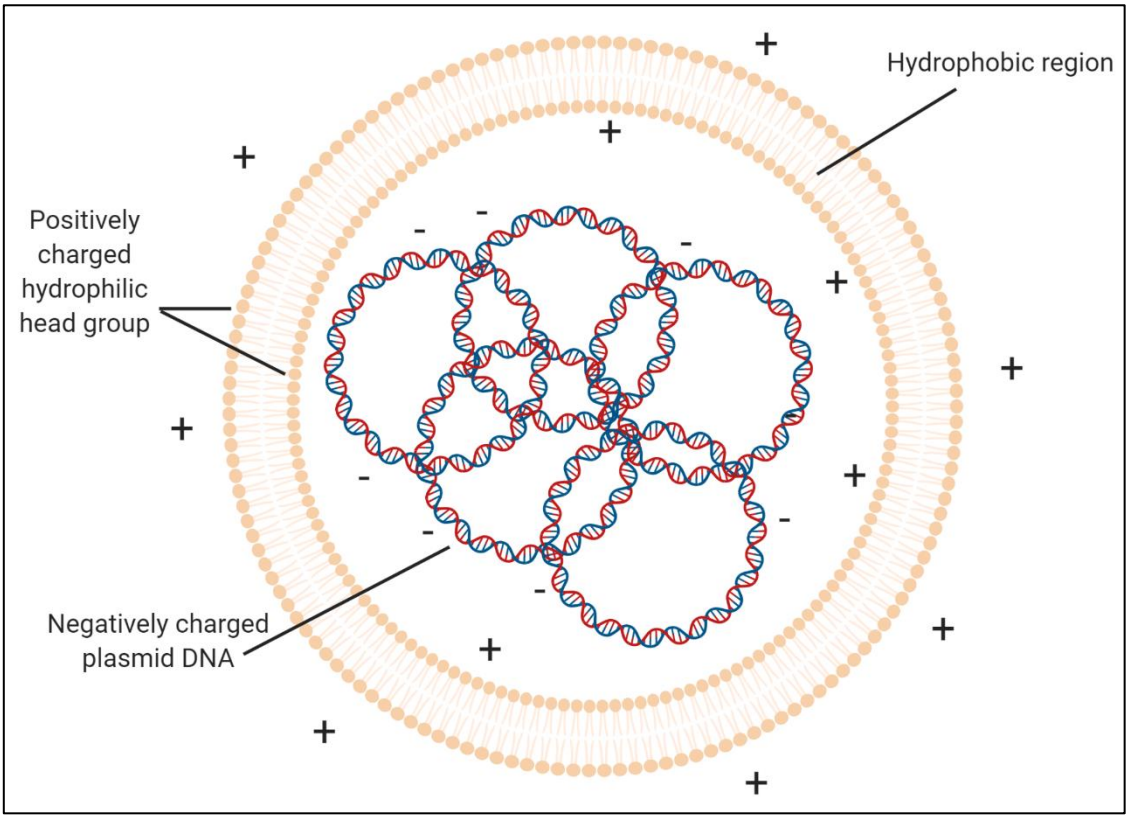

Figure 3: Illustration of a lipoplex that is formed during transfection with cationic lipids. Cationic lipids form vesicles and the positively charged head group binds to the negatively charged phosphate of the backbone of nucleic acids and forms unilamellar complexes. Created with Biorender.com

The second transfection method tested in this project is electroporation and is the physical method that is most widely used. One advantage of using physical transfection is that it is less dependent on the physiochemical and biological properties of the cell, and cells that are difficult to transfect might produce a much higher transfection efficiency through the physical methods (Kaestner et al., 2015). The mechanism behind electroporation is still under debate, but the short electrical pulse is predicted to make the transmembrane potential reach values over a certain threshold that triggers the increase of cell membrane permeability. There is an agreement that the formation of pores in the membrane makes it more permeable. The cell type and size, solution matrix, and electric field parameters are factors that the pore formation is dependent on and that must be optimized for each cell line (Ruzgys et al., 2019).

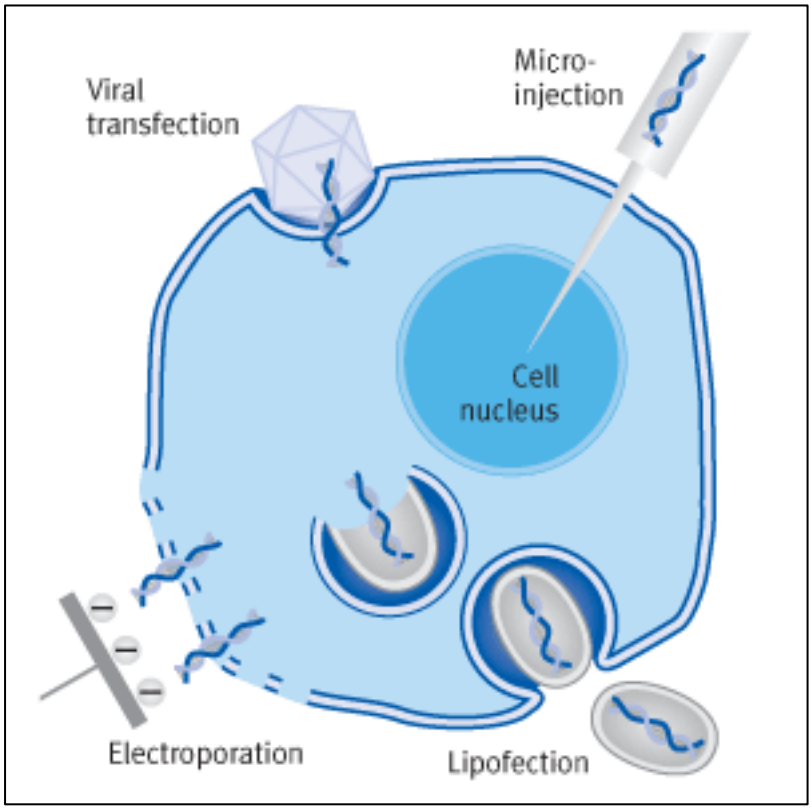

Figure 4: Illustration of four widely used transfection methods (https://www.biontex.com/en/transfection/) (Biontex). Genetic material can be incorporated into a virus, and the protein of interest is transduced into the infected cell. Microinjection injects the genetic material directly into the target cell. Electroporation changes electrical potentials to form pores of the cell membrane for the genetic material to enter. Lipofection is based on cationic lipids that encapsulate the DNA followed by uptake into the cell (Kaestner et al., 2015).

The third transfection method in this project was mRNA transfection with a chemical based transfection method using engineered cationic polymers. This method has several similar characteristics with lipid-based transfection systems as they both encapsule nucleic acids and fuse with the membrane of the target cell. The difference between DNA and mRNA transfection is that the mRNA is not dependent on entering the cell's nucleus, and the rate of cell divisions will be insignificant. mRNA transfection is therefore thought to gain higher transfection efficiency of hard to transfect and slow growing cells (PolyplusTransfection, 2019).

1.5 Viral infection and host protection

The immune system protects the fish against diseases by identifying and eliminating the pathogen. The immune system is also involved in processes to maintain stable conditions during development and growth as well as following inflammatory reaction on tissue damage (Magnadottir, 2010) The immune system can be categorized into two systems: the innate immune system is the primary defense mechanism from infection, with a rapid response, and the adaptive immune system develops to defend against specific invaders after contact (Sompayrac, 2012).

1.5.1 Innate antiviral immune responses

The innate immune system is the first line of defense of the fish and can be commonly divided into three sections: the epithelial/mucosal barrier, the humoral parameters and the cellular components. Since the fish is constantly exposed for potentially harmful agents, the epithelial and mucosal barriers of the skin, gills and alimentary tract are very important physical disease barriers. The humoral parameters can either be secreted from cells or be expressed receptors, and also includes the complement system. The humoral parameters also include interferons that acts against viral infections and cytokines that leads to recruitment and activation of immune cells. The cellular components consist of phagocytes and non-specific cytotoxic cells. Phagocyting cells recognize pathogen associated molecular patterns (PAMPs) by Pattern Recognition Receptors (PRR). Important PPRs are the Toll-like receptors that provides a exceptional specificity in recognizing foreign antigens (Magnadottir, 2010).

Interferons (IFNs) plays a central part in viral infections and are being produced by virus infected cells (Klepp, 2020). Effects of interferons are very important as they inhibit virus replication in the early stage of infection (Cann, 2001). Interferons do not have antiviral effects by themselves but bind to other cells via interferon receptors and induces several changes inside these target cells, including antiviral activity. Interferons can be grouped into three types: α-, β- and γ-interferons. α-and β- interferons are called type I interferons, while γ-interferons are called type II interferons. Class I interferons are most important during a viral infection since their activity is primarily antiviral (Degrè et al., 2010). Production of interferons are regulated following detection of viruses by PPRs. In a viral infection, the cellular protein synthesis is usually inhibited by the cell to avoid production of virus proteins. As an example, double stranded (ds) RNA and DNA with unmethylated CpG-sequences do not naturally appear in eukaryotic cells and are therefore detected as foreign by endosomal and cytoplasmic receptors that function as inducers of interferon (Brencicova and Diebold, 2013).

DNA viruses are mainly poor interferon inducers, while RNA viruses are in general most effective. Poxviruses are an exception from this as they are very potent interferon inducers (Cann, 2001). Type-I interferons bind to a common receptor that exists on most cells in the organism (Degrè et al., 2010). When an interferon binds to a receptor, it triggers a cascade reaction inside the cell, that eventually leads to activation of transcription of several genes (Cann, 2001)

1.5.2 Adaptive antiviral immune responses

The adaptive immune system develops relatively slowly compared to the innate immune system, and adapts to defend against specific pathogens (Sompayrac, 2012).The key humoral parameter of the adaptive immune system are antibodies that are proteins with high specificity against foreign substances. B-lymphocytes, a cellular compartment of the adaptive immune system produce antibodies that will either be anchored in the cell membrane or secreted (Magnadottir, 2010). Another cellular compartment are T-lymphocytes that are responsible for cellular immunity (Sompayrac, 2012). Especially during a viral infection, presenting the antigen (a part of the pathogen) for T-cells by Major Histocompatibility Complexes (MHCs) is important for activation of the adaptive immune system (Sompayrac, 2012). MHC class I is present on all nucleated cells in the body, while MHC class II is solely expressed on antigen presenting cells (APC) that can either be macrophages or B-lymphocytes. (Cann, 2001). T- cells have membrane-bound receptors that can recognize antigens presented by the MHC and when they detect a foreign antigen, they are activated to multiply into effector T-cells. Antigens presented by MHC I activate T-cells to multiply into Cytotoxic lymphocytes (CTLs). These can detect presentation of the specific foreign antigen in MHC I on other target cells infected by the same virus. When foreign material is recognized, the killer T-cell triggers the target cell to undergo apoptosis (Sompayrac, 2012). Antigens presented by MHC II activate T-cells to multiply into helper T-cells. Helper T-cells secrete cytokines that activates macrophages and B-lymphocytes, that will lead to a humoral adaptive response (Abbas and Lichtman, 2009). CTLs also need stimulation by several cytokines secreted by T-helper cells (Cann, 2001).

1.5.3 Viral hijacking of cellular functions

Viruses have evolved several mechanisms to escape the immunological defenses by the host. The cell has several host antiviral mechanisms that can trigger apoptosis, translational inhibition and block viral release during a viral infection. However, many viruses have developed ways to defeat these mechanisms to keep the host cell alive and the virus production ongoing. Some examples of viral mechanisms are inhibition of the antiviral response molecules of the cell, blocking of cell signaling, or inhibition of negative regulators of apoptosis. (Cann, 2001). The virus can also inhibit the MHC-I-restricted antigen presentation. In this way, the CTL will not be able to “see” that there is an invader inside the cell. Some viruses can also inhibit MHC class II restricted-antigen presentation on APCs, and CTLs will not be able to detect the infection. Some viruses can also directly inhibit the expression of certain chemokines, a group of cytokines involved in recruiting immune cells. Poxviruses can encode homologues for cytokine

receptors that will compete with the cells own receptors for binding of the cytokine. Binding to the viral homologue results in no transmembrane signals. Viruses can also interfere the other way around by producing inactive cytokine-like molecules to block the host receptors. The virus may also produce molecules with high affinity to cytokines and neutralize them directly (Cann, 2001). In conclusion, viruses inhibit antiviral protection through numerous of mechanisms.

1.6 Pox viruses

Poxviruses are among the largest and most complex DNA viruses. The most notorious member in this family is variola, the causative agent of smallpox. Smallpox was one of the deadliest infectious diseases in human history and the first disease to be extensively prevented by vaccination, due to the English scientist Edward Jenner's work using the cowpox virus for immunization. Humans inoculated with the cowpox virus were also immunized against the variola virus. Vacca means cow in Latin, and the vaccinia virus is closely related to the cowpox virus and is the active constituent in the vaccine that eradicated smallpox (Condit et al., 2006). The variola virus is not used in the lab due to biosecurity precautions. However, the vaccinia virus serves as a laboratory model for other poxviruses and is the best studied poxvirus (Haller et al., 2014). Therefore, the general description of poxviruses in this thesis is mostly based on what is known about the vaccinia virus. Poxviruses can be grouped into two subfamilies: *entomopoxvirinae*, which infects insects and *chordopoxvirinae*, which infects vertebrates (Haller et al., 2014). Phylogenetically, SGPV is the deepest representative of the *chordopoxvirinae* so far discovered (Gjessing et al., 2015).

1.6.1 Poxvirus structure and genome

Poxviruses make up a large family of viruses that replicate in the cytoplasm of their host cell (Haller et al., 2014, Condit et al., 2006). Poxviruses are large, complex viruses with linear, double stranded DNA and a complex and unique virion morphology (Condit et al., 2006). They are membrane-enveloped, slightly flattened and barrel-shaped particles with an internal structure that has a walled, biconcave core flanked by lateral bodies as shown in figure 5 (Moussatche and Condit, 2015). A poxvirus virion can exist in three different forms: mature virion (MV), wrapped virion (WV) and extracellular virion (EV). As shown in figure 6, MV is the simplest form of the virus and are usually located inside their host cell and are only released by cell lysis. WV, also located inside the cell, is a MV with two extra lipid bilayers deriving from the hosts Golgi apparatus. Characteristic viral proteins can be found attached to the outer

membranes of WV. The outer membrane of WV fuses with the plasma membrane and leaves the host cell by exocytosis. The virion does now have an EV form, which is an MV with an additional membrane as shown in figure 5 (Condit et al., 2006).

The genomes of currently sequenced poxviruses vary in length (Haller et al., 2014). Poxvirus genes do not contain introns because of the cytoplasmic replication site, and the viral mRNAs are therefore not being spliced. This makes it easier to study genomic sequences of poxviruses. Each gene seems to have a promotor that control transcription, and genes are closely spaced in the genome (Condit et al., 2006). Conserved genes that are important for the general biology of poxviruses are primarily located in the central regions of the genome, while genes involved in the interaction with the host are usually found at the end of the genome, having more sequence diversity. The latter genes are usually considered virulence genes and their protein products as virulence factors (Haller et al., 2014). The gene order of SGPV differs from other chordopoxviruses (Gjessing et al., 2015) and will be further explained in chapter 1.7.2.

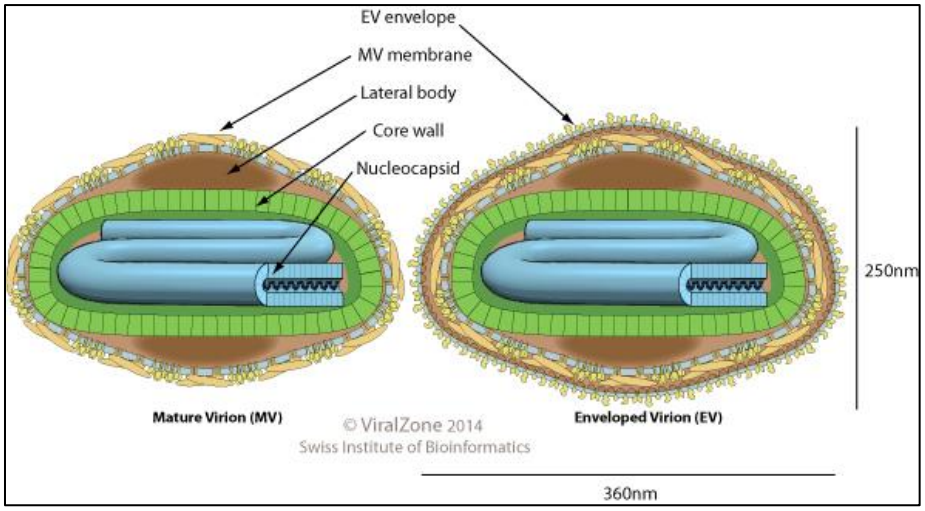

Figure 5: Pox virus structure. The left figure shows a mature virion and the right figure show the virus with an extra membrane envelope. (ViralZone, 2014).

1.6.2 Pox virus replication and host interaction

Most poxviruses enter the host cell by self-determined species-specific receptors. When the virus is taken up by the cell, it undergoes uncoating and the core is released into the cytoplasm (Tesgera et al., 2019). Poxviruses encode a complete set of genes involved in transcription that enables exclusive replication in the cytoplasm of their host cells (Moussatche and Condit, 2015). Before the genome is replicated, early genes being important for replication are

expressed (Tesgera et al., 2019). When the early gene expression peaks, the replication starts and are placed in so called "factories" in the cytoplasm (See figure 6). Intermediate transcription factors are also encoded by early genes, while intermediate genes encode late transcription factors. The genes are therefore expressed in a well-coordinated order (Condit et al., 2006). The late genes that encode structural proteins are expressed after the genome is replicated. Lastly, the complete virus is formed and assembled (Tesgera et al., 2019).

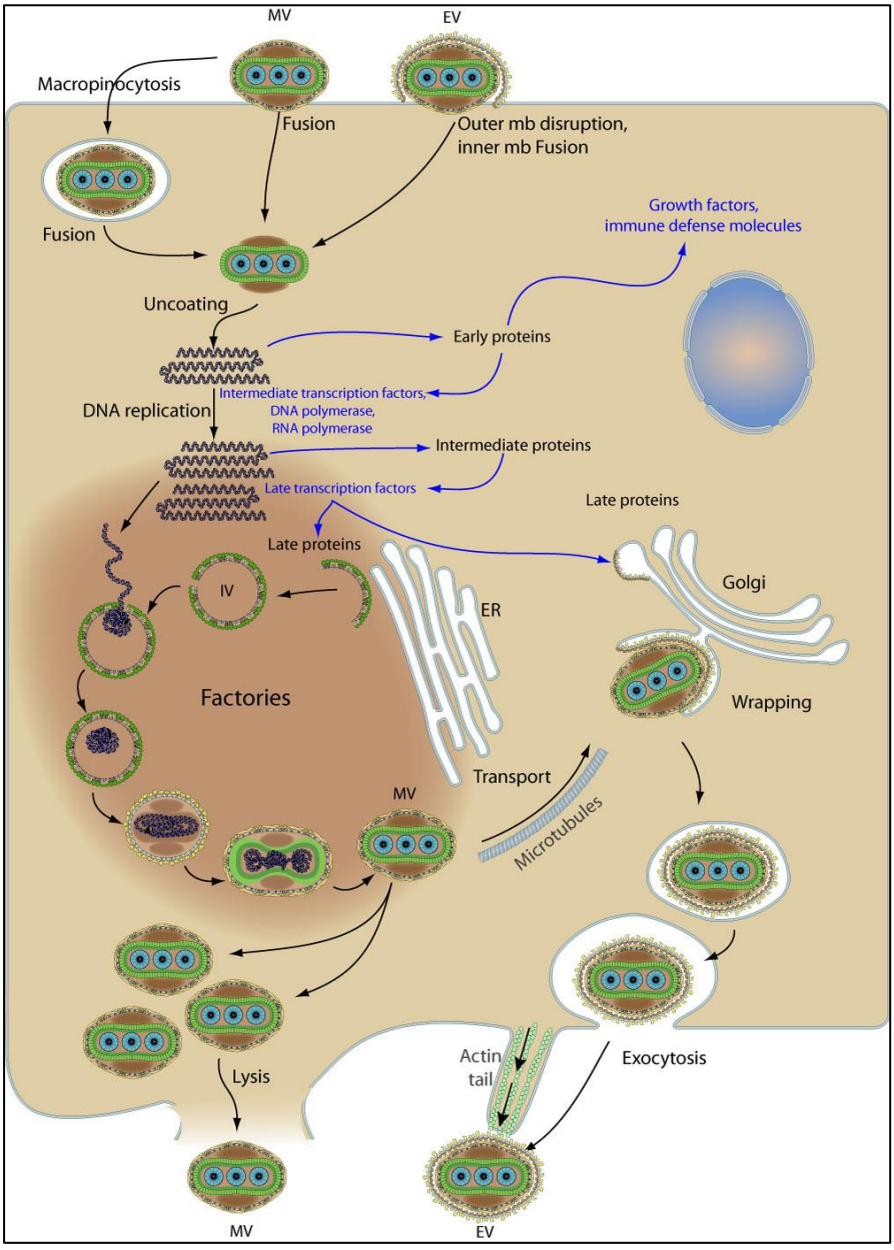

Figure 6: Poxvirus replication cycle showing different ways of infection and release (ViralZone). See text for details.

Viral infection leads to an early innate immune response to limit the replication of the virus and an adaptive immunity that develops later (described in 1.5). During the course of evolution, viruses have developed numerous ways to evade or suppress the hosts' immunological defenses and poxviruses encodes many proteins dedicated to this task. Some proteins function inside the infected cell to inhibit apoptosis or signaling pathways that produces chemokines, pro-inflammatory cytokines and interferons. Other proteins are secreted from the cell, where they bind and neutralize cytokines, chemokines, complement factors and interferons (Smith et al., 2013).

1.7 Salmon Gill Pox Virus (SGPV)

The salmon gill poxvirus (SGPV) is the focus of this master project. SGPV infects gill epithelial cells in farmed salmon and is associated with acute high mortality during disease outbreaks in Norwegian aquaculture. Poxvirus related diseases with high mortalities have been described in farmed Atlantic salmon, koi and common carp (*Cyprinus carpio*), and ayu (*Plecoglossus altivelis)*. A commonality is that poxvirus has an affinity for the gills and compromise the gill functions. The only published fish poxvirus genome so far is SGPV. One study claims to have successfully cultivated SGPV (LeBlanc et al., 2019), but no fish poxvirus has yet been successfully cultured in cells at the NVI. More experimental studies are needed to be able to get more knowledge about poxviruses and their disease manifestations in fish.

1.7.1 The disease caused by SGPV

Specific manifestations of gill disease resembling that caused by SGPV infection has been observed since the 1990's. The virus was first observed by electron microscopy described by Nylund et. al in 2008 (Nylund et al., 2008). In 2015, SGPV was sequenced and characterized in association with apoptosis of gill epithelial cells, and the first full genome of SGPV was published. This work led to the establishment of diagnostic tools that included immunohistochemistry and real-time PCR assays. The combined use of these analyses enabled characterization of virus association with gill pathological changes during an infection. (Gjessing et al., 2015). As more studies were performed following the development of diagnostic tools, it was discovered that SGPV is more widespread than previously believed. Improved detection strategies also made it possible to detect the presence of SGPV in archived samples, and it has been suggested that the role of SGPV has been largely overlooked as the presence of other agents have been regarded as more conspicuous (Gjessing et al., 2017b). SGPV is now confirmed to be a key pathogen responsible for gill disease in farmed salmon

(Thoen et al., 2020, Gjessing et al., 2017a, Gjessing et al., 2017b, Gjessing et al., 2015). Thoen et. al presented the first experimental infection model for SGPV disease (SGPVD) in 2020, showing that an acute disease development and mortality was associated with a combination of infection and stress(Thoen et al., 2020).

The virus infects the gill epithelial cells, compromising the barrier function of the gills, and also affects the chloride cells. Based on transcriptomic studies, SGPV compromise the gill immune system and probably paves the way for secondary infections (Gjessing et al., 2017b). SGPV infections has been detected both in the fresh- and seawater phase of salmon production. The disease outbreaks are acute and spread rapidly in freshwater farms. Since most fish display disease manifestations, the morbidity is thought to be high, but the number of diseased fish vary considerably. Mortality also varies a lot in the seawater phase, and losses between 2 % to 70 % have been reported (Gjessing et al., 2016). In the seawater phase SGPV is detected amongst several other pathogens and appears in association with complex gill disease (Gjessing et al., 2017b). SGPV has also been detected in wild salmon (Garseth et al., 2018).

1.7.2 Genetic characterization and tracing of SGPV variants

SGPV is the deepest representative of the *Chordopoxvirinae* discovered so far. The genome is a single linear dsDNA molecule of 241 kilobases (kb) and is predicted to contain 206 unique genes. Similar to vaccinia virus, SGPV is predicted to harbor all the essential elements for genome replication and expression. Like most other poxviruses, its genome also includes inverted terminal repeats (ITRs). The gene order of SGPV differs from other chordopoxviruses, and its genome is predicted to encode several unique proteins with unknown function. There are several conserved proteins in other chordopoxviruses, including some involved in interactions with host defense systems, that are missing in SGPV. One exception is the conserved B22R-like giant membrane proteins. Functional studies of these proteins could provide important information on virus-host interactions, with possible links to SGPV pathogenesis (Gjessing et al., 2015).

A Multi-locus variable-number tandem-repeat analysis (MLVA) for genotyping SGPVs has been established. MLVA is based on variable numbers of tandem repeats (VNTRs) that are short, repeated gene sequences in a genome. The sequences only consist of a few base pairs in a certain order that is repeated several times. VNTR regions appear several places in a genome and the length of each VNTR-region can vary between closely related viruses. An MLVA profile of a genome is based on the different lengths of several VNTR sites. Eight VNTRs have

been selected to map the MLVA profiles for SPGVs, having various locations throughout the genome. The MLVA assay enables specific, high-resolution genotyping of the virus directly from gill samples. Sequencing of more SGPV genomes and phylogenetic analysis revealed that one main SGPV cluster dominates in samples from Northern Europe, with a distinct variant found on the Canadian east coast. MLVA revealed specific sub-lineages and indicated “house strains” in freshwater smolt farms and similarities in individual fjord systems for wild salmon. In some wild fish samples, more than one strain of SGPV was found in the same individual (Gulla et al., 2020).

1.7.3 B22R genes

The poxviral B22 family of proteins are of particular interest when it comes to interactions between the virus and the host immune system. B22 proteins are encoded by the largest genes of several poxviruses. It has been found that when the T-cell ability to control the dissemination of some poxviruses is reduced, this might be directly related to virulence. Alzhanova et. al identified a gene product from Monkeypox virus (MPXV) causing T-cells to be non-responsive to stimuli. This is a predicted transmembrane protein belonging to the B22 family of proteins that has also been found in several other poxviruses including variola virus and SGPV, but not vaccinia virus. Alzhanova et al. showed that vaccinia virus strongly stimulates virus-specific T-cells with CD4 and CD8 receptors that produce the cytokines IFNγ and TNFα. On the other hand, poxviruses that contain B22R encoding genes, had a T-cell response that was extremely low. They also showed that B22R interference occurs after the T-cell receptor (TCR) has bound the antigen presenting MHC, and most likely inhibits the signaling pathway downstream of TCR binding. Since the inhibitory factor is not a secreted protein, the T-cells are thought to be inhibited by cell to cell contact (Alzhanova et al., 2014).

Three paralogous genes (SGPV154, SPGV159 and SGPV162) are located close to the end of the genome of SGPV. These genes are all homologous to the B22R gene in the variola virus (Gjessing et al., 2015). In this master thesis, it has been decided to rename the three genes to B22R1, B22R2 and B22R3 respectively, and these names will be used hereafter. B22R1 has about the same length as the homologues in other poxviruses, but B22R2 and B22R3 are much shorter, which suggests that these two genes have been truncated during the evolution of the SGPV, and may have evolved by duplication events (Gjessing et al., 2015). It is interesting to investigate whether these genes may play a role in SGPV virulence. Since assays and tools to analyze T-cell interactions are not yet well established in salmon, a first step is to clone the

genes encoding these proteins, express them in relevant cells and conduct some initial investigations to prepare for such a study.

2.0 Aims

Main aim: Cloning and characterization of three genes from the Salmon Gill Pox Virus that resembles the B22R gene from the vaccinia virus, in which are shown to inhibit immune function.

Specific aims:

- Characterize SGPV B22R genes *in silico*
- Clone B22R genes from two genetic variants of SGPV into an expression vector
- Optimize transfection methods in fish epithelial cell lines
- Transfect and express B22R in fish epithelial cells
- Study localization of B22R variants using confocal microscopy
- Analyze expression of B22R transcripts in gills *in vivo*

3.0 Materials and methods

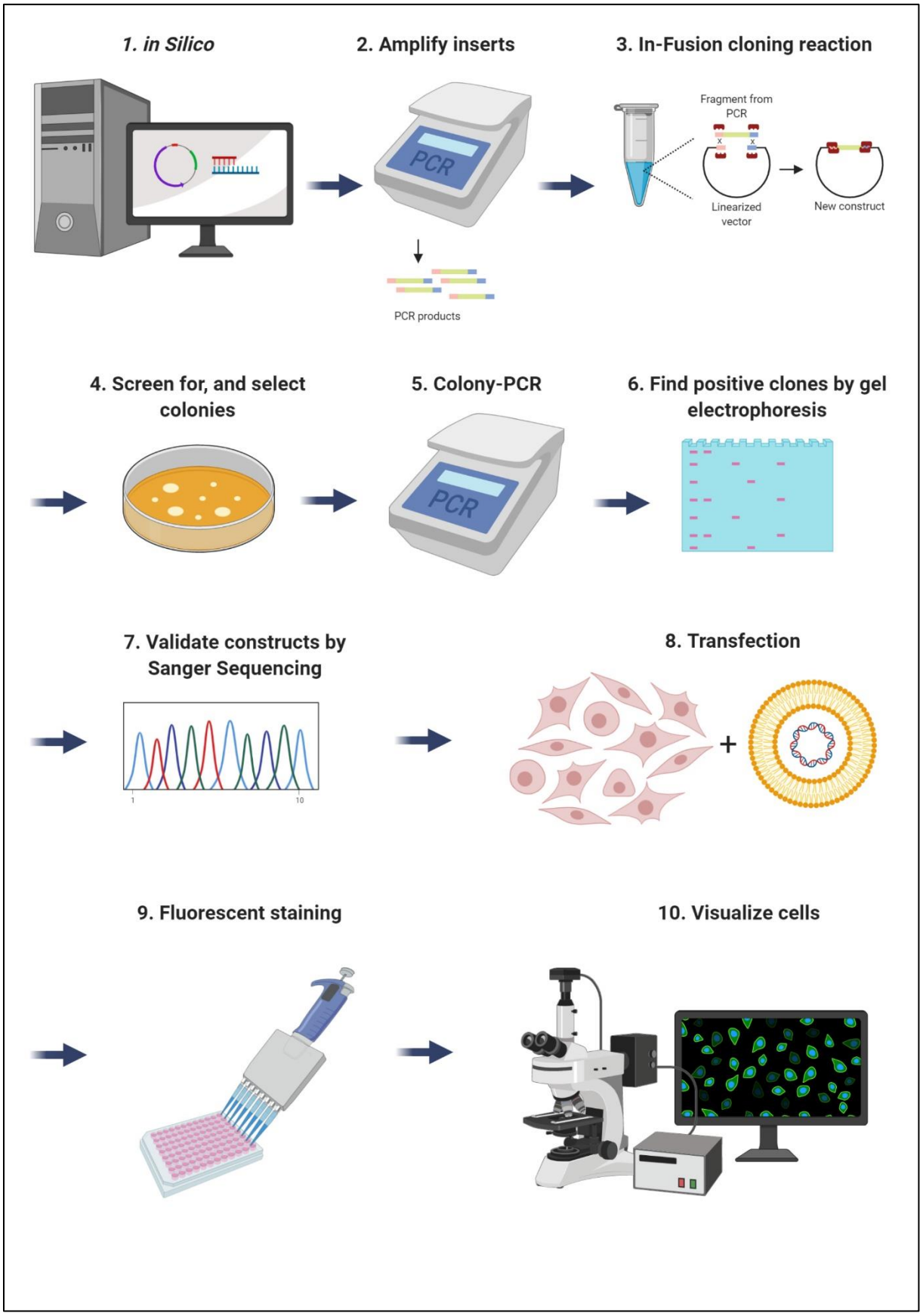

Figure 7: Overview of the main experimental steps performed in the thesis work. **1:** Characterization of the reference genes and preparation of cloning by analyzing gene sequences, vectors and designing primers. **2:** Amplify inserts by PCR. **3:** Set up the In-Fusion cloning procedure, plate out cells and let incubate overnight. **4:** Screen for colonies the day after. **5:** Use bacteria from selected clones to set up a colony PCR. **6:** Investigate the PCR products on a gel and pick the ones with the right length. **7:** Sequence the selected clones to ensure that the right sequence has been inserted into the vector. **8:** Transfection procedure. Lipofection has been used as an illustration here. **9:** Fluorescent staining of the cells, to be able to visualize specific targets in the cells. **10:** Visualize and examine the cells by a fluorescence or confocal microscope (Created with Biorender.com).

An overview of the main experimental steps performed in the thesis work is presented in figure 7.

3.1 Sequence analysis

With the arrival of Next Generation Sequencing genetic information has become more and more accessible, and today it continues to become cheaper and faster to sequence DNA due to the rapid development of sequencing technologies. This has resulted in an increasing abundance of genome sequences available in public genomic databases. This sequence information that can be used, among others, to perform comparative studies of genes and gene products within and across species. Investigations of protein function often starts *in silico* with analysis of a DNA sequence, predicted to represent a functional gene, and its translated protein product. The first step is often to use available databases and search for homologous nucleotide or amino acid sequences. In the latter case, well-characterized proteins with identical and/or similar amino acid sequences to that of your target protein can provide valuable early information about its structural and biological properties (Alberts et al., 2015).

In the present work, several bioinformatic tools and software programs have been used to study the nucleotide and amino acid sequences of three SGPV genes and their gene products. The recombinant viral proteins were studied *ex vivo* with the aim to gain new functional information.

3.1.1 Bioinformatic analyses and primer design

3.1.1.1 Online bionformatic tools and databases

The SGPV sequences were analyzed *in silico* to predict physiochemical and functional properties. The BLAST search tool at NCBI (https://blast.ncbi.nlm.nih.gov/Blast.cgi) was used to find other similar proteins in the database. Default settings were used. SignalP (http://www.cbs.dtu.dk/services/SignalP/) was used to search for signal peptide sequences. PSORTII (https://psort.hgc.jp/form2.html) provides a number of useful predictions of protein structural elements and motifs, including cellular localization, presence of nuclear localization

signals (NLSs), transmembrane regions and dileucine motifs, to mention a few. PSIPRED (http://bioinf.cs.ucl.ac.uk/psipred/) was used to predict protein secondary structure with special focus on the N- and C-terminal ends of the proteins, relevant when considering where to add the FLAG-sequence for detection of expression (see 3.1.1.2) . The presence of putative N-glycosylations was investigated using NetNGyc 1.0 (http://www.cbs.dtu.dk/services/NetNGlyc/). N-glycosylations indicate that the proteins have been in the Endoplasmic Reticulum (ER) and may have followed the secretory pathway. Potential NLSs were predicted using both PSORTII and NLS Mapper (http://nls-mapper.iab.keio.ac.jp/cgi-bin/NLS_Mapper_form.cgi). NetNES 1.1 was used to predict nuclear export signals (http://www.cbs.dtu.dk/services/NetNES/). As the three SGPV proteins are potential transmembrane proteins and could contain fatty acid modifications, N-terminal myristoylation was examined using Myristoylator (http://web.expasy.org/myristoylator/). Kyte & Doolittle hydrophobicity plots were made using Protscale (https://web.expasy.org/protscale/) to indicate potential transmembrane regions. TMpred, another program to predict localization of transmembrane regions was also used (https://embnet.vital-it.ch/software/TMPRED_form.html). Molecular Weight (MW) of the proteins were also predicted (http://web.expasy.org/compute_pi/). PFAM is a large collection of protein families and was used to find motifs in the protein sequences that was consistent with a protein family (https://pfam.xfam.org/search/sequence). Identity and similarity between protein sequences was found using SIAS (http://imed.med.ucm.es/Tools/sias.html).

3.1.1.2 Sequence data analysis

The software program CLC Main Workbench (Qiagen) was used to view and analyze sequence data, to assemble contigs from sequencing and compare with a reference sequence, and perform multiple sequence alignments. This software was also used for sequence data management, *in silico* translation, primer design, preparation and planning of cloning (Qiagen).

The pcDNA™ 3.1 (+) vector from Invitrogen was used for cloning (described in section 3.3). The vector is 5.4 kilobases (kb) in size and some relevant features are: multiple cloning sites, Human Cytomegalovirus (CMV) enhancer promoter, T7 phage promoter, Bovine Growth Hormone (BGH) polyadenylation signal and an ampicillin resistance gene. Figure 8 shows a map of the pcDNA™3.1 vector. CLC Main Workbench was used to visualize and locate the various restriction sites and promoter regions in the vector. The gene sequence must be inserted downstream of the CMV promoter region for transcription in the eukaryotic cell. The CMV promoter is an immediate early gene promoter encoded by the Human Cytomegalovirus and is

widely used as a constitutive promoter to drive gene expression in eukaryotic cells. (Yu et al., 2017). A multiple cloning site is located immediately downstream of the CMV promoter, and selected restriction sites for vector linearization and cloning was determined *in silico*. Section 3.3.1 describes how it was done experimentally.

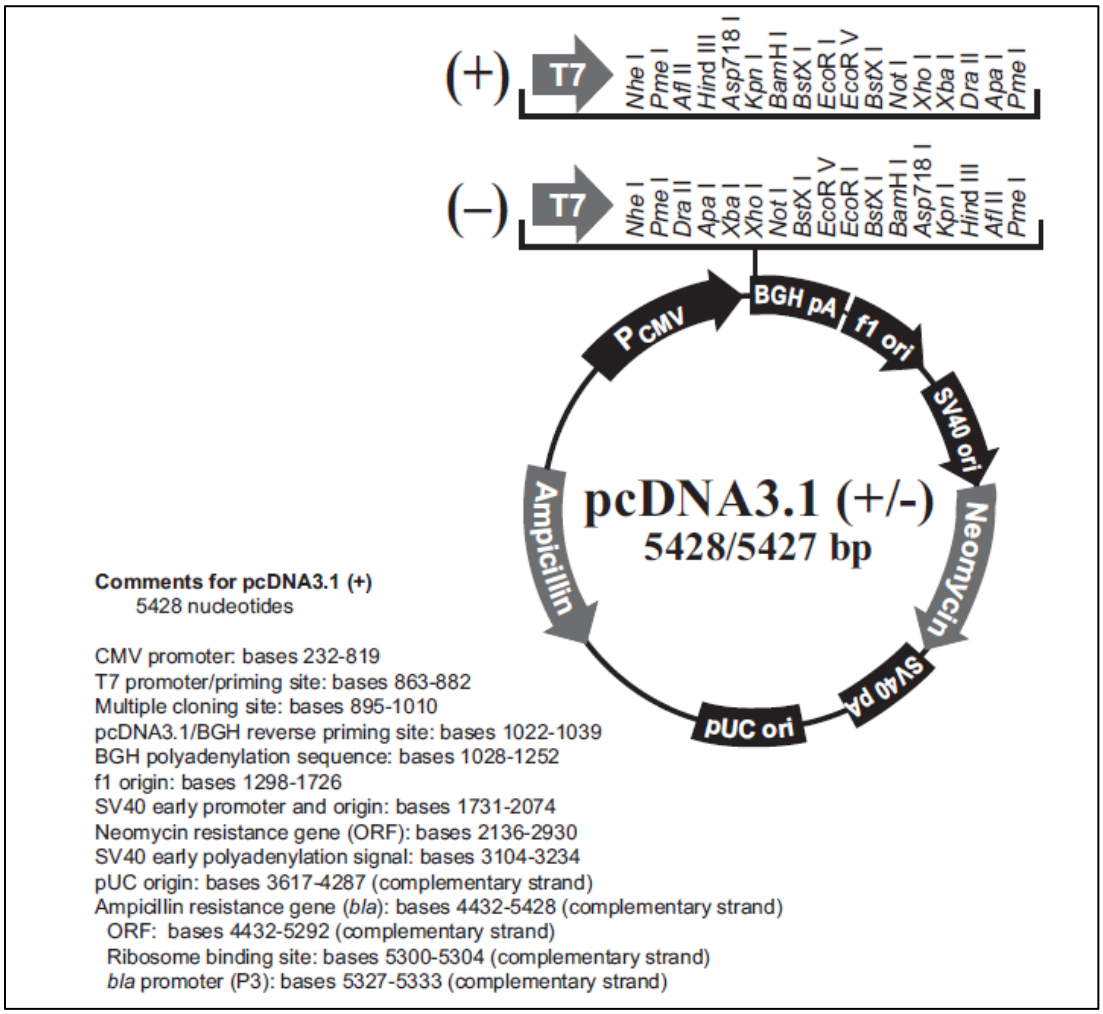

Figure 8: The pcDNA 3.1 (+/-) plasmid used in cloning of the three SGPV genes.

Both CLC Main Workbench and the TaKaRa Clontech web program were used to design cloning primers. Several parameters were taken into consideration when designing the primers. As described in the In-Fusion manual, the 3'-portion of the primer (the gene-overlapping part) should be gene-specific, have a melting temperature (T_m) of 58-65 °C while the T_m difference between the forward and reverse primer should be ≤ 4 °C, be between 18-20 bases in length and have a GC-content between 40-60 %, not contain identical runs of nucleotides and the last five nucleotides at the 3' end of each primer should not contain more than two cytosines (C) or guanines (G), and avoid complementarity within each primer and primer pairs. The primers must also contain 15 bases that are complementary to the ends of the linearized vector.

The fusion tag included in each construct is called FLAG™. The coding sequence of the FLAG tag (AspTyrLysAspAspAspAspLys) was present at the start or end of the gene sequence so that both were expressed together creating a fusion protein. The tag can be targeted by several commercially available antibodies (Einhauer and Jungbauer, 2001). The DNA sequence encoding the FLAG-tag (5'- GACTACAAAGATGACGACGATAAG –3') was included in the primer design.

3.2 Quality and concentration measurements

3.2.1 Gel electrophoresis

Electrophoresis is when electrically charged particles migrate under the influence of an electric field. A porous gel is used as medium, soaked in a solution of dissolved electrolytes. Nucleic acids contain phosphate groups that are negatively charged at physiological pH and higher and will travel against the positive pole (anode). Samples can be pipetted side by side in wells in the gel. By adding a constant electrical field, it will be possible to separate the nucleic acids by size (Jacobsen, 2019). Short nucleic acid fragments will not get much resistance while travelling through the gel and will travel faster, while longer nucleic acid fragments will have more resistance and travel slower. The nucleic acids must be stained to enable visualization (Jacobsen, 2019).

Electrophoresis was used here for running plasmids and PCR products. A protocol from the electronic database at the Norwegian Veterinary Institute (NVI) was followed. A 50 mL gel was prepared with 0,5 g agarose, 50 mL 1x Tris-Borate-EDTA (TBE)-buffer and 5 µL GelRed™ DNA stain from Biotium (binds to DNA). After the gel had cooled, it was put into an electrophoresis chamber with electrodes. The samples were mixed with 6X Loading dye from Thermo Fisher -1/6 of the total volume. The samples were added to their respective wells in the gel. GeneRuler 1 kb DNA Ladder was added directly onto a well on the gel. The gel was run at 100 V and the migration of the loading dye was monitored. The run was stopped when the dye had travelled approximately 2/3 of the length of the gel (see Appendix page 1 for materials and detailed protocol). The stained DNA in the gel was visualized using either a UV Transilluminator or a ChemiDoc XRS. The ChemiDoc XRS was used to take photos of the gel. When cutting out DNA bands from the gel for downstream cloning, the UV Transilluminator and a face shield was used. The DNA was purified using the NucleoSpin® Gel and PCR Clean-up kit from Macherey-Nagel.

3.2.2 Bioanalyzer

The Bioanalyzer 2100 Expert instrument assay from Agilent Technologies is based on traditional gel electrophoresis principles (capillary electrophoresis) using specialized chips. A chip includes wells for loading the gel, samples and ladder and contains micro-channels to create interconnected networks between the wells. When preparing the chip, a gelmix with dye molecules that intercalates into DNA or RNA strands are added and spread out to all the wells. Markers, ladder and samples are added before the chip is placed in the instrument cartridge. The markers function as internal standards used to align the sample with the ladder and is necessary to compensate for the probable occurrence of drift effects during a chip run. The polymers in the gelmix allow charged molecules to migrate through the gel and be separated by size. Detection is based on laser-induced fluorescence detection (LIF), and the data are translated into electropherograms showing peaks and gel-like images showing bands. The ladder contains components of known sizes and creates a standard curve that shows the correlation between migration time and size of the fragments. The ladder also contains markers with known concentration, and the concentration and size of each product from the samples can be calculated.

The DNA 12000 Reagents kit was used for separation of large DNA strands like linearized vectors and large gene sequences. DNA 1000 reagents kit was used for separation of shorter DNA strands like PCR products. RNA 6000 Nano Reagents were used for separation of mRNA strands made *in vitro*. The chips were prepared according to each user manual included in the kits (AgilentTechnologies, 2020).

3.2.3 Nanodrop

Concentrations of RNA and DNA were determined using NanoDrop 2000 Spectrophotometer according to the user manual from Thermo Fisher Scientific. 1 µL of a sample is added to a measurement pedestal where it bridges between two optical fiber cables. Light passed through the sample is measured and shown in a diagram in the computer software connected to the instrument. Concentration of nucleic acids are based on absorbance at 260 nm, and quality evaluation also includes absorbance at 280 nm (260/280). (ThermoFisherScientific, 2009)

3.3 Cloning

Cloning a gene sequence into a vector requires several steps including vector linearization, fragment preparation, insertion, amplification in bacterial culture and confirmation of successful cloning by PCR and sequencing.

3.3.1 Preparation of components for cloning

3.3.1.1 Vector Linearization

According to the In-Fusion user manual, the vector must be linearized before starting the cloning procedure and this was done by a restriction enzyme digestion. A restriction enzyme recognizes and cuts at specific locations in a DNA sequence (Børresen-Dale, 2018). The vector pcDNA™3.1(+) was linearized using the Anza™ Restriction Enzyme Cloning System from ThermoFisher, a kit containing several restriction enzymes. The enzyme Anza 16 HindIII was selected because the vector has a restriction site for this enzyme in the cloning region. Additional restriction enzyme cutting sites were also present in the cloning region so other enzymes could also have been used. The digestion protocol from the Anza™ Restriction Enzyme Cloning System user guide was followed (ThermoFisher, 2015a). Gel electrophoresis was performed as described in section 3.2.1 to confirm the linearization of the vector. An uncut vector was also included in the setup as a control to confirm linearization. A linearized vector travels slower than the supercoiled circular vector in the gel. The uncut vector should generate two characteristic bands in the gel because of a mix between supercoiled and relaxed plasmid. The supercoiled form of the plasmid migrates faster than the relaxed form.

3.3.1.2 PCR for amplification of gene sequences

Polymerase Chain Reaction (PCR) is an important tool that is broadly used in scientific research and in human and veterinary diagnostics. PCR is an *in vitro* amplification of DNA or cDNA. Heat stable DNA polymerases are used to amplify a region of the DNA on a denatured single stranded DNA (ssDNA) template (Watson et al., 2014). The target region to be amplified is determined by two different oligonucleotide primers around 20 bases in length, each of which bind in a sequence dependent manner (complementarity) to either end of the target region. Upon hybridization of the primers, the DNA polymerase binds to these regions and initiates chain elongation. The PCR is divided into three steps that is repeated 25-35 times (cycles) making it possible to produce many copies of the template DNA:

1. Denaturing: The dsDNA is denatured (becomes ssDNA) at a high temperature (94-98°C).
2. Annealing: The temperature is lowered according to the optimal temperature for the primers (55-65°C) so they can hybridize to the complementary sequence in the template ssDNA.

3. Elongation: The temperature increases to 72°C which is the optimal temperature for the heat stable DNA polymerase that elongates the DNA strand from the primers.

4. In the PCR used in the cloning procedure, a 15 bp sequence overlapping with the vector and flag sequences will be incorporated into the ends of the PCR product through additional sequence stretches included at the end of the primers (Figure 9). See appendix page ii for full list of materials and PCR setup and program used.

3.3.2 In-Fusion Cloning

The In-Fusion® HD cloning kit from Takara Bio USA, Inc. was used to perform the cloning. This system was selected because it is a fast and easy cloning protocol with relatively few steps and high cloning accuracy compared to traditional cloning methods. (Takara Bio USA, 2016). The target gene sequences were amplified by PCR, using primers with an overlap with the vector sequence, and the insertion is based on annealing and recombination of complementary ends instead of restriction sites (Park et al., 2015). The cloning mechanism eliminates the need to consider restriction sites within the cloning design, restriction digestion of the insert, and the ligation reaction. The method is also seamless, which means that there are no extra bases between joined fragments (Raman, 2015). Because of the PCR primer design, the insert and vector will have 15 bp homologous ends. The insert and the linearized vector are incubated with the In-Fusion enzyme that removes nucleotides at the 3'- ends of linear DNA. This allows the complementary base pairs of the vector and insert to join and anneal in the right direction. (Takara Bio, 2020). When the plasmid is transformed into the competent *E. coli* cells, any remaining gaps will be repaired by mechanisms in the bacteria. Screening for clones takes much shorter time compared to traditional cloning technologies because of the high cloning efficiency and accuracy (Raman, 2015).

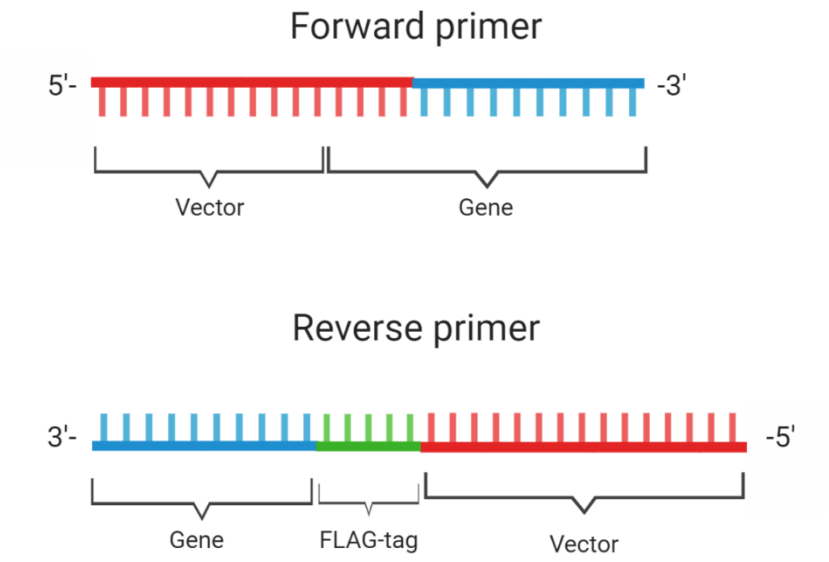

Figure 9: Illustration of the primer designs used. In this figure, FLAG-tag will be in the C-terminal end of the PCR product (Created with Biorender.com)

The lab-manual from Takara Bio USA was used to perform the In-Fusion reaction and the transformation. The flow chart of the In-Fusion cloning system is presented in figure 10. The transformed E. *coli* was plated out on plates containing Luria-Bertani (LB)-agar and 100 mg/L Ampicillin (see section 3.3.3 for more details) and put into an incubator at 37°C overnight and screened for clones the day after.

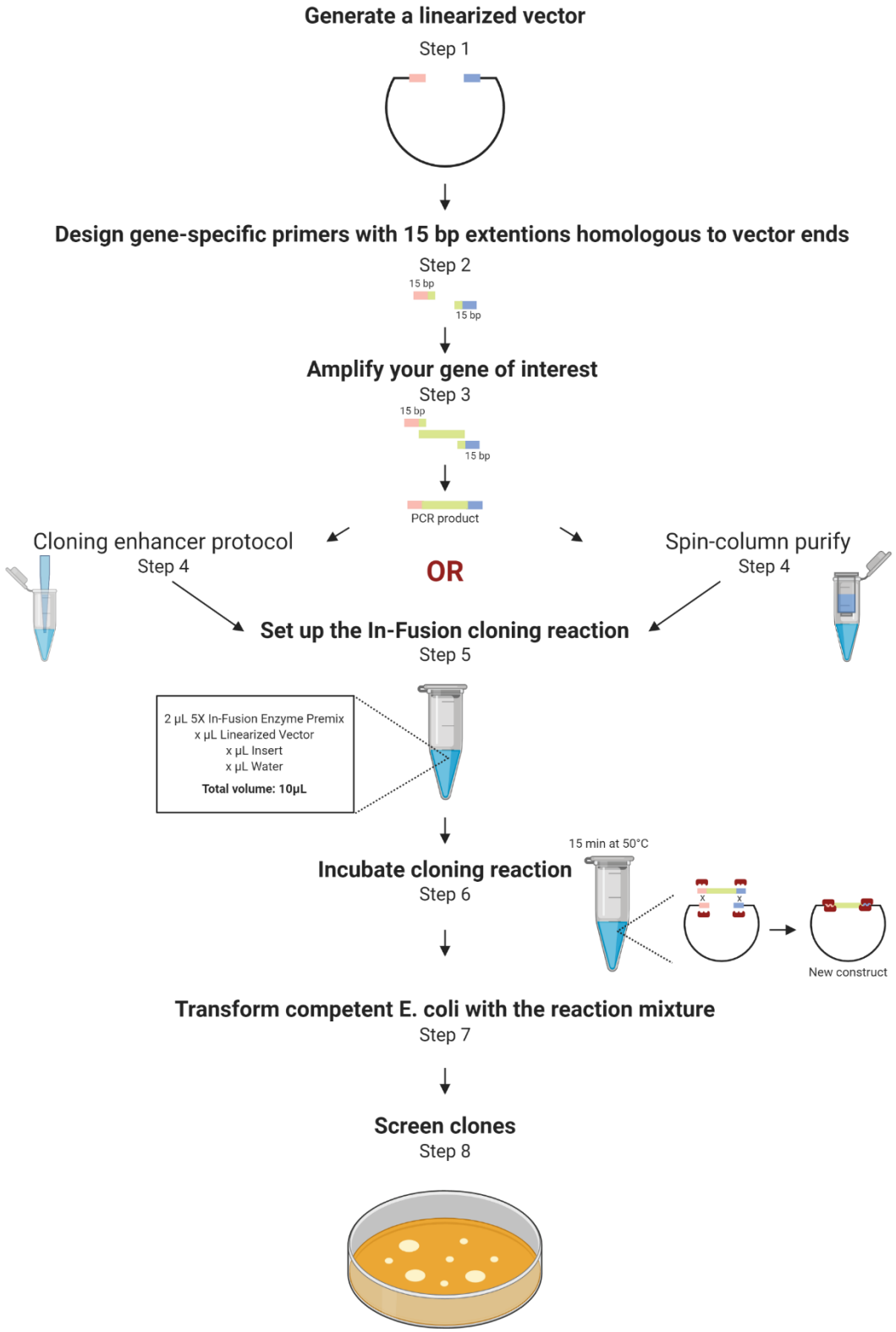

Figure 10: overview of the In-Fusion cloning protocol based on a figure from the user manual (Created with Biorender.com).

3.3.3 Cultivation of bacteria

A growth medium must contain several nutrients required for bacterial growth, and different bacteria have different requirements. Bacteria are usually cultured using either solid or liquid nutrients-containing medium. Here, liquid LB broth with 50 mg/L ampicillin and petri dishes containing LB agar with 100 mg/L ampicillin have been used to cultivate the bacteria. LB medium is a medium rich on nutrients that is commonly used for culturing bacteria. The In-Fusion® HD cloning kit includes Stellar™ Competent Cells. The Stellar™ Competent Cells are an E.*coli* HST08 strain that has been prepared to achieve high transformation efficiency (Takara Bio). All incubations were done at 37°C. The liquid media containing bacteria were incubated with shaking, and rpm is specified in each topic.

The *E. coli* was diluted in SOC medium after transformation during the In-Fusion cloning procedure. SOC medium is a glucose-containing and nutritionally rich medium that is specialized on improving transformation efficiency (Sun et al., 2009).

3.3.4 Colony PCR

A colony-PCR is used to confirm that the gene sequences have been inserted into the vector. Sequencing will later be the final verification. To ensure that at least one clone had the right insert, 10 bacterial colonies were collected for each of the constructs and incubated in 200 µL LB medium containing 50 ng/µL ampicillin on a 96 well plate for three hours at 37°C with shaking at 130 rpm. Then 1 µL of each bacterial suspension was used directly in the PCR setup (see setup in appendix pg. iv). Primers that bind to the T7 promoter sequence and the BGH polyadenylation sequence in the vector were used (see Figure 11 and Table 2). These sequences are located close to each end of the insert, and the PCR product will therefore include the gene sequence if it has been inserted. A forward primer from a primer set available from another project with binding site within the gene B22R1 was also used instead of T7 for this gene. With this primer, no bands should be visible on the gel if there were no insert. The length of each PCR product was calculated so it was possible to confirm with high probability that the right gene sequence had been inserted.

Table 2: T7 and BGH primers used for colony PCR.

***Primers**		
Name	**Target**	**Sequence**
T7 Promoter primer (F)	Vector	5'- TAATACGACTCACTATAGGG -3'
BGH Reverse primer (R)	Vector	5'- TAGAAGGCACAGTCGAGG -3'

* For the B22R1 forward primer, see table 9 in section 4.6.

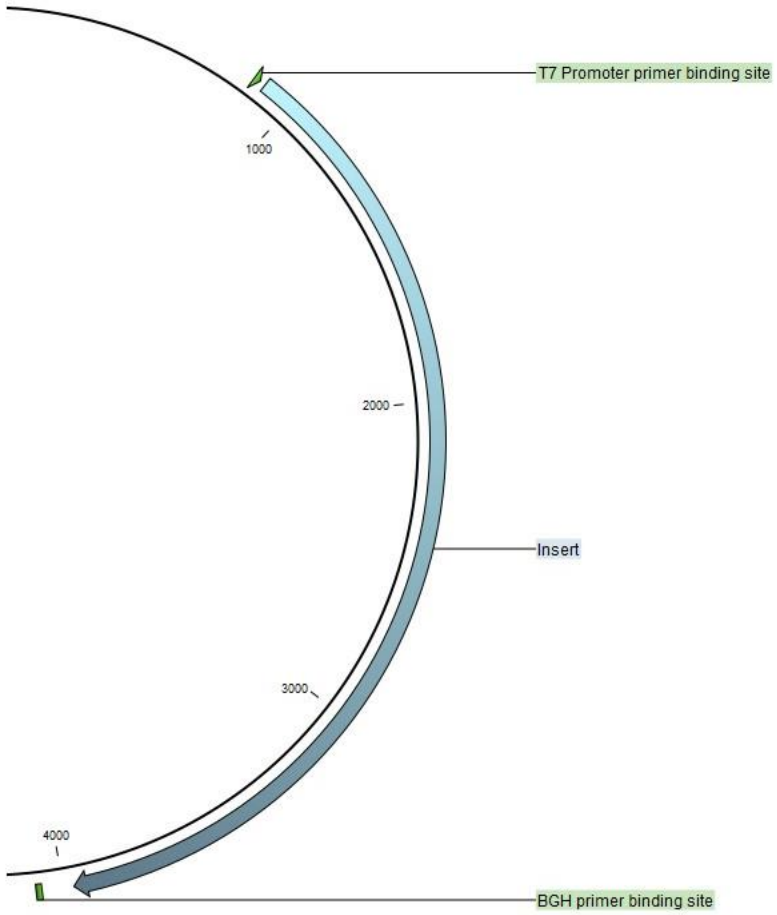

Figure 11: T7 and BGH primers hybridize with the vector directly upstream and downstream of the inserted sequence.

If the PCR products had the expected size as estimated by gel electrophoresis, 50 µL of the bacterial suspension was added to a sterile tube containing 3-5 mL LB broth with 50 mg/L ampicillin, incubated overnight and prepared for purification with a miniprep kit the day after.

3.3.5 Mini- and midiprep of plasmids

The Quick Plasmid Miniprep kit (Invitrogen, Thermo Fisher) was used to purify the three overnight cultures containing the different constructs. Miniprep is a quick and easy way to purify plasmids. This method does not give a high-level output of plasmid and is therefore most suitable for applications where abundant product is not needed. Here, miniprepped clones were used to prepare templates for the first sequencing step.

A HiPure Plasmid Midiprep kit from Thermo Fisher was used to perform a midiprep of the selected clones. This kit produces higher output and a purer product with less contaminants compared to the Miniprep kits. Thoroughly purified constructs are important for subsequent transfection into cells. Here, 50 µL bacterial culture from the colony-PCR plate was added to 50 mL LB broth with 50 ng/µL ampicillin in a sterile tube and incubated over night with shaking at 130 rpm and 37°C. The next day, the plasmids were purified using the Purelink™ HiPure Plasmid DNA Midiprep Kit (Invitrogen, Thermo Fisher). The purified plasmids were aliquoted to avoid repeated freezing and thawing and then stored at -20°C (ThermoFisher, 2015b).

3.3.6 Sanger sequencing

Sanger Sequencing is the traditional way of sequencing and has been the gold standard for many years. Sanger sequencing is based on dideoxy-modified deoxynucleotides (ddNTPs), meaning that the dNTPs used are missing a hydroxyl group at the 3’ position in the deoxyribose component. The four different ddNTPs (A, T, C and G) are labelled with specific fluorescent dyes that makes them possible to be detected and distinguished by an instrument. A standard PCR is set up with a mix including a DNA polymerase, the DNA template, specific primers, normal dNTP’s and ddNTPs with a specific ratio between those different groups. When the PCR runs, some of the dideoxy-dNTPs will be incorporated into the growing strand, and the elongation will stop. The PCR results in a series of many strands with different lengths. The fragment sizes are then separated by electrophoresis in an instrument. As the fragments move through the gel, the instrument detects the fluorescence from each of the four different fluorescently labeled dideoxy-dNTPs. A software processes the data and assembles the different signals to one continuous sequence. This method was considered as sufficient for sequencing the different constructs in this project. (Goodwin et al., 2016)

The sequencing was performed in-house at the sequencing facility at the Norwegian Veterinary Institute (NVI).

3.4 *In vitro* mRNA production

The mMESSAGE mMACHINE® T7 Ultra Kit (Life Technologies, cat.: AM1345) was used for synthesis of translation enhanced capped and polyadenylated mRNA transcripts. The constructs made by In-Fusion cloning was used as mRNA production templates, in addition to a Monster Green® Fluorescent Protein Vector (phMGFP). The kit is specialized for producing mRNA suitable for eukaryotic transfection and contains reagents for capping and polyadenylation, and section 1.4.1 explains the importance of this. An overview of the procedure is shown in fig. 12.

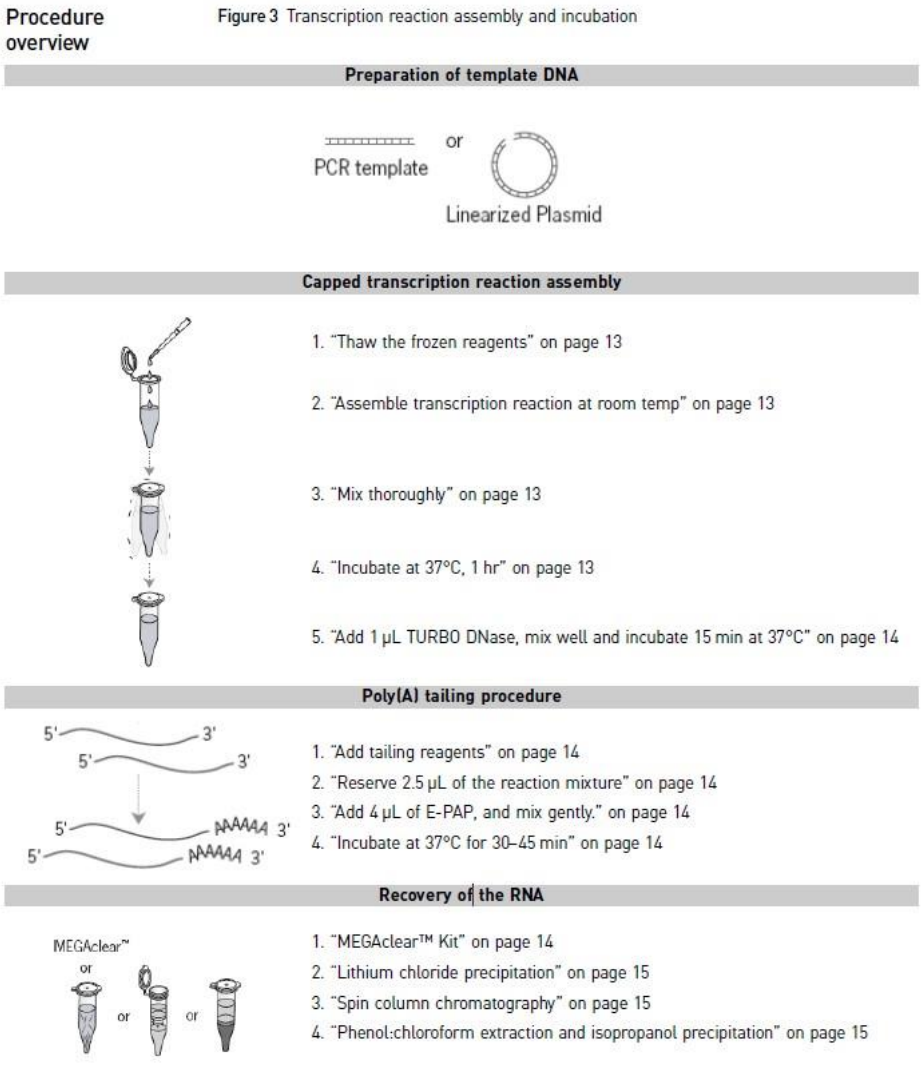

Figure 12: Overview of the *in vitro* mRNA synthesis procedure taken from the mMESSAGE mMACHINE® T7 Ultra Kit.

The plasmids were cut by restriction enzymes using the Anza™ Restriction Enzyme Cloning System kit from Thermo Fisher. The vector must have a T7 promoter region because the kit

includes a T7 polymerase that will transcribe from here. Figure 8 shows that the vector pcDNA3.1 has the T7 promoter region. The restriction enzymes were selected based on the insert sequences and localization of the restriction site in the vector sequence. It is important that the restriction enzyme does not cut in the insert sequence which would lead to incomplete translation. The restriction site must be located downstream of the insert for it to be transcribed and so that the transcript would not be too long. If the plasmid was circular, the RNA polymerase would keep on transcribing, and the products would be extremely long. The restriction cutting was examined by Bioanalyzer 2100 to confirm complete linearization.

The translation, capping and polyadenylation was performed following the mMESSAGE mMACHINE® T7 Ultra Kit procedure. Recovery of DNA was done with NucAway spin-columns™ from Thermo Fisher Scientific. Completed translation and incorporated polyA was confirmed with the Agilent 2100 Bioanalyzer system. According to the Agilent RNA 6000 Nano Kit Quick Start Guide, the samples should have a concentration of 5 – 250 ng/µL. The concentrations of the purified RNA were measured using NanoDrop 2000, and if necessary diluted before the Bioanalyzer run.

3.5 Cell lines

The complexity of intact tissues makes it difficult to study or purify particular molecules. Animal welfare and being able to replace experimental animals are also important issues. Most animal and plant cells can survive, multiply and express differentiated features in a culture dish if they are given suitable surroundings. Cell cultures are convenient to work with in the laboratory where several properties can be systematically investigated. The cells can be observed continuously in a microscope or analyzed biochemically. Most tissue cells require a solid surface to grow and attach to, and cultured cells are often attached to the surface of a plastic dish, as opposed to bacteria who live in suspended form. Cultured cells can be removed from the dish and be cultured again repeatedly in subcultures that can go on for weeks or months. An advantage is that such cells often display many differentiated properties that are maintained in culture, properties that often are not possible to study in intact tissues. Epithelial cells form large sheets displaying many of the features of an intact epithelium. Cell lines can also be stored in liquid nitrogen at -196°C and retain their viability after thawing. One important note though is that cell lines will differentiate from their progenitors after being cultured for some cycles (Alberts et al., 2015).

The two cell lines *Epithelioma papulosum cyprinid* (EPC) and Atlantic salmon gill-10 (ASG-10) described in section 1.3.3, have been cultivated and were used for transfection experiments. The cell cultures were split using the same protocol (full protocol in Appendix) by using 10 mL PBS to wash the cells, and 2 mL TrypLE to detach the cells from the surface. The EPC cells were incubated with TryLE for about 6-8 minutes, and the ASG-10 cells were incubated about 2-4 minutes. The flasks were gently agitated and the trypsination was observed using a phase contrast microscope. The cells were resuspended in 5-10 mL complete growth medium that will inactivate the trypsinization process.

When preparing a transfection experiment of each cell line, the number of cells per milliliter were counted using a Moxi™ Z Mini Automated Cell Counter by ORFLO Technologies and used for calculating the number of cells to be seeded per cm^2.

3.5.1 Cultivation of EPC cells

The EPC cell line was acquired from the central cell culture laboratory at the NVI and derives from the European Collection of Cell Cultures (ECACC). The cells were cultured at 20 or 15°C, split 1:3 once a week, grown in a T75 cell culture flask, with Leibovitz L-15 medium containing 5% Fetal Bovine Serum (FBS), 1% Penicillin and 1% streptomycin according to the electronic manual from the NVI.

3.5.2 ASG-10 cell culturing

The ASG-10 cell line has recently been established at NVI as explained in section 1.3.3. The cells were cultured at 20 or 15°C, split 1:2 around 7-14 days, grown in a T75 cell culture flask with Leibovitz L-15 medium containing 10% FBS, 1% Penicillin and 1% streptomycin. To reduce oxidation, 30 µM β-mercaptoethanol (BME) per 100 mL medium was added.

3.6 Transfection

3.6.1 Lipid-based transfection

The kits METAFECTENE® (Biontex), K2® Transfection System (Biontex), Lipofectamine 2000 (Thermo Fisher), Lipofectamine 3000 (Thermo Fisher) are all based on the transfection method using cationic lipids as explained in section 1.4.2.

METAFECTENE® and K2® Transfection System is a part of a development series of transfection reagents from Biontex. The K2® Transfection System is an improvement of the

METAFECTENE® transfection kit. This is also the case for Lipofectamine™ 2000 and Lipofectamine™ 3000, where the latter is the latest improvement.

Positive controls: Monster Green® Fluorescent Protein phMGFP Vector and pGFP (GFP=green fluorescent protein). phMGFP has been used for most of the transfection experiments and a vector chart is presented in figure 13.

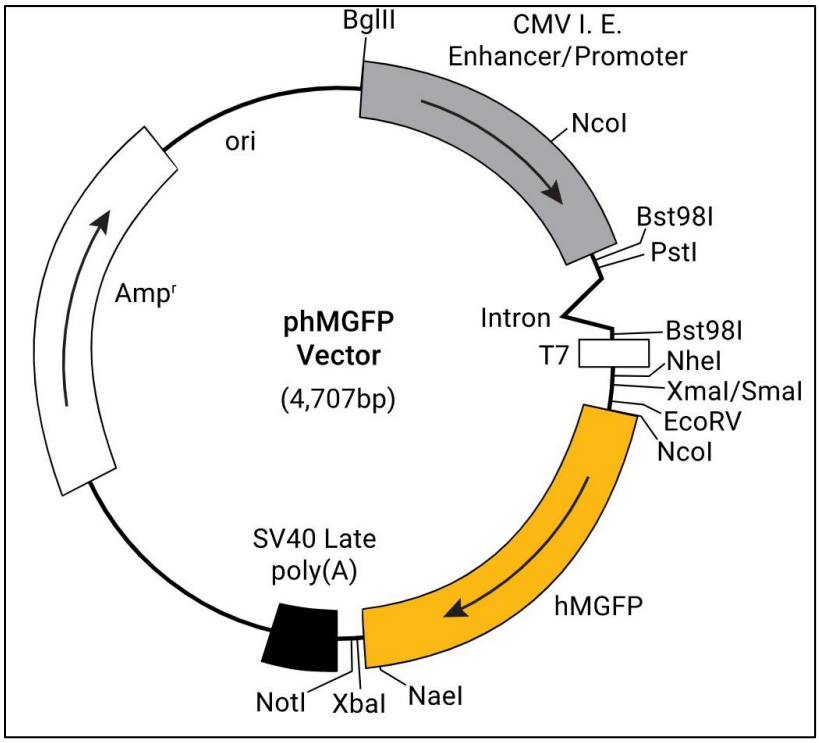

Figure 13: phMGFP vector chart (positive control)

3.6.2 mRNA transfection

For mRNA transfection (explained in section 1.4.2), the jetMESSENGER kit by Polyplus transfection® was used and the user manual was followed. A GFP-encoding mRNA intended for transfection from Oz Biosciences was used as a positive control.

3.6.3 Electroporation

Electroporation was the third tested transfection method (explained in section 1.4.2) using the Amaxa® Cell Line Optimization Nucleofector® Kit (Cat.: VCO-1001N). Cells were electroporated with the instrument Nucleofector™ 2b Device (Cat.: AAB-1001). The user manual was followed, and an optimization protocol with buffer V and different electroporation programs at the instrument were done.

3.7 Flow cytometry

Flow cytometry is a method that measures many physical characteristics of a single cell such as size, granularity and fluorescence. The cells must be in suspension, and the characteristics are measured simultaneously as one cell after the other flow through a measuring device (See Figure 14). Each cell forms a light scatter when it flows through the laser beam, and different wavelengths are detected by different photo detectors. The light signals are converted to voltages by photodetectors. Cells are normally stained with different fluorescent probes (fluorochromes), enabling detection of a variety of cellular compounds, as the fluorochromes have a known emission spectrum. (Adan et al., 2017)

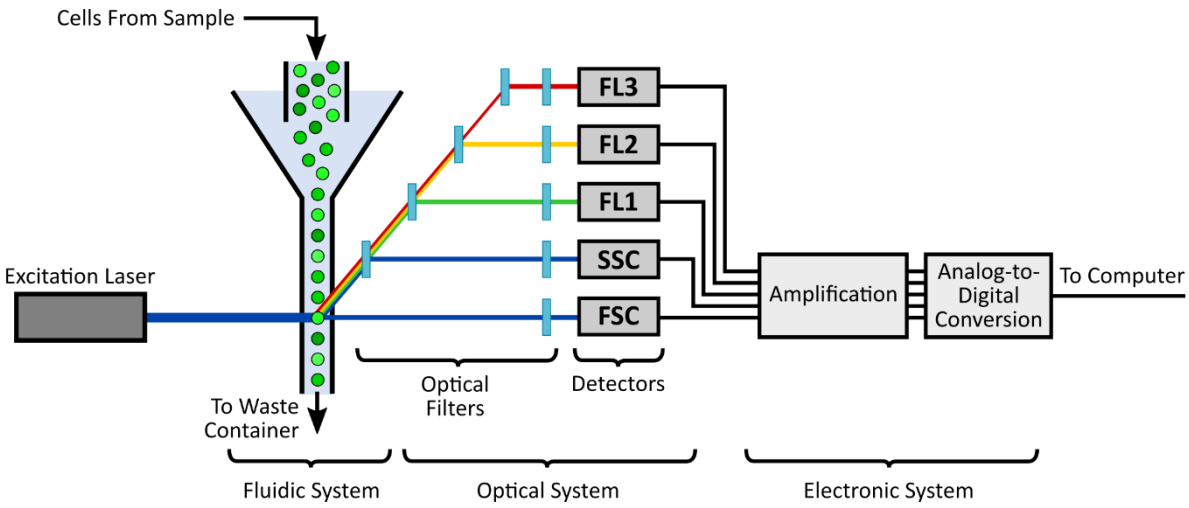

Figure 14: Illustration of the principles behind a common flow cytometer. Cells from a sample flow through a fluidic system, and one by one the pass through a laser beam. Emitted light from the cells are scattered into different directions, filtered through an optical filter, and then into a detector. The light signals are amplified and converted into digital data, that can be displayed by a computer (AAT Bioquest, 2019).

The flow cytometer used here is called Novocyte Flow Cytometer from ACEA. Flow preparation of cells from a 48 well plate is described on page iv in Appendix. The cells are stained with Propidium Iodine (PI) to enable exclusion of dead cells during flow cytometry. PI binds to double stranded DNA if cellular membranes have been damaged. The light scatter from the cells was visualized by three types of plots. Plot one excludes debris by gating the cell population, plot two excludes the population of dead cells stained with PI, and plot three displays all cells except from debris and dead cells. A gate was added to define GFP positive cells.

3.8 Immunochemical staining

Antibodies are widely used tools enabling specific targeting and labelling of extra- or intracellular antigens within cells and tissues. Antibodies can either be monoclonal in that they are identical and target only one specific part of the antigen, or polyclonal consisting of a pool of antibodies with varying specificities against many parts of the antigen(s). The antibodies used here are fluorescently labelled allowing visualization in a fluorescent microscope (Bauer, 2014).

Here, a monoclonal antibody (DYKDDDDK Tag Monoclonal Antibody (FG4R) DyLight 488, cat.: MA1-91878-D488) was used. This antibody recognizes and binds to the FLAG-tag incorporated in the protein sequence, and will hereafter be named Anti-FLAG. DyLight 488 is the name of the fluorescent label on the antibody and 488 describes the excitation wavelength in nanometers. Two different staining protocols were used, one for visualization in a fluorescent microscope, and one for visualization in a confocal microscope (details for both staining protocols are described in the appendix).

The first protocol (fluorescent microscope) used the Cytofix/Cytoperm™ kit (Cat. No. 554714) from BD to fix and permeabilize the cells. Cells were stained with anti-FLAG and 4′,6-diamidino-2-phenylindole (DAPI). DAPI excites at 405 nm. Antibody was diluted (2 µg/mL) in Perm/wash, and DAPI was added into the last was step (0,01 µg/µL).

The second protocol (confocal microscope) used 4% Paraformaldehyde (PFA) for fixation, PBS with 3 % Bovine Serum Albumin (BSA)/0,05% saponin for permeabilization/blocking, and anti-FLAG diluted (2 µg/mL) in PBS with 1 % BSA/0,05% saponin. Prior to staining, the cells were seeded on cover slips at the bottom of the culture plate well. At the end of the staining protocol, the cover slips were mounted on a microscope slide with mounting media and let dry overnight. This protocol was split into three different combinations of staining:

1. Anti-FLAG, DAPI and LysoTracker™ Deep Red (668 nm emission) (from here on named LysoTracker).
2. Anti-FLAG, DAPI and Wheat Germ Agglutinin (WGA), Alexa Fluor™ 555 conjugate, (from here on named WGA).
3. Anti-FLAG, DAPI and Alexa Fluor™ 568 Phalloidin (from here on named Phalloidin).

DAPI stains nucleic acids and is used to visualize the nucleus. LysoTracker labels acidic organelles in live cells and can permeate cell membranes. The cells were therefore stained

with this dye before the permeabilization step. WGA binds to sialic acids and *N*-acetylglucosaminyl residues and will mainly stain the ER and Golgi apparatus. Phalloidin stains actin, a part of the cell skeleton.

3.9 Microscopy

Fluorescent molecules absorb light at one wavelength, and it is emitted at another, longer wavelength. A fluorescent microscope is similar to an ordinary light microscope, except that the light source is more intense and passes through two set of filters. One filters the light before it reaches the specimen and the other filters the light obtained from the specimen. The first filter can switch between letting through specific wavelengths, and block others out. When a sample is put in a fluorescence microscope, the light passing through the first filter will excite a specific fluorescent dye. The second filter blocks out this light, and only passes the emitted wavelengths when the dye fluoresces. This light will glow against a dark background (Alberts et al., 2015). Here, Zeiss AXIO observer A1, invert fluorescence microscope was used.

A confocal microscope excludes out-of-focus light and produces optical sections. The optical details are complex, but the basic arrangement of optical components is similar to a standard fluorescent microscope. Instead, a laser is passed through a pinhole to illuminate a single point at a specific depth in the specimen. The emitted light from the specimen is collected by a detector. Another pinhole is placed in front if the detector, at a position that is confocal with the first pinhole. This means that the second pinhole is placed exactly where the emitted light from the specimen come to focus. At this point, the light converges and then enters the detector. Here, the Zeiss LSM 710, Axio Observer confocal microscope was used.

3.10 cDNA synthesis and RT-qPCR

Reverse Transcriptase quantitative PCR (RT-qPCR) can be used to measure gene expression and is widely used in diagnostics and in research. The main differences compared to traditional PCR is that the template is ssRNA, which must first be converted into complementary DNA (cDNA) though a reverse transcriptase step before the PCR is performed (as explained in section 3.3.1.2). Quantitative PCR (qPCR) includes a fluorescent reporter dye that increases in signal intensity proportional to the amount of dsDNA produced during the amplification process. The dye can be a DNA binding agent such as SYBR green, which binds to the PCR amplification product in a non-specific manner, or a sequence specific fluorescent ssDNA probe such as TaqMan probes that bind to a region between the primer binding sites during the PCR.

In the latter case, the probe is degraded more and more upon amplification, releasing fluorescent signal with an intensity proportional the amount of PCR product (Jia, 2012).

In this work, the reverse transcriptase step was done by using the QuantiTect® Reverse Transcription kit (Qiagen) and following the user manual. 2,5 ng/µL cDNA was used as template in the qPCR and SYBR green was used as reporter dye. CFX384 and CFX96 qPCR instruments (Bio-Rad) were used, and the software CFX Manager was used to examine the results.

4.0 Results

4.1 SGPV B22R reference sequences

The SGPV NOR2012 full genome sequence was published in 2015 Gjessing et al. (2015) and is the complete SGPV sequence from Norway. Recently, the poxvirus group at NVI had partially sequenced four additional genomes (Gulla et al., 2020), of which one was from wild salmon gills (SGPV NOR2009-W) . The B22R1-3 sequences from SGPV NOR2012 have here been used as main references because they are from the original published full SGPV genome. Basic information on the proteins are shown in table 3.

Table 3: Overview of the three B22R sequences from SGPV NOR2012 and SGPV NOR2009-W used as reference.

B22R reference sequences			
Isolate/accession number	***Protein***	***Nucleotide length (nt)***	***Protein Length (aa)***
SGPV NOR2012/ YP_009162526.1	AL387_gp154 (B22R1)	6681	2226
SGPV NOR2012/ YP_009162531.1	AL387_gp159 (B22R2)	3015	1004
SGPV NOR2012/ YP_009162534.1	AL387_gp162 (B22R3)	3906	1301
SGPV NOR2009-W	AL387_gp154 (B22R1)	6681	2226
SGPV NOR2009-W	AL387_gp159 (B22R2)	3015	1004
SGPV NOR2009-W	AL387_gp162 (B22R3)	3909	1302

4.2 *In silico* characterization of SGPV B22R proteins

Predictions regarding different properties of the SGPV NOR2012 B22R1-3 proteins were performed using online databases and software programs. These types of *in silico* studies can

provide valuable information prior to performing functional studies in the laboratory. All proteins contain a predicted signal peptide sequence, indicating that the proteins are translated into the Endoplasmic Reticulum (ER). The proteins also have several predicted N-glycosylated sites (see Figure 15) that further indicates ER involvement. Furthermore, all three proteins are predicted to contain several transmembrane regions (see Figure 15), supported also by the profiles observed in hydrophobicity plots (Appendix pg. xxii). The results are summarized in Table 4. Altogether, these results indicate that all three proteins function as transmembrane glycoproteins. Secondary structure predictions of the B22R1-3 proteins was also performed (see pg. xvii-xxi in appendix), and the SGPV NOR2009-W and SGPV NOR2012 sequences show some structural differences. A B22R protein motif was found for all three proteins as shown in Figure 15. A BLAST search for the B22R1-3 proteins found hits that roughly cover the region of the B22R family motif, indicating that the BLAST hit regions are conserved (see table 5). B22R3-NOR2009 was predicted to contain a dileucine (LL) in the C-terminal end of the protein. Dileucine motifs are known to act as signals for endocytosis and/or post endocytic sorting of various membrane proteins (Awwad et al., 2010). The identities between the three B22R proteins from SGPV NOR2012 was between 19-26% while the protein similarity was between 31-37%.

The predictions show that all proteins have a low probability of localizing to the cell nucleus, but the B22R1 protein does have a predicted Nuclear Localization Signal (NLS). The protein was though not detected in the nucleus during microscopy in this study. Because of the predicted NLS, further investigations were done with nuclear export signals (NES), but the B22R1 did not contain NES. The B22R proteins are not expected to have any nuclear functions.

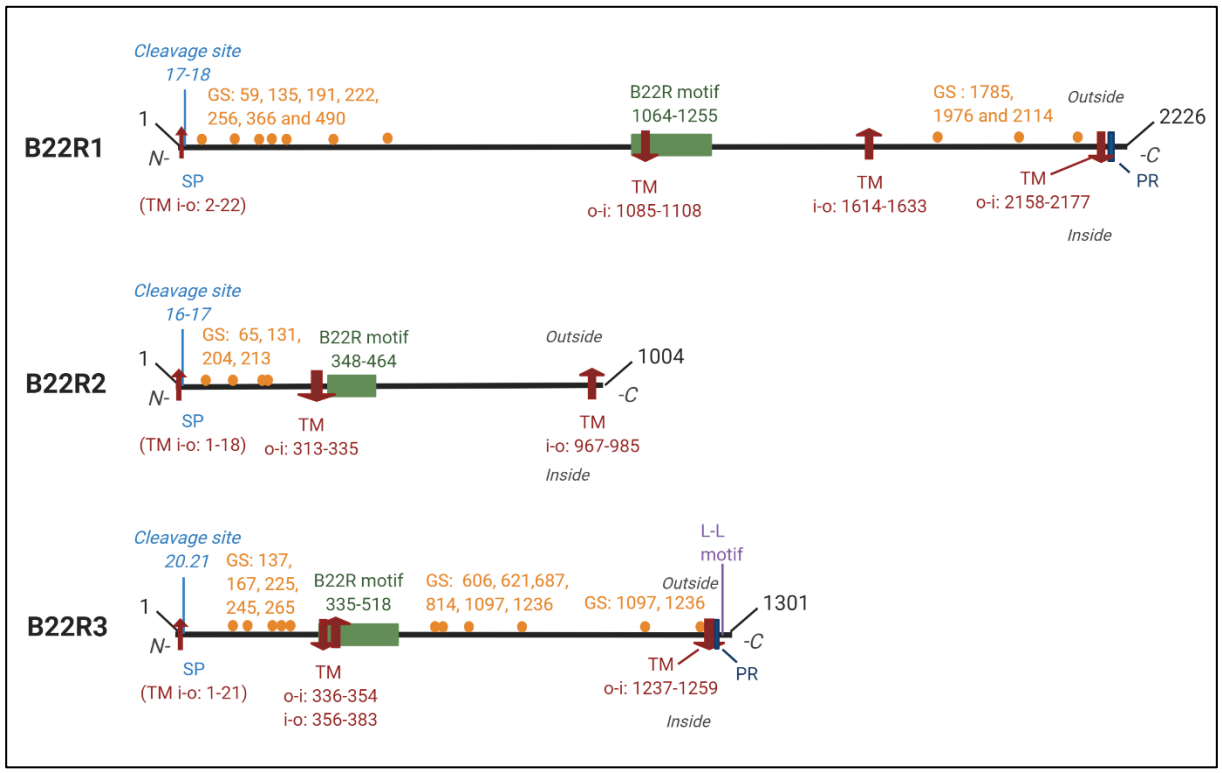

Fig. 15: Overview of the three paralogous proteins in the SGPV NOR2012 genome, homologous to the B22R protein from the variola virus. The sequence information provided here, is based on predictions from several databases. The numbers indicate amino acid positions in the sequence. Outside is at the cell exterior and inside is in the cytoplasm. SP: Signal peptide, TM: transmembrane regions (going in or out of the plasma membrane, indicated with arrows), GS: glycosylation site. PR: Polybasic region. Created with Biorender.com

Table 4: Several sequence predictions of the SGPV NOR2012 B22R 1-3 proteins.

Reference sequence predictions				
Protein	*NLS mapper*	*Cytoplasmic/nuclear*	*N-terminal*	*Dileucine in tail*
B22R1-NOR2012	Yes: PFRNKKMCLV	70,6 % cytoplasmic	inside	none
B22R2-NOR2012	none	89 % cytoplasmic	inside	none
B22R3-NOR2012	none	89% cytoplasmic	inside	at 1277 aa
Protein	*Signal sequence*	*MW (kDa)*	*Myristolator*	
B22R1-NOR2012	Yes. Cleavage site: 17-18 aa	251,1	none	
B22R2-NOR2012	Yes. Cleavage site: 16-17 aa	113,7	none	
B22R3-NOR2012	Yes. Cleavage site: 20-21aa	146,0	none	

Table 5: Basic Local Alignment Search Tool (BLAST) searches from the database of the National Center for Biotechnology Information (NCBI) for the SGPV NOR2012 B22R 1-3 proteins. The coverage ranges from 17-49%, and identity ranges from 25-29%. B22R2 only got one hit.

Top hits following BLAST search of B22R1-NOR2012 (Accession number: YP_009162526.1)				
Accession number	Description	Identity	Coverage	Coverage localization (aa)
QIM55319.1	membrane protein [Cyprinid herpesvirus 2]	29 %	44 %	1039-2022
ADZ29521.1	7-transmembrane-G-protein-coupled-receptor-like protein [Cowpox virus]	25 %	41 %	1024-1942
AXY04803.1	variola B22R family protein [Fowlpox virus]	25 %	49 %	834-1942
Top hits following BLAST search for B22R2-NOR2012 (Accession number: YP_009162531.1)				
Accession number	Description	Identity	Coverage	Coverage localization (aa)
YP_009362347.1	hypothetical protein [Ranid herpesvirus 3]	25 %	17 %	442-620
Top hits following BLAST search for B22R3-NOR2012 (Accession number: YP_009162534.1)				
Accession number	Description	Identity	Coverage	Coverage localization (aa)
YP_784230.1	B22R-like protein [Nile crocodilepox virus]	25 %	30 %	284-676
YP_009281948.1	surface glycoprotein [Volepox virus]	28 %	27 %	335-686
AYO89701.1	variola B22R family protein [Fowlpox virus]	28 %	26 %	336-682

4.2 SGPV B22R PCR and cloning

The isolates SGPV NOR2019 and SGPV NOR2009-W was selected to be investigated in this thesis. SGPV NOR2019 is associated with severe gill disease and mortalities from a disease outbreak in farmed salmon in Nordland and has been used to recreate SGPVD experimentally (Thoen et al., 2020). SGPV NOR2009-W is a virus sequenced from wild salmon gills (Gulla et al., 2020) and is associated with a moderate gill pathology with other agents present. These isolates were selected because of their potential difference in virulence. DNA was isolated from gills containing these viruses, and concentration measured to prepare for amplification of B22R gene sequences (see Table 6). SGPV NOR2009-W and SGPV NOR2019 has an identity and similarity between 98-99%.

Table 6: The two SGPV isolates used for the B22R cloning and DNA concentration of their corresponding gill sample

*Isolate	Full name	Gill DNA-concentration measured by Qubit (ng/µL)
SGPV NOR2009-W	2016-60-F377 L1	21,8
SGPV NOR2019	2019-05-287/F2	25,0

*SGPV NOR2009-W is a virus sequenced from wild salmon gills (Gulla et al., 2020), and SGPV NOR2019 origins from a disease outbreak in farmed salmon in Nordland and has been used to recreate SGPVD experimentally (Thoen et al., 2020)

4.2.1 Cloning preparation

In CLC Main Workbench, the different SGPV isolate sequences were used to design primers to amplify B22R genes for the In-fusion cloning. Using CLC Main Workbench, several primers were found with properties that met the primer requirements from the In-Fusion cloning protocol. The primers included both a 18-25 base long sequence complementary to the B22R gene end regions and a 15 base long sequence complementary to the vector. The primers were optimized for an annealing temperature of 60°C. The downstream primer in the primer pair also included a FLAG-tag encoding sequence as illustrated in figure 9. For B22R3, an additional construct was made expressing the FLAG tag fused to the N-terminal of the encoded protein. Here, the upstream primer contained the FLAG-tag encoding sequence. The primers are listed in table 7. The amplified and flag-tagged sequences B22R1, 2, 3-C and 3-N from the isolates NOR2009-W and NOR2019 were then cloned into the vector pcDNA3.1.

Table 7: Primers used to PCR amplify eight different B22R sequences for cloning.

Primers			
Name	Target	Flag location	Sequence (5'-3')
B22R1 F	Gene	C-terminal	GTTTAAACTTAAGCTATGTTGAGTTATTACATTTTCGT
B22R1 R	Gene	C-terminal	GCTCGGTACCAAGCTCTACTTATCGTCGTCATCTTTGTAGTCCACT CTTGTCACAGGGA
B22R2 F	Gene	C-terminal	GTTTAAACTTAAGCTATGCTGACTCTTATCTTTCTCCTG
B22R2 R	Gene	C-terminal	GCTCGGTACCAAGCTTCACTTATCGTCGTCATCTTTGTAGTCGGAG GAAGGGTCAGTG
B22R2 R-Nor2009	Gene	C-terminal	GCTCGGTACCAAGCTTCACTTATCGTCGTCATCTTTGTAGTCGGAG GAAGGTTTAGTG
B22R3-C F	Gene	C-terminal	GTTTAAACTTAAGCTATGGGAAAGTCAGTGTTCTTCA
B22R3-C R	Gene	C-terminal	GCTCGGTACCAAGCTTCACTTATCGTCGTCATCTTTGTAGTCTACA GTTACCATACTTTTGTTACCT
B22R3-N F	Gene	N-terminal	GTTTAAACTTAAGCTATGGACTACAAAGATGACGACGATAAGGGA AAGTCAGTGTTCTTCA
B22R3-N R	Gene	N-terminal	GCTCGGTACCAAGCTTCATACAGTTACCATACTTTTGTTACCT

Flag
Gene
Vector

4.2.1 Vector linearization

Figure 16 shows the difference between uncut and cut pcDNA vector. The pcDNA vector appeared completely linearized since only one band was visible with a migration length between the relaxed and supercoiled uncut plasmid. The length corresponded to approximately 6000 bp according to the ladder. The linearized vector was stored at -20 °C for later use.

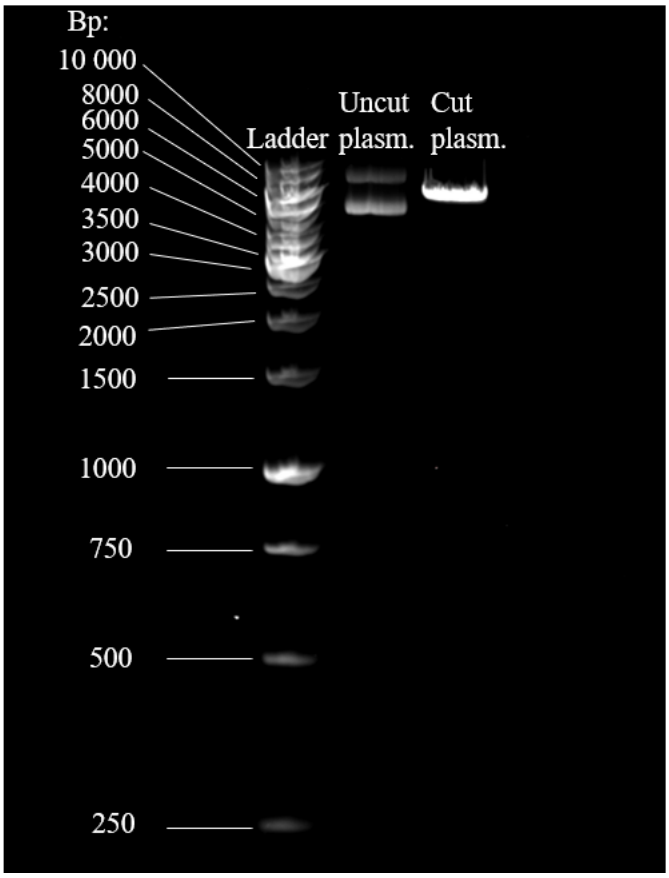

Figure 16: Gel image showing bands representing uncut and cut plasmid. Molecular weight standard is the GeneRuler 1 kb ladder.

4.2.2 Amplification of B22R sequences

B22R genes from gills infected with the SGPV isolate NOR2009-W were PCR amplified using the Phusion High-fidelity PCR master mix from Invitrogen (Thermo Fisher). As the primers were optimized for 60°C, the annealing temperature was set to accommodate for this. A negative control sample was also included with each B22R gene amplification run. The negative control originated from a gill sample from salmon that was poxvirus negative. A gel electrophoresis was performed to examine the PCR results. This first PCR setup only gave products for B22R3-N-flag. Therefore, the next day the PCR was instead done with the protocol and reagents from ClonTech (TaKaRa), with the premix called CloneAmp^{TM} HiFi PCR Premix (see table 2 in appendix). Here, the annealing temperature was lowered to 57°C to increase hybridization between primer and template. The setup contained both NOR2009-W and NOR2019. This was done to eliminate the possibility that sequence differences in NOR2009-W was the reason for the negative results obtained from the first PCR setup. Two negative controls for B22R3-C-FLAG and B22R3-N-FLAG were also added because of the results from the first setup. This time, all the PCR reactions gave bands of correct sizes on the gel, except

from B22R1 were no visible bands could be observed. The negative controls produced some unspecific background amplification products.

There were some challenges with the cloning of the genes B22R1-19, B22R2-19, B22R2-NOR2009-W and B22R1-NOR2009-W. These genes were attempted amplified by PCR and went through the cloning procedure more than once. One challenge was the primers for the gene B22R1. When running the first HiFi PCR protocol, there was no band on the gel for the B22R1 gene. The gene B22R1 from NOR2019 was set up in a new PCR to be run at new conditions in an attempt to increase primer and template hybridization and to include more time to copy the whole gene. Therefore, the annealing temperature was changed from 57°C to 55°C and the annealing time from 15 to 20 seconds because of the long gene target. Also, the elongation step was extended from 1 to 2 minutes. This time the PCR of B22R1-19 was successful. There was still problems amplifying the gene sequence of B22R1-NOR2009-W. New primers were tested for B22R1, and this time the amplification of B22R1-NOR2009-W was successful. An extra base was added to each primer so they may bind stronger to the template. A weak presence of the primers and a weak bond of amplified DNA was observed on the gel, so the modification of the primers did not seem to help much. On the other hand, it worked having freshly prepared primer solutions.

It was challenging to amplify the gene sequence B22R2-NOR2009-W. The gene B22R2 gave a weak band of the correct length, but also another unspecific shorter band. It was attempted to extract the correct band from the gel, but after a new PCR run and gel electrophoresis only an unspecific band was seen. It was discovered later that the B22R2 reverse primer sequence was not 100 % identical to the target sequence in the NOR2009-W sample. This may explain why it was problematic to get sufficient amplification product of this gene. New primers with 100% sequence identities to this isolate were ordered, and the HiFi-PCR went well.

The length of each PCR product should be about the same length of each gene: B22R1; 6681 bp, B22R2; 3015 bp and B22R3; 3906 bp. Figure 17 shows that each PCR product had the expected length. The ladder was smeared, (When running gel electrophoresis, it was noticed that the stated amount of ladder to be added to the gel (5 µL) from the protocol, resulted in a “smear” on the gel. This occurred in some of the following results. Later, 2 µL was used instead). but it was still possible to figure out the right lengths.

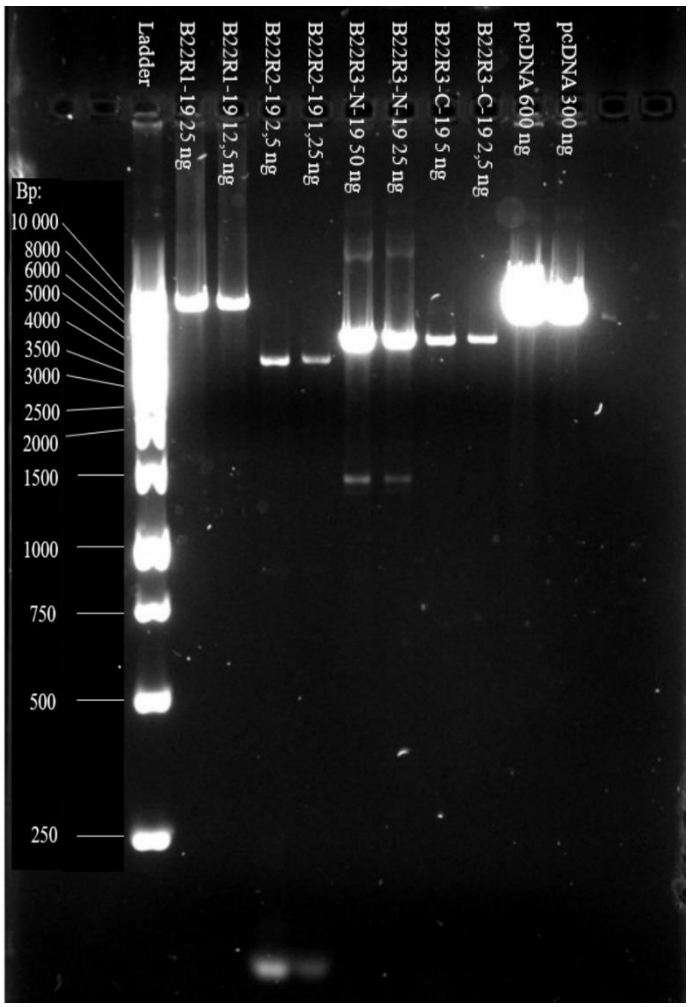

Figure 17: Dilution of PCR products and vector to be able to calculate the amounts to be used in the In-Fusion cloning reaction. The ladder is smeared (5µL ladder was too much), and it is not possible to distinguish between the different lengths (lengths are placed approximately). It was still possible to see that the bands had the right lengths. B22R1 travelled slow because of the large size. The pcDNA3.1 (5427 bp) travelled a bit longer compared to B22R1 as expected but was smeared because of too much amounts of plasmid were added on the gel. B22R2, the shortest gene, travelled farthest and B22R3 is observed right behind.

4.2.3 Cloning of B22R genes and transformation

The first cloning setup in this experiment was with the genes B22R1-2019, B22R3-N-2019, and a positive and negative control from the cloning kit. The cell suspensions were diluted with SOC-medium and plated out at four different dilutions (2:10, 4:10, 6:10 and 8:10). The pelleted cells from the remainder of the transformation reaction was plated out on a fifth plate (1:1). The negative control was only plated out on one plate (1:1). There were colonies on every plate, also a few on the negative control plate. The dilutions 4:10 and 6:10 were most suitable for the genes B22R1-2019 and B22R3-N-2019, and for the positive control the dilution 2:10 which had a lot of growth. These three dilutions were generally used for the rest of the cloning

performed in this work. Concentration of B22R1-NOR2009-W after amplification was low. Therefore, the concentration for this cell suspension was raised to 6:10, 8:10 and 10:10.

4.2.4 Cloning confirmation

To identify successful insertion into the vector, a colony-PCR were performed, and the results were examined on a gel. B22R1-NOR2019 and B22R3-NOR2019 was included in the first cloning experiment and almost all the PCR products were of the expected size when being compared to the ladder (see Figure 18). A forward primer specific for B22R1 and a reverse primer specific for the vector was used for the B22R1-NOR2019 clones. The colony-PCR would only give products is the insert was present. The band size for B22R3-NOR2019 should be about 3900 bp. The bands were smeared, but the size was possible to interpret. Three colonies of each clone with the correct size on the gel were selected and purified with a miniprep kit. After purification, each sample was analyzed using Nanodrop for measuring DNA concentration. The samples were then stored at -20 until first step sequencing analysis.

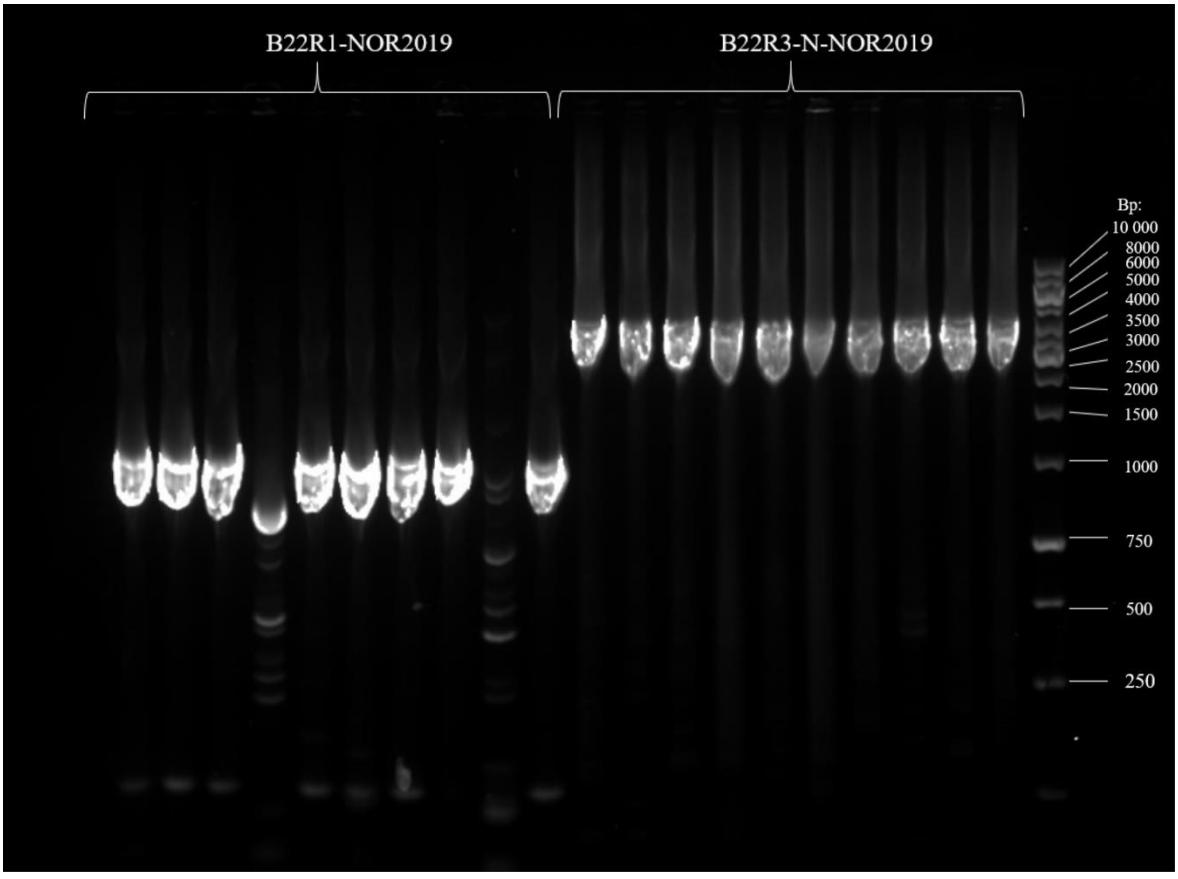

Figure 18: A gel showin the result from colony-PCR on B22R1- NOR2019 and B22R3-N-FLAG-NOR2019.

In the In-Fusion cloning kit, the user can choose between two different methods to prepare the fragments for insertion. Either by cloning enhancer treatment or by spin-column purification. It

was decided to give the cloning enhancer treatment a try. This method worked well for the genes B22R1-NOR2019, B22R3-N-FLAG-NOR2019, B22R3-C-FLAG-NOR2019, B22R3-N-FLAG-NOR2009-W and B22R3-C-FLAG-NOR2009-W. However, for the genes B22R2-NOR2019, B22R2-NOR2009-W and B22R1-NOR2009-W, it might not have been the best solution because the In-Fusion protocol recommends doing cloning enhancement only with abundant PCR products. The colony PCR showed that for B22R2-NOR2019 and B22R2-NOR2009-W, the fragments inserted were very short. When a spin-column purification of these genes was done instead of a cloning enhancer treatment, the cloning worked well.

After performing the HiFi PCR protocol for B22R1-NOR2009-W, the PCR product showed a weak band with the correct size on the gel. A spin-column purification was done with this amplified gene. Because of the weak bands on the gel, there were also a low number of fragments in the purified product. When doing a new transformation, there were more colonies on the plates than before, but still relatively few. Colony-PCR had to be done on up to 30 colonies to find two having the correct insert.

4.2.5 Sequence confirmation

The three colonies from each clone were sequenced by Sanger sequencing at the sequencing facility at NVI. The most important confirmation in the first step of sequencing was to confirm that the B22R genes had been inserted correctly into the vector, that the start codon, the FLAG-tag and the stop codon was intact. The primers used in the first sequencing step were the T7 Promoter primer and the BGH polyadenylation sequence primer which were the same primers used in the colony-PCR described earlier. These primers are used for sequencing parts of the vector, and the start and the end of the gene inserts. The sequencing data were analyzed using CLC Main Workbench. The cloned sequences were aligned with existing sequence files that were used as reference sequences (see section 4.1). Those inserts that were successfully sequenced and had intact start codons, FLAG-tags and stop codons were selected onto the next sequencing step. Only one cultured colony from each B22R construct were chosen. A midiprep was performed to get a high yield of plasmids (see Table 8).

Table 8: Concentrations of each construct after midiprep was measured using NanoDrop.

Gene	NOR2009-W (µg/µL)	NOR2019 (µg/µL)
B22R1	1,94	1,67
B22R2	1,87	1,60
B22R3C	1,20	1,37
B22R3N	0,36	1,63

The midiprep prepared plasmids were again sequenced by Sanger sequencing at the sequencing facility at NVI, but now with primers that covered the entire gene (see Table 9). The sequences were assembled and aligned to the reference sequences as before. The reference sequences (SGPV NOR2012) used for the cloned SGPV NOR2019 sequences were not from the same outbreaks, and some nucleotide differences were detected. The cloned sequences from the isolate SGPV NOR2009-W were supposed to be identical to existing sequence data for this isolate. However, some differences in the sequences was observed, and will be discussed later. Some B22R sequences got better coverage than others, and some sequencing reactions had more background noise than others. Many initially apparent ambiguous nucleotides could be called correctly following detailed analyses of the chromatograms obtained from the sequencing in CLC Main Workbench. Some nucleotides were though challenging or even impossible to call, as shown in figure 19. B22R3 NOR2019-N-FLAG had an additional lysine as shown in figure 19. A consensus sequence was extracted from each of the sequenced genes. Some of the contigs from the Sanger Sequencing of B22R2-19 and B22R2-W were of poor quality and without full coverage. It was not possible to finish the sequencing of these constructs because of reduced operations at NVI during the COVID-19 pandemic. A complete consensus sequence was therefore not obtained for these genes; B22R2-19 is missing coverage between positions 2099-2280 and B22R2-W between 2084-2278 (numbering relative to ATG start codon).

Table 9: Primers used to obtain the complete gene sequence of each B22R gene from Sanger Sequencing.

Gene	Binding localization (bp)	Primer sequence
B22R1	942	FP: 5'- GAGACCATACGCAACAGATC -3'
B22R1	1922	RP: 5'- ACTTGTCTGCTCCTGTGAA -3'
B22R1	1810	FP: 5'- TTCTCAGATGATGACATGTTCAC -3'
B22R1	2815	RP: 5'- ACATACAGCGGATCTCTTCA -3'
B22R1	2785	FP: 5'- CCAGGATGTAAAGGAGGAGC -3'
B22R1	3752	RP: 5'- GGAGATGCTAGGATACATGGA -3'
B22R1	3671	FP: 5'- TCAGGTCCAATCAGGTCAC -3'
B22R1	4559	RP: 5'- AATAGTCTGTCGTTTCCGATGA -3'
B22R2	1330	FP: 5'- GACCATCATCTTCGGACACA -3'
B22R2	750	RP: 5'- CGTCGTGAGCTGATTGG -3'
B22R2	2231	FP: 5'- CCCACTCACGTTTCAATTCA -3'
B22R2	2696	FP: 5'- CGGTGGATTTGTTTGATGTGT -3'
B22R2	1490	RP: 5'- TGTTTCAGGGGGTGTTCG -3'
B22R3	1129	FP: 5'- ACAGCCATCACTCTCTTTGA -3'
B22R3	635	RP: 5'- AAATCTGGGTGTGCTACC -3'
B22R3	1914	FP: 5'- GAATGACCCAGACACCTG -3'
B22R3	1280	RP: 5'- TGAATATGAGTGTTGTCGTC -3'
B22R3	2490	FP: 5'- CTCACTGACGTTCGAATTT -3'
B22R3	3525	FP: 5'- GCAAATGGCACTGAAGCAA -3'
B22R3	3707	RP: 5'- ACGTTGTAAGCCATTAGC -3'

When analyzing the sequences in CLC Main Workbench, several observations were made.

Other important remarks were noticed when the gene sequences were transcribed to protein sequences. B22R1-NOR2019 had a stop codon at position 3295 in the DNA sequence, meaning that only half of the protein will be translated since the synthesis will stop at this point in the sequence. The presence of the stop codon was covered with two sanger sequences. Surprisingly, originating from the same isolate, B22R3-C-FLAG NOR2009-W and B22R3-N-FLAG NOR209-W had different sequences. B22R3-N-FLAG NOR2009-W also had a stop codon at position 2674 that was covered with two sanger sequences.

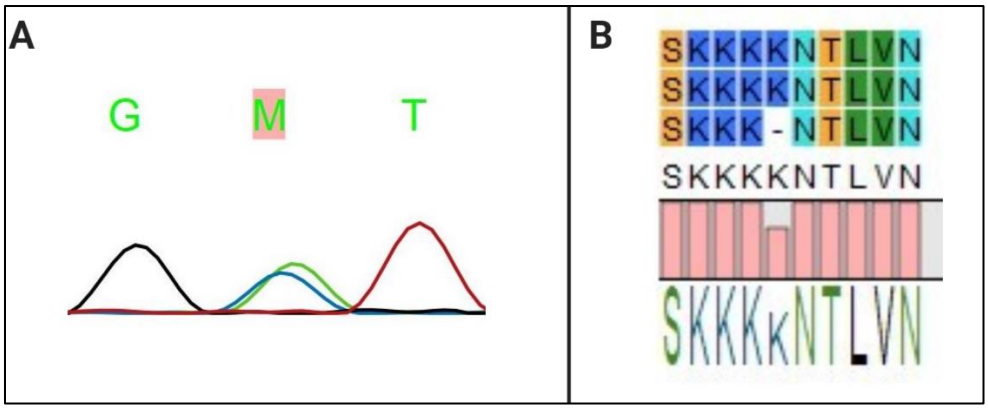

Figure 19: Screenshots from CLC Main Workbench showing two different examples of observations. **1:** There are two peaks of almost identical size and shape, blue (cytosine), and green (adenine) at the same position. From cloned NOR2009-W aligned with the reference sequence NOR2009-W of B22R2. **2:** Showing the two constructs B22R3 NOR2019-C-FLAG and B22R3 NOR2019-N-FLAG having an extra Lysine (K) compared to the reference sequence B22R3-NOR2012.

4.3 SGPV B22R and GFP mRNA production

In addition to producing plasmids for B22R expression it was also desirable to test transfection and expression from mRNA produced by *in vitro* transcription. The constructs from isolate NOR2019 and phMGFP were used in the transcription procedure. According to the mMESSAGE mMACHINE® T7 Ultra Kit (Life Technologies), the vector must be linearized before transcription. As shown in Figure 20, the linearized vectors produced the expected sizes except the one with the B22R1 gene that produced a size being too small. Non-cut vectors were also included, but it did not seem like they migrated through the gel.

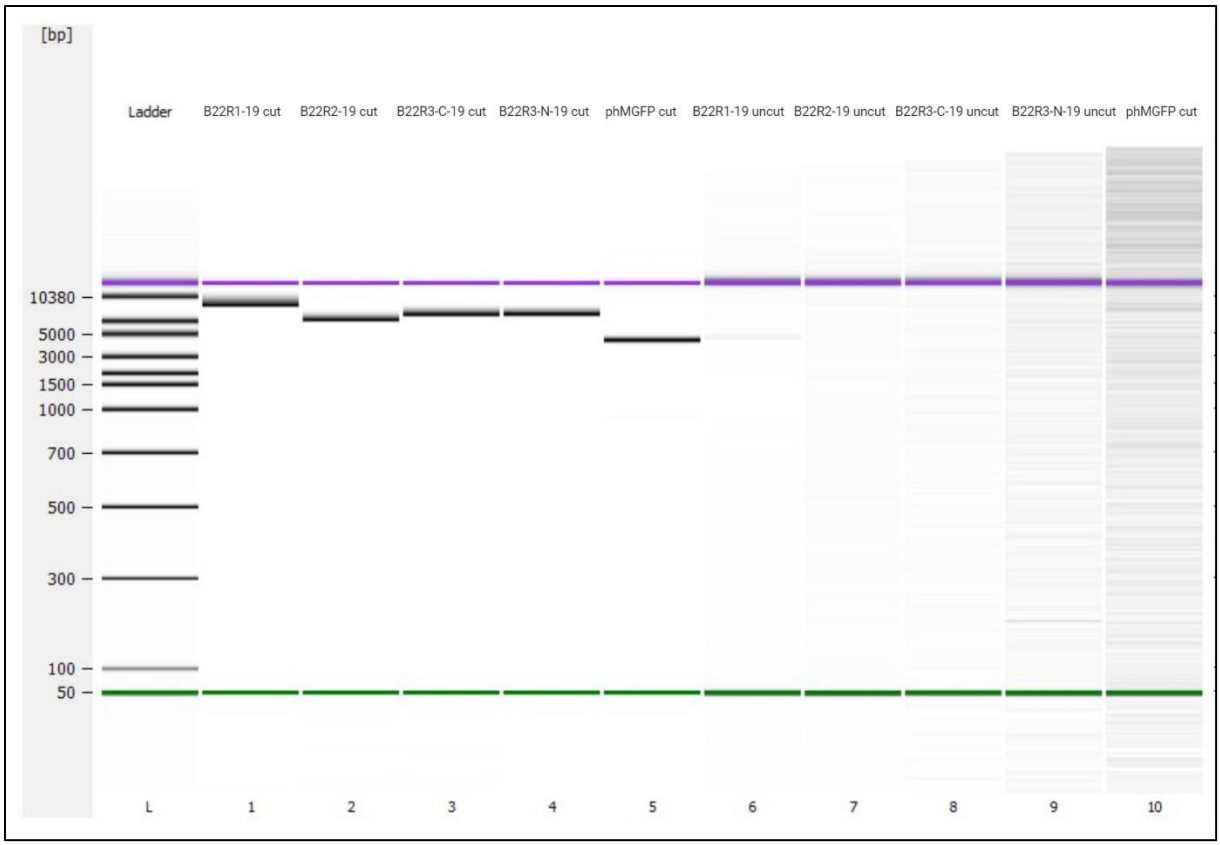

Figure 20: Linearization of vector constructs from isolate SGPV NOR2019 and phMGFP using Bioanalyser 2100. Uncut vectors were also included but do not seem to have migrated through the gel.

The products resulting from the mRNA transcription show that there might be some degradation of the B22R1-19 construct (other attempts showed two bands at the gel, but this is not shown here), and these transcripts were shorter than expected (see Figure 21). At the same time, the molecular weight ladder did not contain the expected upper, largest band. Several attempts were made with the *in vitro* transcription and bioanalyzer run, but the products were either seen as a smear, weak or not of the expected size.

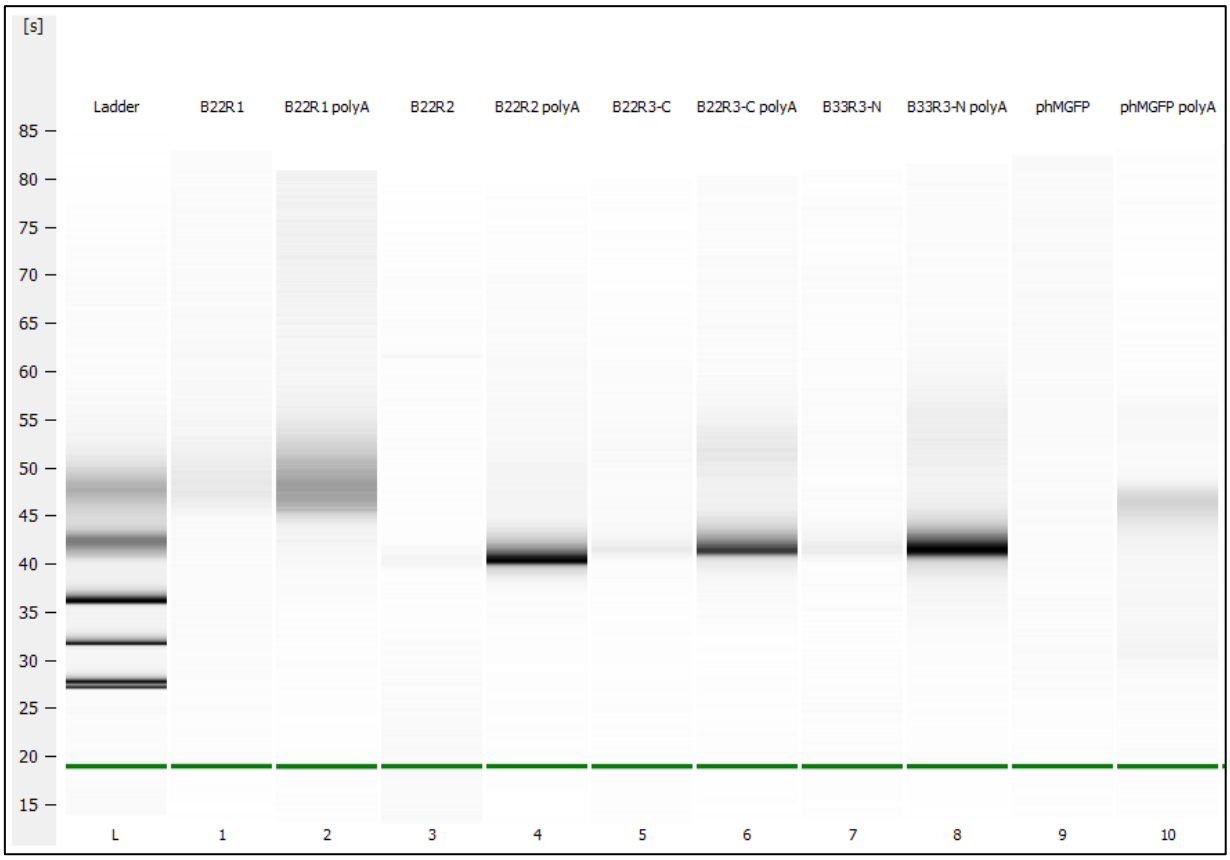

Fig. 21: Results from the *in vitro* mRNA transcription of constructs from the NOR2019 isolate and phMGFP. Expected approximate sizes of the mRNA strands before adding polyA: B22R1: 6700 bases, B22R2: 3000 bases, B22R3: 3900 bases.

4.4 Transfection optimization of EPC and ASG-10 cells

It is desirable to study the three different B22R proteins when expressed inside the host cell to obtain information on their putative functional properties. A way to do this is to transfect a cell line with a plasmid containing the gene encoding the protein of interest. The experiments should be performed as close to *in vivo* conditions as possible for most accurate results. Different cell lines have different characteristics and may hence respond differently to transfection. It is therefore necessary to find the optimal transfection procedure for each cell line. The most attractive cell line for transfection in this work is the ASG-10 cell line as it represents the target cell type and species for SGPV. Therefore, these cells were chosen as the priority cell line in the present work. However, these cells have never been transfected before, and to ensure a successful transfection procedure, the EPC cell line was also included. The EPC cell line is well known, has been used in many research projects and are known to be easy to transfect.

4.4.1 Transfection optimization of EPC cells

4.4.1.1 K2 and METAFECTENE transfection optimization

The first transfection test was performed in EPC cells with the MGFP vector and two transfection kits called K2 and METAFECTENE, both based on the lipid-based transfection technology described in chapter 3.6.1. On the first day the cells were seeded on a 48 well culture plate in two different concentrations: 150 000 cells/cm^2 and 250 000 cells/cm^2 (see table 4 in appendix for plate setup). The cells were transfected on the second day. The cells were incubated at 20°C during the whole process. On the third day the medium was replaced, and the cells were examined in a fluorescence microscope. All wells contained transfected cells one day after the transfection. The cells transfected with K2 had more transfected cells compared to METAFECTENE. Flow cytometry analyses was performed on the samples, and those showing highest transfection efficiency are shown in figure 22. The run did not include a negative control, and the sample showing a smaller number of transfected cells (METAFECTENE transfected with pGFP) was used as a "negative control" and the gate settings in the whole run was based on this sample. See table x in appendix showing % transfected cells in all wells.

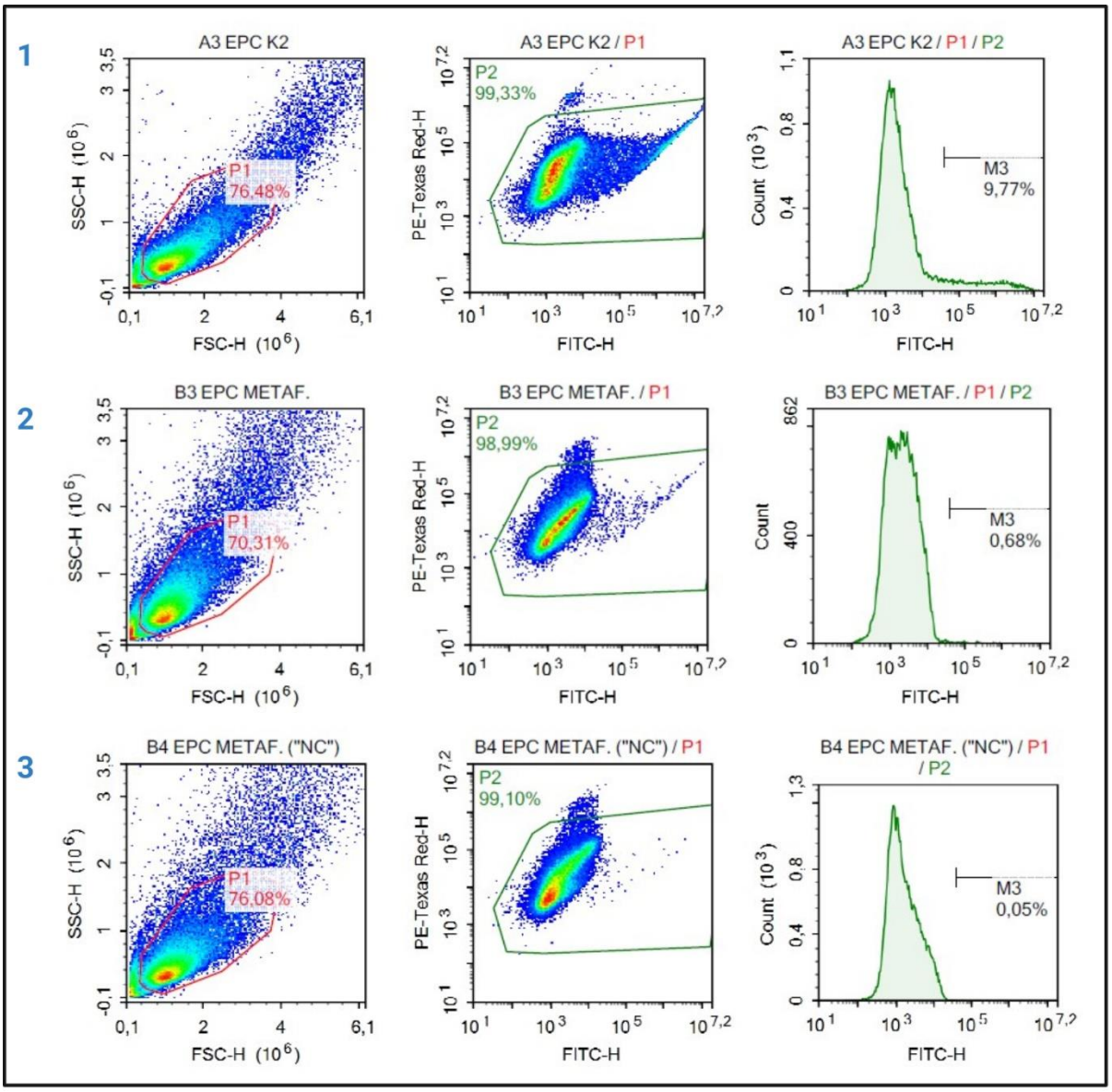

Figure 22: Flow Cytometry results from transfection optimization of EPC cells using the K2 and METAFECTENE transfection kits. **1**: K2 Transfection system, 0,3 µg phMGFP, 250 000 cells/cm^2. **2**: METAFECTENE, 0,2 µL phMGFP, 250 000 cells/cm^2. **3**: METAFECTENE, 0,2 µL pGFP, 250 000 cells/cm^2, used as negative reference.

The second transfection test was performed with the eight different B22R constructs from the two SGPV isolates using the K2 transfection kit and MGFP as positive control. The cells were seeded with 250 000 cells/cm^2 and transfected the day after. The cells were incubated at 20°C during the whole process. On the third day, the medium was changed and in wells where construct had been added the cells were fixed and stained with an anti-FLAG (DyLight 488) antibody overnight. The cells, after washing with buffer, were examined in a fluorescence microscope. Some background staining could be observed, but it was still possible to distinguish between non-transfected and transfected cells, although some cells were a bit hard

to confirm as transfected. Cells transfected with B22R2-19 showed some prominently transfected cells as shown in figure 23. Transfected cells were not observed for every construct.

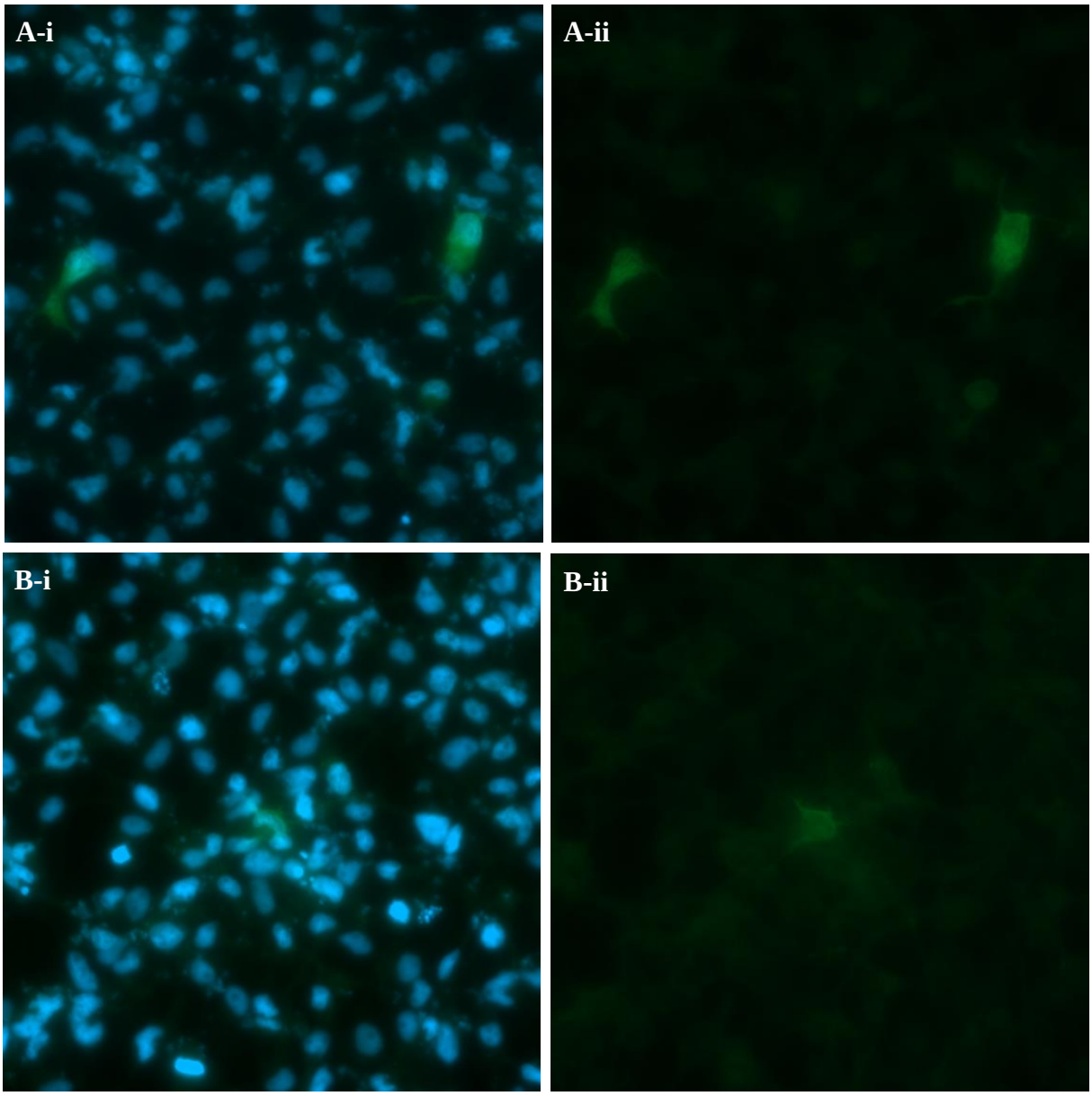

Fig. 23: Fluorescence microscopy of EPC cells transfected with K2® Transfection System stained with anti-FALG DyLight 488 (green), nuclear staining with DAPI (blue). **A**: B22R2 construct, **B**: B22R3-C construct. Both genes from the NOR2019 isolate.

4.4.1.2 K2, Lipofectamine 2000 and Lipofectamine 3000 optimization

The third transfection optimization of EPC cells was performed in a 96 well plate with three different transfection kits to determine which one would give best results. Different cell densities and amount of transfection reagents was varied while the DNA amount was held constant. Two different cell culture media, L-15 and Opti-MEM, were tested in the transfection

mixture. For both media, the cells were incubated at 20°C during the whole experiment. Only the K2® transfection system protocol recommended replacement of the growth medium 6-24 hours after transfection, but the medium for cells transfected with Lipofectamine 2000 and 3000 was also changed after 6-24 hours. The transfected cells were examined one, two and three days after performing the transfection procedure. A substantial increase in fluorescence was detected from day to day (se fig. 24 and 25). The K2® transfection system had most visibly transfected cells after three days with 0,6 µL transfection reagent. The Lipofectamine™ 3000 had the most visibly transfected cells after three days using L-15 and 0,5 µL transfection reagent.

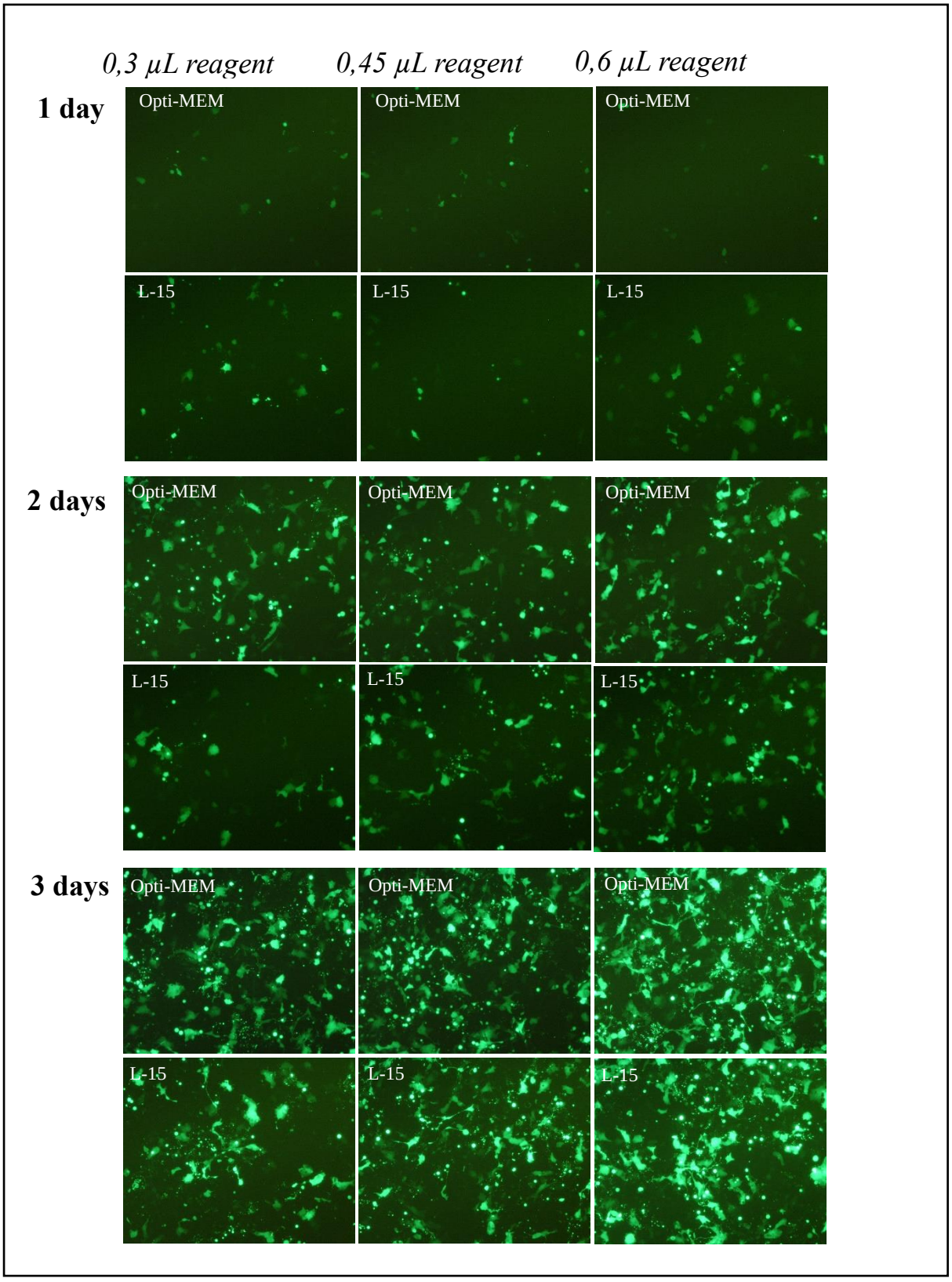

Figure 24: Fluorescence microscopy showing transfection optimization of EPC cells with the K2® Transfection System and MGFP plasmid. All photos taken with 10x magnification.

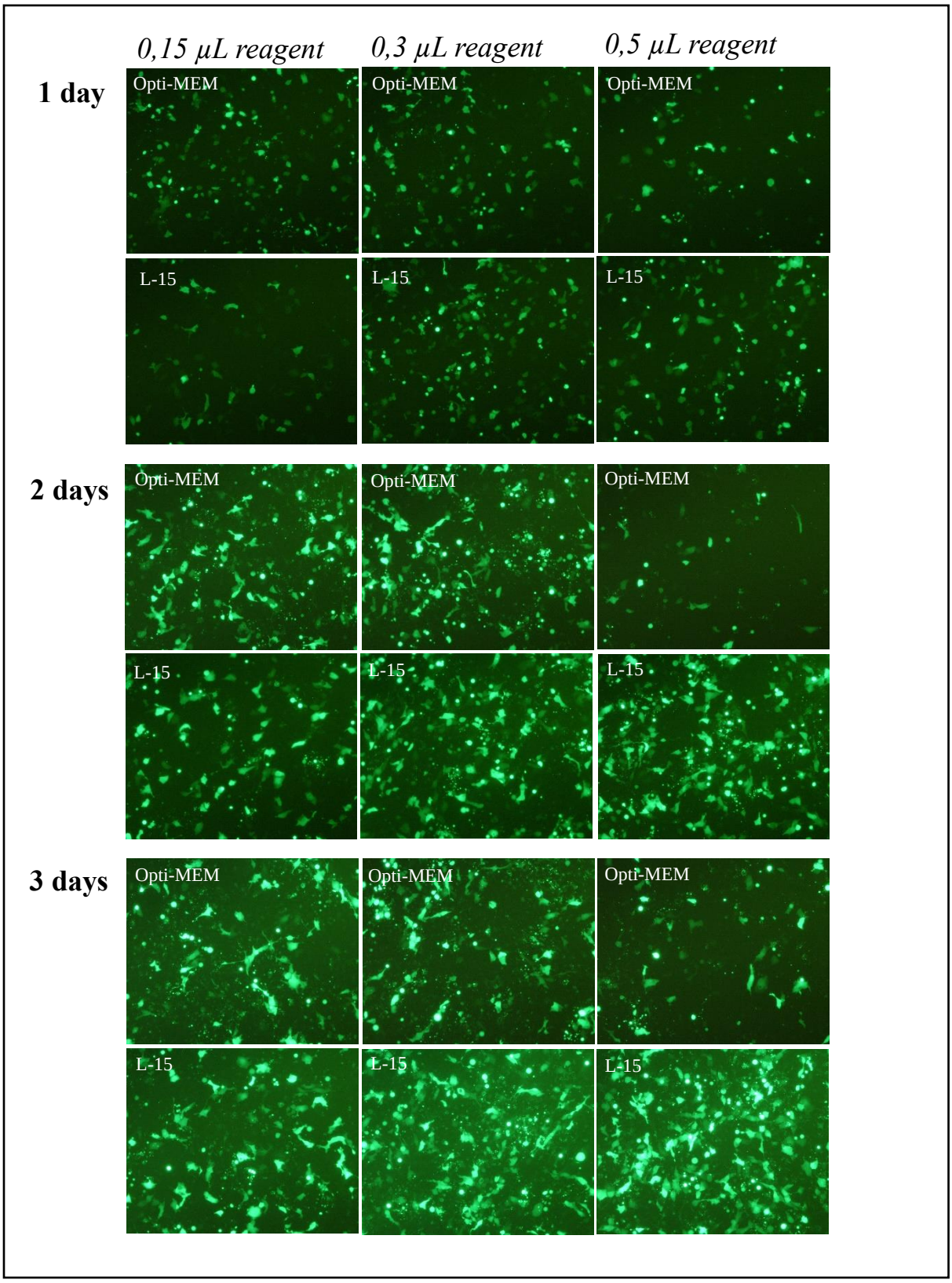

Figure 25: Fluorescence microscopy showing transfection optimization of EPC cells with Lipofectamine 3000™ reagent and MGFP plasmid. All photos taken with 10x magnification.

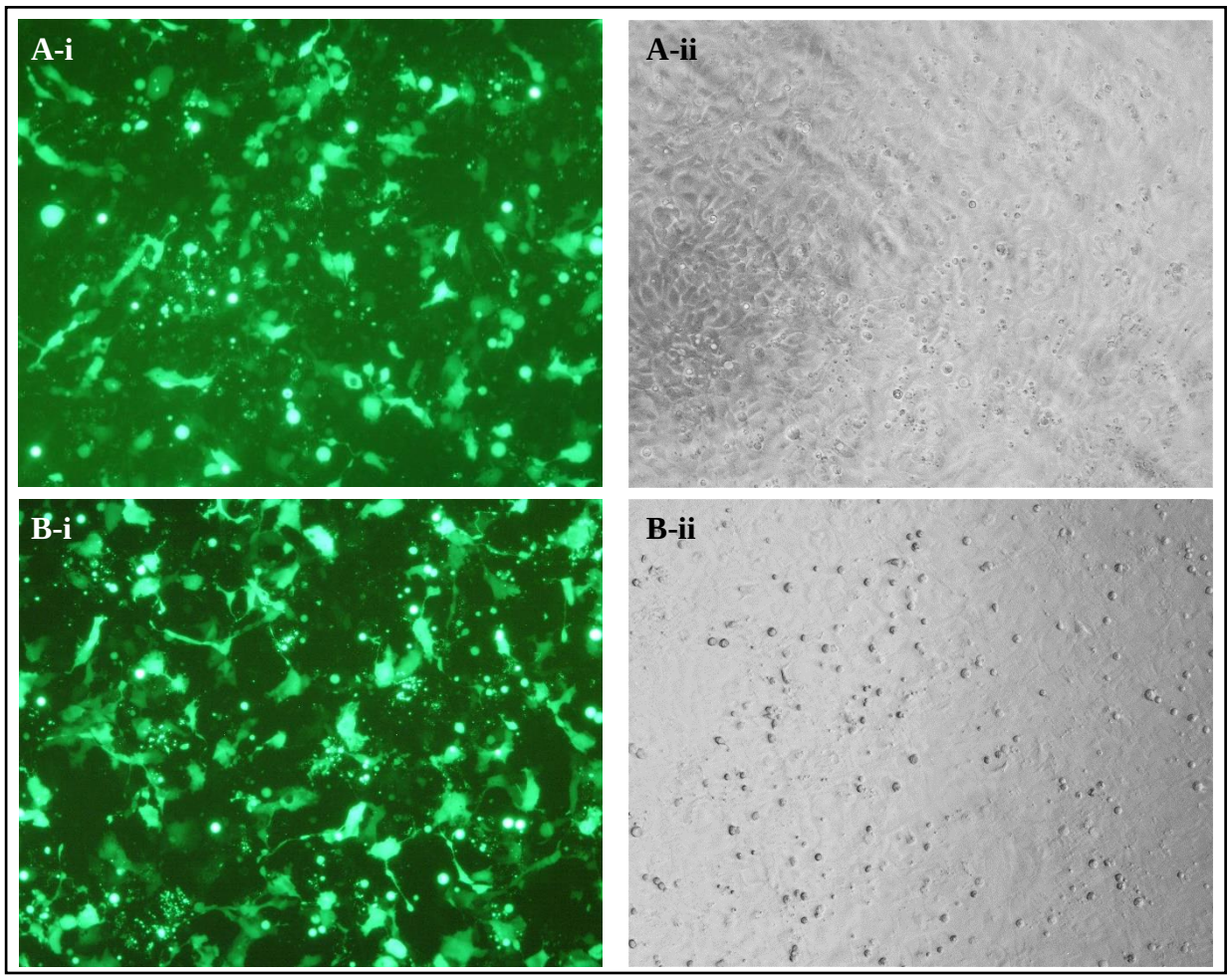

Fig. 26: Comparing two different kits for transfection of EPC cells. **A-i**: Lipofectamine 3000, 40 000 cells/well, 0,2 µg phMGFP and 0,3 µL transfection reagent. **A-ii:** Phase contrast image. **B-i**: K2® Transfection System, 40 000 cells/well, 0,15 µg phMGFP and 0,6 µL transfection reagent. **B-ii**: Phase contrast image. All photos are taken with 10x magnification.

4.4.1.3 mRNA transfection

An attempt of transfecting EPC cells with synthesized mRNA from the different B22R constructs was done. The jetMESSENGER® kit by Polyplus was used to synthesize the mRNA *in vitro*. Cells were seeded at 70 000 cells/cm^2 in a 48 well plate, incubated at 20°C and transfected the day after. The cells were transfected with mRNA B22R3-C-19. A transfection control plasmid was also included with the K2® Transfection System, and a negative control. The medium in the wells containing cells transfected with mRNA were changed after four hours, and those with plasmid transfected cells were changed the day after as indicated by the producers. The wells were fixed and stained on day 3. It was difficult to distinguish background staining and transfected cells (figure 26). At this time, no positive mRNA control was available.

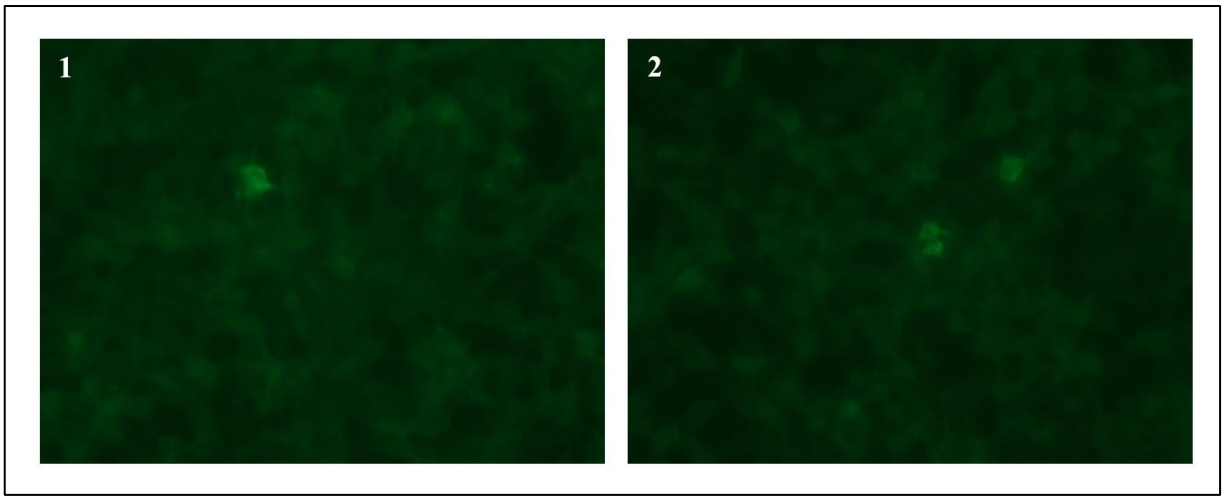

Figure 27: Fluorescent microscopy of EPC cells transfected with *in vitro* synthesized target mRNA. **1:** B22R3-C-FLAG mRNA (NOR2019 isolate), JetMESSENGER (transfection kit). **2:** negative control (no nucleic acids added). Photos were taken with 40x magnification but are somewhat off scale because of image processing.

4.4.2 Transfection optimization of ASG-10 cells

4.4.2.1 K2 and METAFECTENE transfection optimization

It is highly desirable to be able to transfect the ASG-10 cells because of their similarity to the *in vivo* target cells for SGPV. A transfection procedure had never previously been conducted on these cells and it was therefore necessary to test different transfection methods and different kits. The first method that was tested was a liposome-based technology. Three different reagent kits based on lipofection technology (see section 3.6.1) were tested: METAFECTENE®, K2® transfection system and Lipofectamine™ 3000.

In the first round, METAFECTENE® and the K2® transfection system was tested. Six wells (on a 24 well plate) of cells were made available, three for each kit. The setup was made by following the two different user manuals (see table 10 in appendix). The cells were seeded with 132 000 cm^2 cells/well and incubated at 20°C during the whole experiment. Cells were seeded 3 days before adding DNA and transfection reagents. After adding the transfection reagents, the cells were incubated for two days and then studied under a fluorescence microscope. The cells were also examined after four days.

From fluorescent microscopy, it was concluded that the K2 transfection system produced best results. It was possible to observe weak fluorescence after one day from the two different concentrations of DNA that were tested. After four days, the fluorescence was more intense. It was concluded that the well with 0,3 µg DNA had most fluorescent cells. It was therefore

decided to do an optimization with the K2 reagent with DNA concentrations ranging from 0,2 µg to 0,4 µg DNA.

A new optimization experiment with K2® only was done to determine which concentrations of each component gave best transfection efficiency (see table 11 in appendix). Some miscalculations of volumes led to the discarding of some wells. 5 µL multiplier, 0,3 ng DNA and a DNA to transfection reagent ratio of 1:5 seemed to produce the best transfection efficiency. The samples were analyzed by flow cytometry, and the results gave 0-0,07% transfected cells. The run did not include a negative control, and the sample showing less transfected cells was used as a "negative control" and the gate settings in the whole run was based on this sample. Plate setup and percentage transfected cells are on page xiii in appendix.

The next setup was done to test transfection of B22R2-W and B22R2-19 and to further optimize the K2® Transfection System. Cells were seeded one day prior to adding transfection reagents. The cells were examined in a microscope before transfection to see if they had achieved 90-100% confluency. The cells were incubated at 20°C during the whole experiment. Here, a few transfected cells were detected. The wells transfected with 0,4 ng DNA showed a few more transfected cells compared to the wells transfected with 0,3 ng DNA. Both pGFP and phMGFP had some transfected cells, with phMGFP having the highest number. Expression of the B22R proteins were not detected.

4.4.2.2 K2 and Lipofectamine 3000 optimization

A new transfection optimization of ASG-10 cells was done with the K2® Transfection System and Lipofectamine™ 3000 reagent kit. The transfection optimization was performed in a 96 well plate. Different cell densities and amounts of transfection reagents were tested while the DNA amount was held constant (for exact details see table 14 in appendix). Two different cell culture media, L-15 and Opti-MEM, were tested in the transfection mixture. The cells were incubated with L-15 and at 20°C during the whole experiment. Only the K2® transfection system protocol recommended to change the medium 6-24 hours after transfection, but the medium in the wells were cells had been transfected with Lipofectamine 3000 were also changed after about 24 hours. The cells were examined by fluorescence microscopy one, two and four days after transfection. There was a substantial increase in fluorescence intensity between the days for the cells transfected with Lipofectamine™ 3000. Fig. 28 show cells transfected with Lipofectamine™ 3000 after two and four days. Day 4 shows higher number of transfected cells compared to day 2. Lipofectamine 3000 gave more transfected cells compared

to K2, and Lipofectamine gave more transfected cells when more reagent was added. K2 produced more “green dots” with more reagent added, which occurred in almost all wells transfected with K2, although a few transfected cells was spotted (see figure 29). The dots may be dead cells that have detached from the well (see fig. 29, A-ii). Flow cytometry was performed on the samples, and the results showing most transfected cells are shown in figure 30. The flow cytometer can manage 48 samples in one run, and the plate had to be divided into two runs. The first run did not include a negative control, and the sample showing no transfected cells (K2 kit, 0,15 µg DNA and 1µL reagent) was used as a “negative control”, and the gate settings in the whole run was based on this control sample. The second run included a negative control and the gate settings here was based on this sample. All wells transfected with K2® Transfection system showed very low transfection efficiency observed by microscopy, and only cells from a few wells were analyzed by flow cytometry.

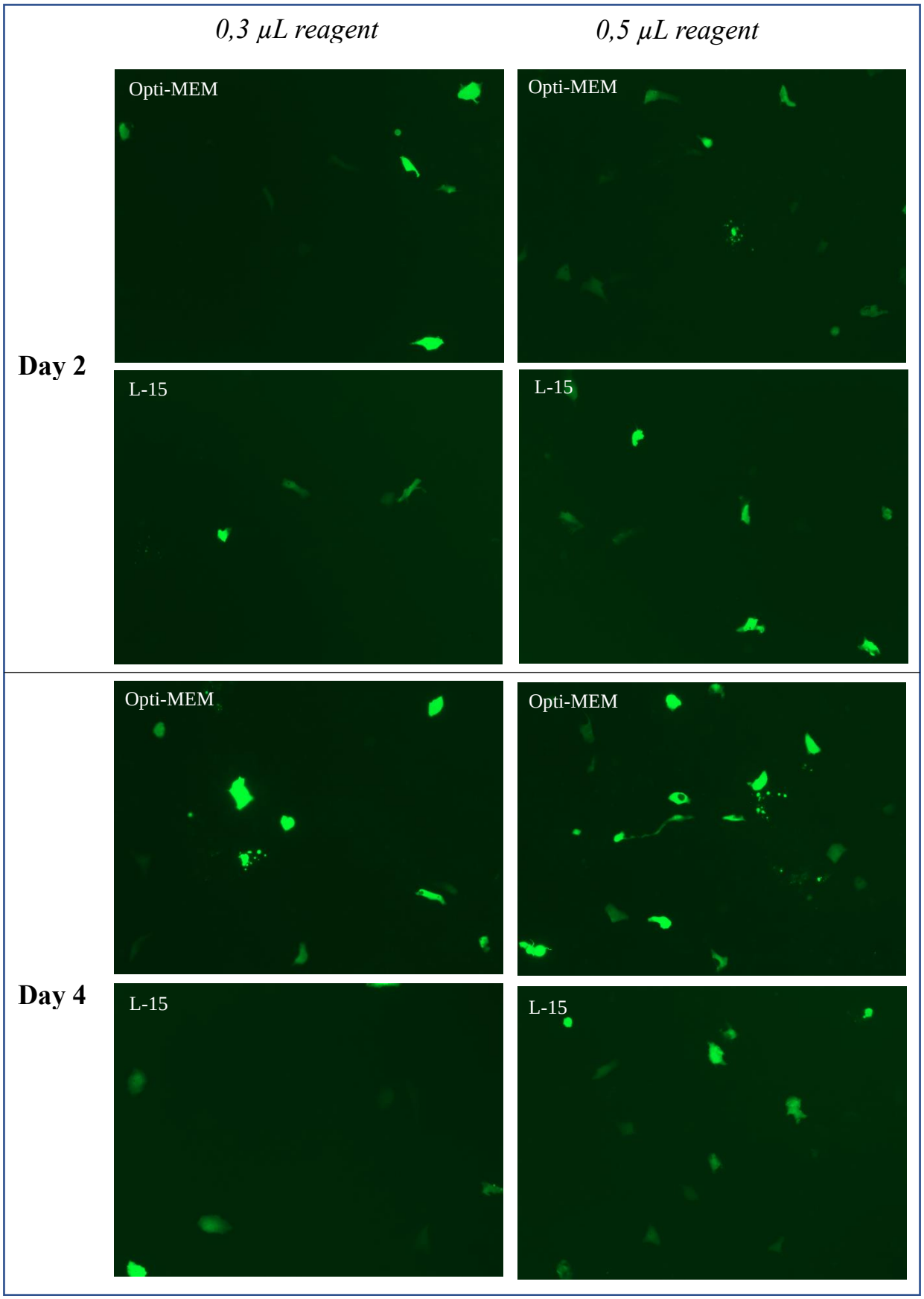

Figure 28: Fluorescence microscopy showing optimization of ASG-10 with the Lipofectamine™ 3000. Pictures are taken with 10x magnification. Differences in transfection efficiencies between 0,3 µL and 0,5 µL transfection reagent, Opti-MEM and L-15 medium were investigated. Day 4 shows higher number of transfected cells compared to day 2.

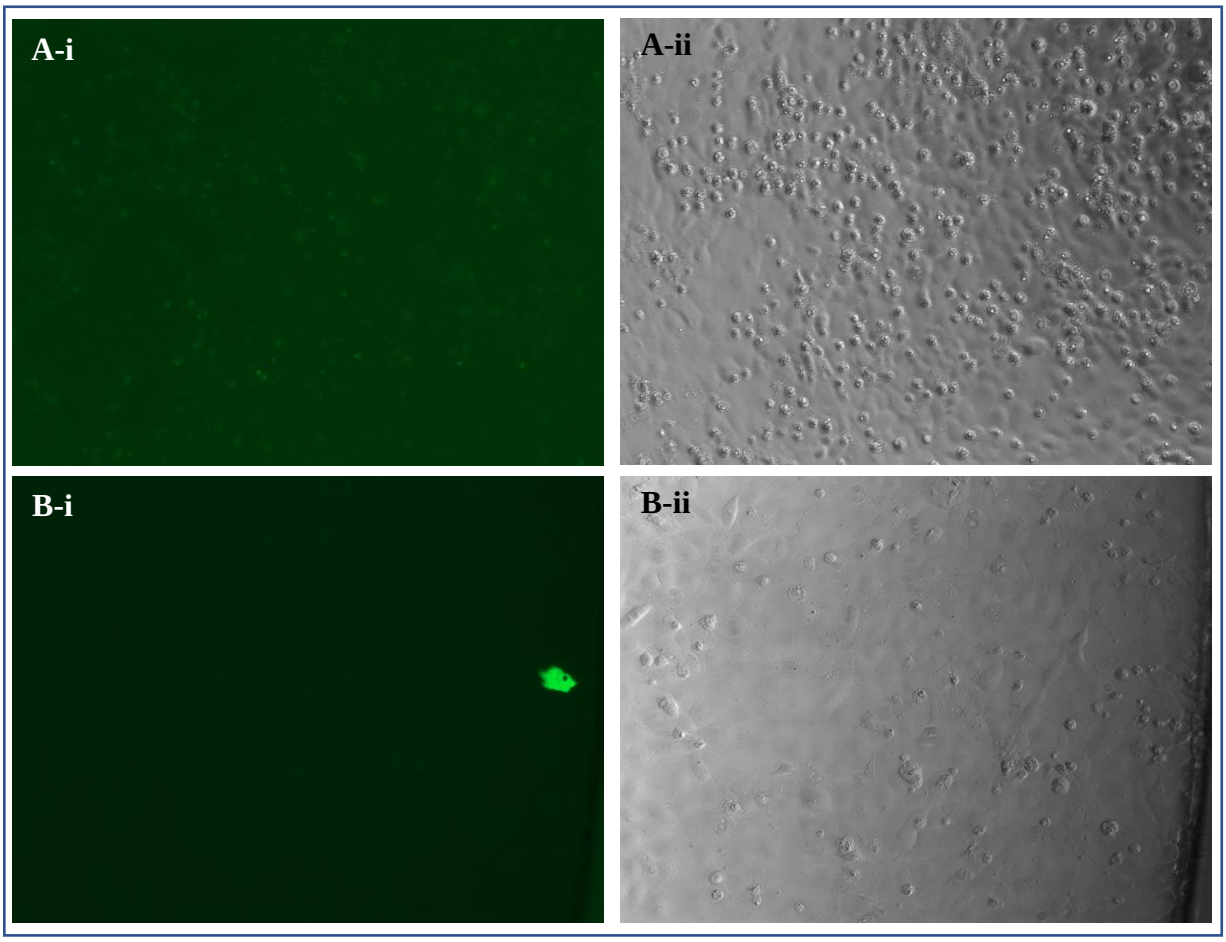

Fig. 29: Optimization of ASG-10 with the K2® transfection system. Photos are taken with 20x magnification. A-i and B-i are pictures taken with fluorescence microscopy, where A-i shows little green dots and B-i shows a transfected cell. A-ii and B-ii are pictures taken with phase contrast microscopy, showing how the cells looks like after transfection.

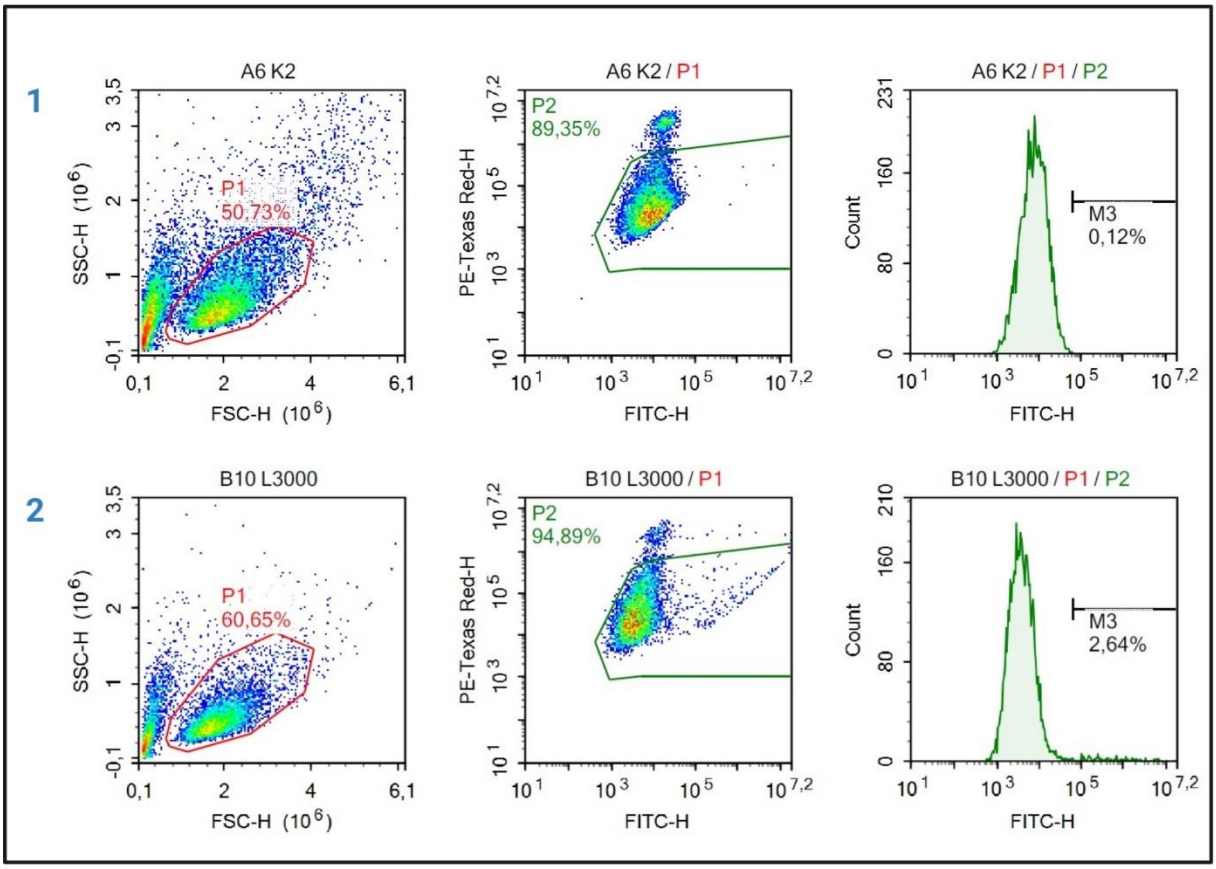

Fig. 30: Flow cytometry results showing the most successfully transfected ASG-10 cells from the two different kits. **1**: K2® Transfection System, 0,15 µg DNA, 0,6 µL transfection reagent. **2**: Lipofectamine™ 3000, 0,2 µg DNA, 0,5 µL transfection reagent.

An attempt was made to transfect ASG-10 cells with all eight B22R constructs and Lipofectamine™ 3000. The transfection experiment was performed in a 96 well plate with a fixed amount of DNA and reagent, and two different cell densities (see table 15 in appendix). Opti-MEM were used while mixing the transfection mixture. The cells were incubated with L-15 medium during the whole experiment and incubated at 15°C after adding the transfection mixture. The medium of the wells with Lipofectamine 3000 was changed after about 24 hours. The control wells with phMGFP were examined by a fluorescence microscope each day after transfection. Few transfected cells were observed, even after four and five days. The wells containing cells transfected with a B22R construct was stained six days after transfection. The results were poor since the cells had been growing for too long, and no transfected cells with a B22R construct was found. The results are therefore not shown.

4.4.2.3 mRNA transfection

GFP-encoding mRNA from Oz Biosciences was transfected using the jetMESSENGER reagents and protocols. A premix of 0,1 µg mRNA and 0,3 µL transfection reagent was added in each well. The cells were examined one, two and four days after the transfection (see figure 31). Figure 32 shows a high transfection efficiency.

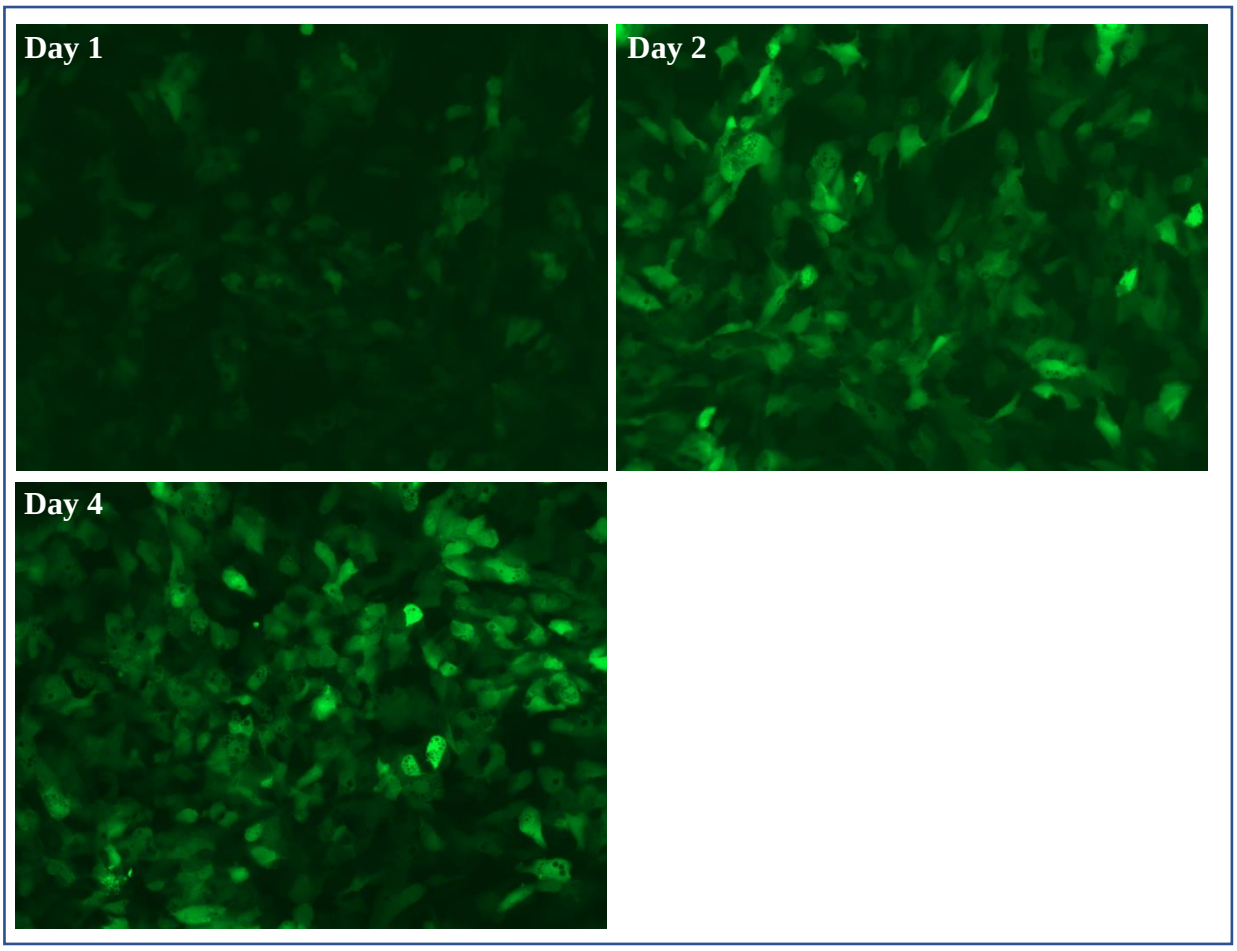

Fig. 31: mRNA transfection of a GFP encoding mRNA examined by fluorescence microscopy taken with 20x magnification. The photos were from the same well (E3) and includes: 60 000 cells/well, 0,1 µg mRNA and 0,3 µL transfection reagent.

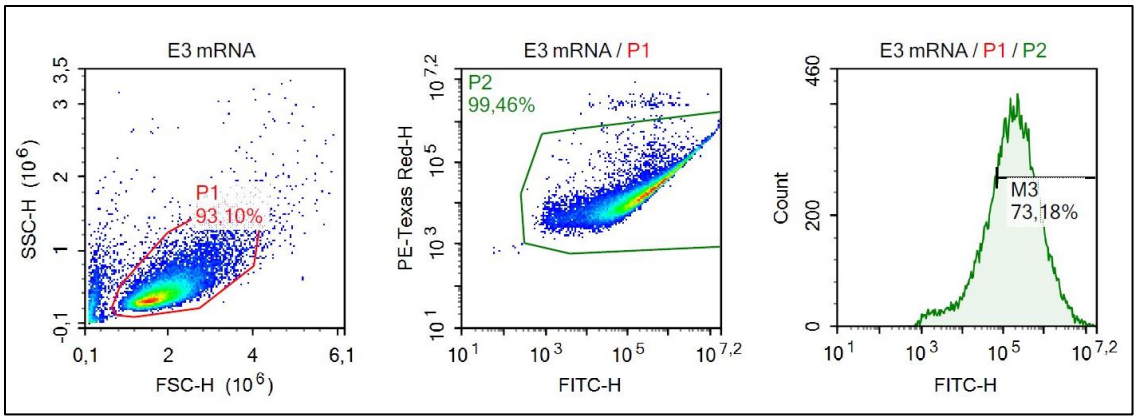

Fig. 32: Flow cytometry of ASG-10 cells transfected with GPF encoding mRNA. The results show very high transfection efficiency. Cells analyzed are the same as in Fig. x (well E3).

4.4.2.4 Optimization of electroporation

The Amaxa® Cell Line Optimization Nucleofector® Kit was used for transfection optimization of ASG-10 cells. In this transfection procedure, the cells must be in suspension, and the ASG-10 cells were suspended in 18 mL growth medium with a concentration of 2,05x10^6 cells/mL. Every sample included: 1 mL cell suspension, 2 µg pmaxGFP® Vector and 100µL buffer. The procedure was performed according to the user manual (see table 10 for setup). It was not possible to perform any further optimization or take pictures due to the COVID-19 pandemic.

Table 10: Overview of the transfection results on ASG-10 cells using the Amaxa® Cell Line Optimization Nucleofector® Kit.

Sample	MaxGFP vector	Buffer	Amaxa program	Status cells viability observed 12.03.20	Transfection efficiency observed16.03.20
1	+	V	A-020	Thin layer OK-	Low
2	+	V	T-020	Thin layer OK-	Low
3	+	V	T-030	Thin layer OK-	Low
4	+	V	X-001	All dead	None
5	+	V	X-005	Thin layer OK-	Low
6	+	V	L-029	Good	Low
7	+	V	D-023	Thin layer OK-	Low
8	+	V	W-001	Thin layer OK-	Low
9	+	V	Y-001	Good	Good
10	+	V	M-003	Good	Low
11	+	V	U-011	Good	Ok
12	+	V	U-029	Thin layer OK--	Ok
13	+	V	T-023	Thin layer OK-	Low
14	+	V	*-	Too many cells – some dead	

*No program used

4.5 Recombinant expression of B22R3 proteins in EPC cells

Based on the results obtained from the transfection optimization of EPC cells, it was decided to set up a transfection of the eight different B22R constructs in EPC with K2® Transfection System (0,6 µL transfection reagent), and Lipofectamine™ 3000 (0,3 µL transfection reagent), 30 000 cells/well in a 96 well plate. One well was transfected with MGFP as a positive control. This made it possible to follow the transfection rate from day to day and decide on when to do the immunochemical staining. This time, the cells were incubated at 15°C through the whole experiment. By following the expression of MGFP it was decided to stain the cells transfected with the B22R constructs three days after transfection (figure 33).

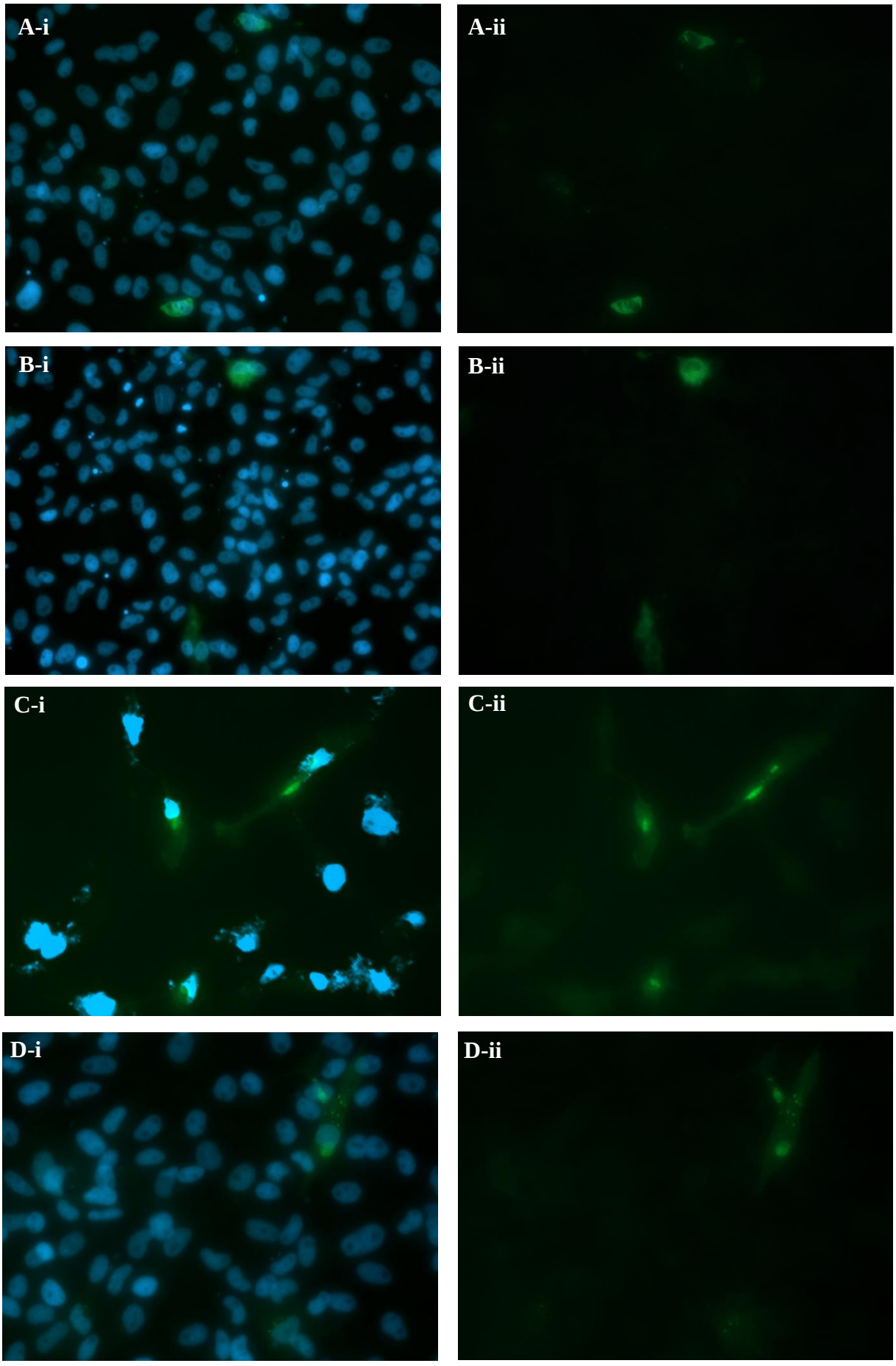
A-i
A-ii
B-i
B-ii
C-i
C-ii
D-i
D-ii

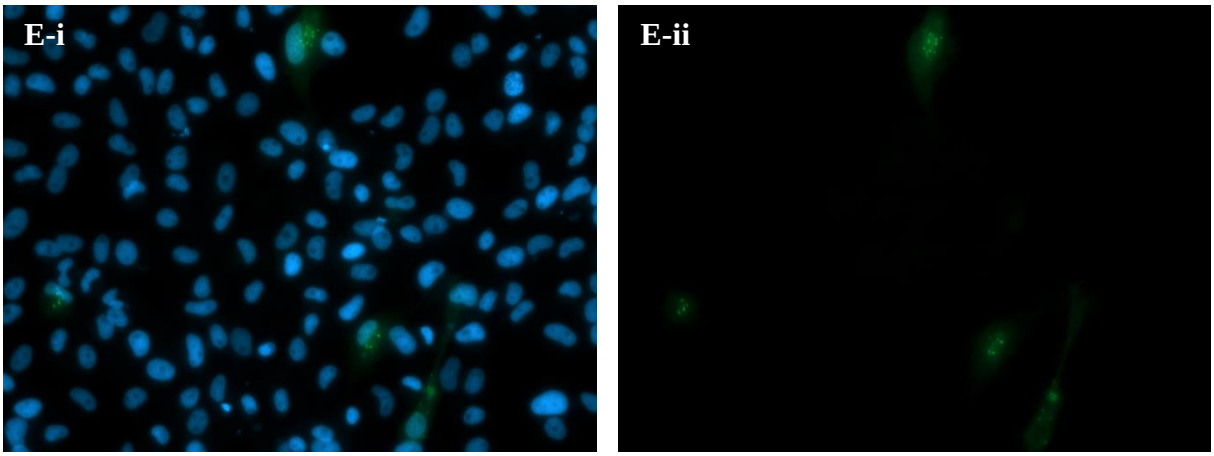

Figure 33: Photos of transfected EPC cells from fluorescence microscopy stained with DAPI (blue) and anti-FLAG antibody (green). Each row represents the same image captured but selected for or without nuclear (DAPI) staining. **A:** B22R1 construct (NOR2009-W isolate), Lipofectamine™ 3000. **B:** B22R2 construct (NOR2019 isolate), Lipofectamine™ 3000. **C:** B22R3-C-FLAG construct (NOR2019 isolate), K2® Transfection System. **D:** B22R3-C-FLAG (NOR2019 isolate), Lipofectamine™ 3000. **E:** B22R3-C-FLAG (NOR2019 isolate), Lipofectamine™ 3000. Every image is taken with 40x magnification but are somewhat off scale because of image processing. See appendix for details about staining of each well.

EPC cells were transfected and examined also by confocal microscopy to be able to observe the appearance and the intracellular location of the different proteins at higher resolution (see appendix table 9 for plate setup). The collagen coating was included because the EPC cells seemed to be washed away during the immunochemical staining of previous transfections.

The previous results of EPC cells transfected with B22R3-C-FLAG display granules of different sizes. It was therefore decided to stain the cells with Lysotracker to evaluate if these granules may be lysosomes. WGA staining was included to investigate if the granules could be endosomes. WGA also stains the Golgi apparatus and ER. If the anti-FLAG fluorescence overlaps with LysoTracker or WGA, it is an indication that the proteins are located in these cell compartments. Phalloidin dyes the cytoskeleton, which gives a nice outline of the cell.

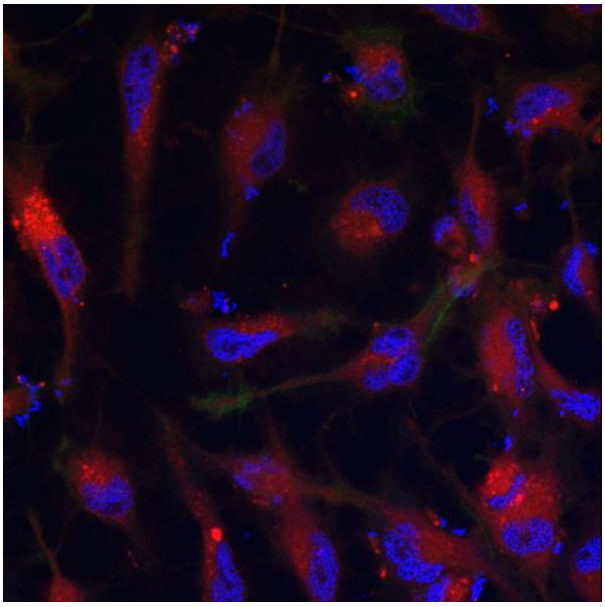

1: Gene/construct: B22R1
Isolate: SGPV NOR2019
Staining: Anti-FLAG (488), DAPI (405) and Lysotracker (668)

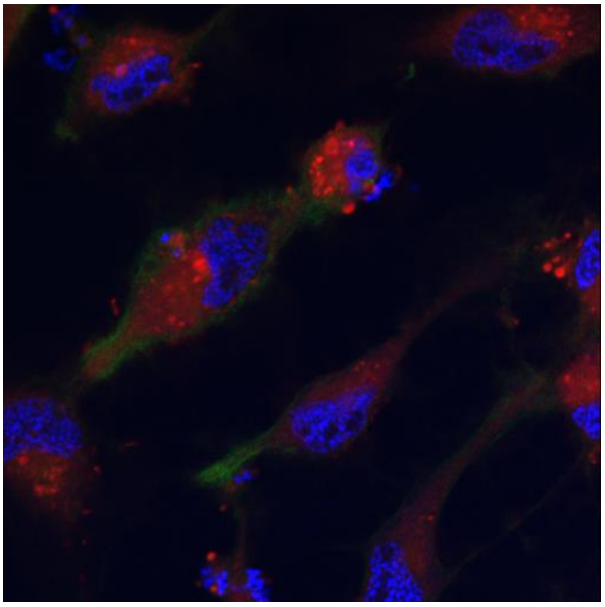

2: Gene/construct: B22R1
Isolate: SGPV NOR2019
Staining: Anti-FLAG (488), DAPI (405) and Lysotracker (668)

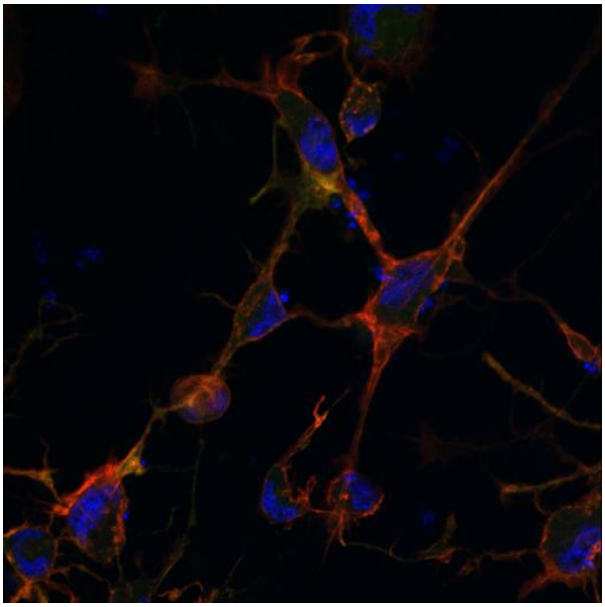

3: Gene/construct: B22R1
Isolate: SGPV NOR2019
Staining: Anti-FLAG (488), DAPI (405) and Phalloidin (568)

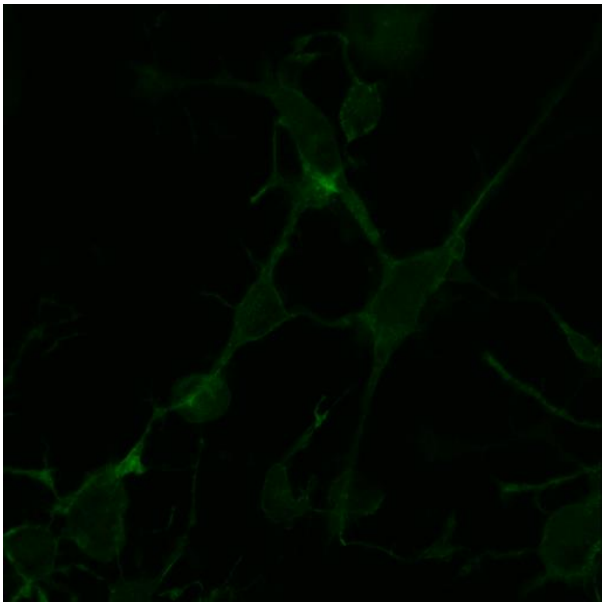

4: Gene/construct: B22R1
Isolate: SGPV NOR2019
Staining: Only viewing Anti-FLAG (488).

Figure 34: from page 74-77: Findings from the EPC transfection. Every picture is taken with 63x magnification but are somewhat off scale because of image processing. See appendix for details about staining.

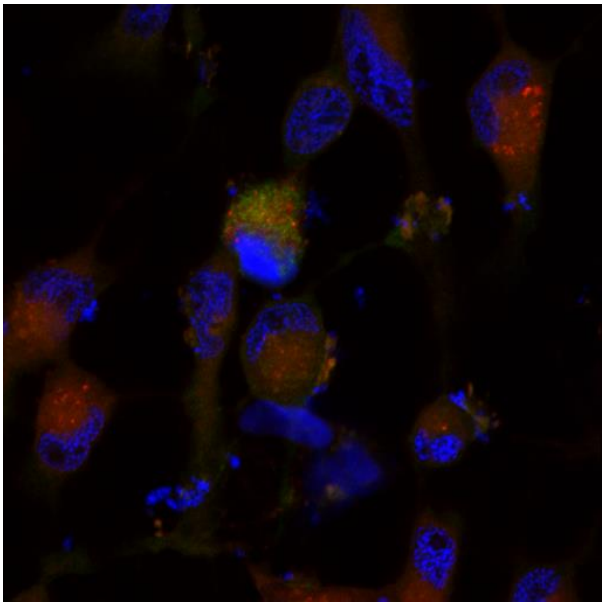

5: Gene/construct: B22R2
Isolate: SGPV NOR2009-W
Staining: Anti-FLAG (488), DAPI (405)
and Lysotracker (668)

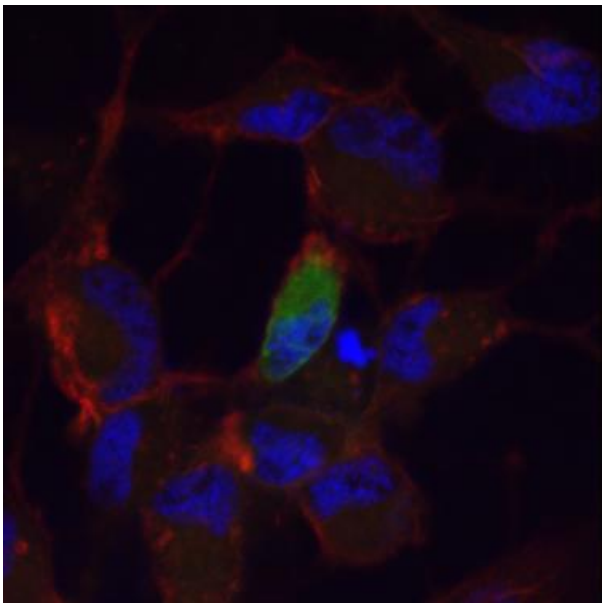

6: Gene/construct: B22R2
Isolate: SGPV NOR2009-W
Staining: Anti-FLAG (488), DAPI (405)
and Phalloidin (568)

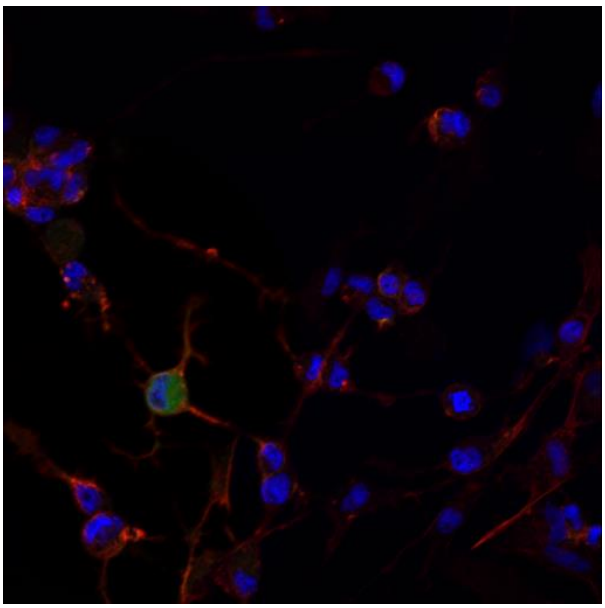

7: Gene/construct: B22R2
Isolate: SGPV NOR2019
Staining: Anti-FLAG (488), DAPI (405)
and Phalloidin (568)

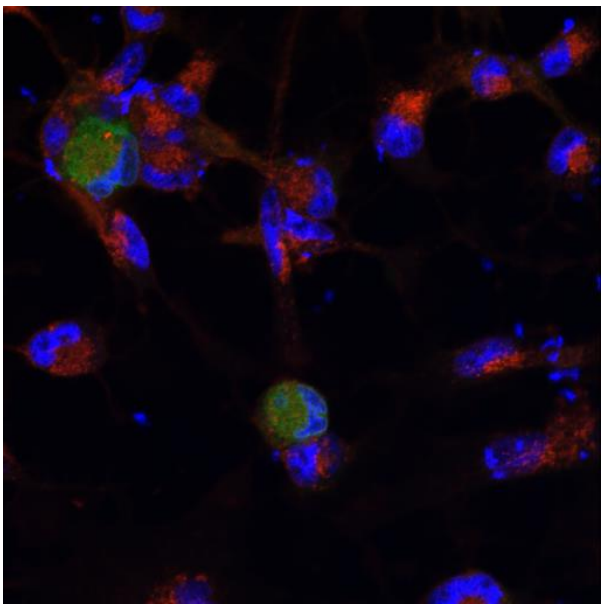

8: Gene/construct: B22R2
Isolate: SGPV NOR2019
Staining: Anti-FLAG (488), DAPI (405)
and WGA (555)

Figure 34: from page 74-77: Findings from the EPC transfection. Every picture is taken with 63x magnification but are somewhat off scale because of image processing. See appendix for details about staining.

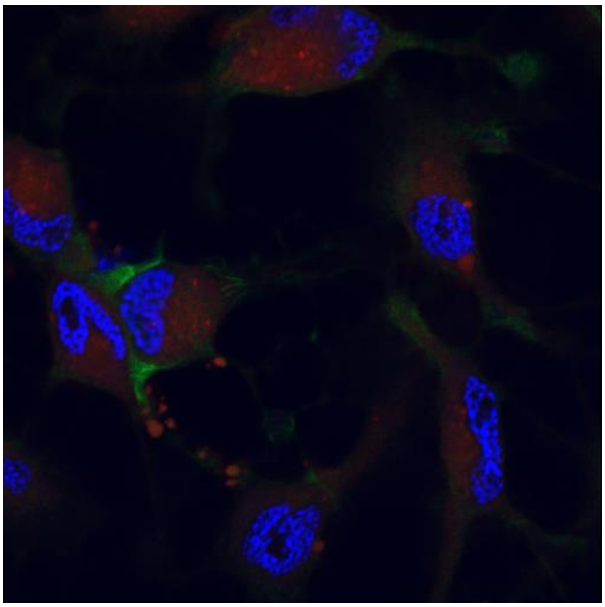

9: Gene/construct: B22R3-C-flag
Isolate: SGPV NOR2019
Staining: Anti-FLAG (488), DAPI (405)
and Lysotracker (668)

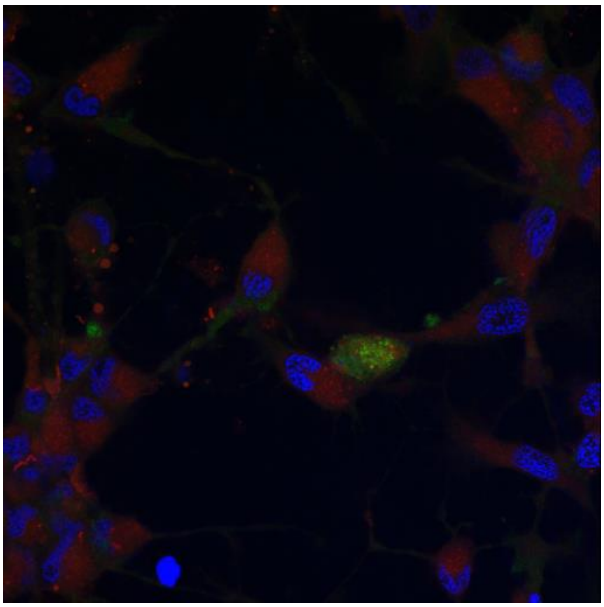

10: Gene/construct: B22R3-C-flag
Isolate: SGPV NOR2019
Staining: Anti-FLAG (488), DAPI (405)
and Lysotracker (668)

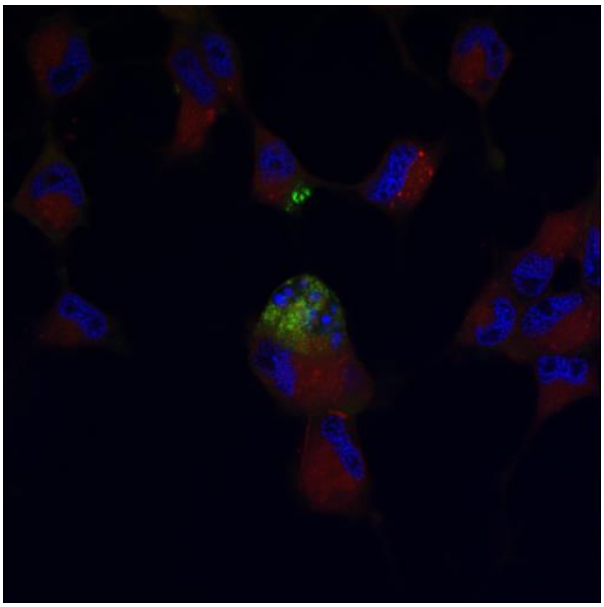

11: Gene/construct: B22R3-C-flag
Isolate: SGPV NOR2019
Staining: Anti-FLAG (488), DAPI (405)
and Lysotracker (668)

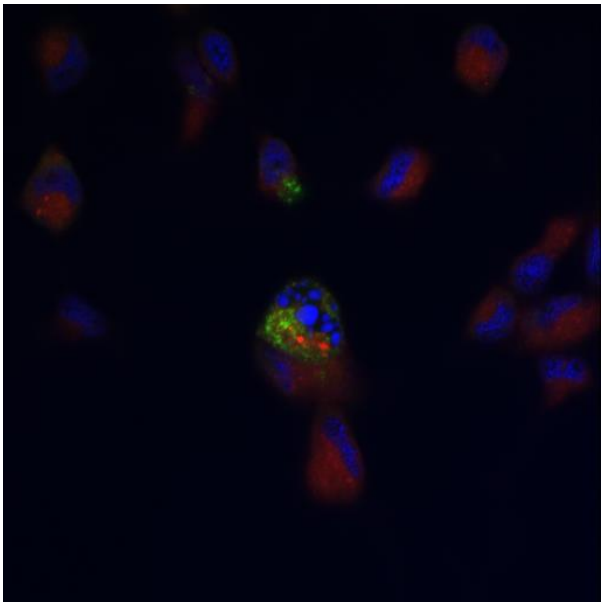

12: Gene/construct: B22R3-C-flag
Isolate: SGPV NOR2019
Staining: Anti-FLAG (488), DAPI (405) and
Lysotracker (668)

Figure 34: from page 74-77: Findings from the EPC transfection. Every picture is taken with 63x magnification but are somewhat off scale because of image processing. See appendix for details about staining.

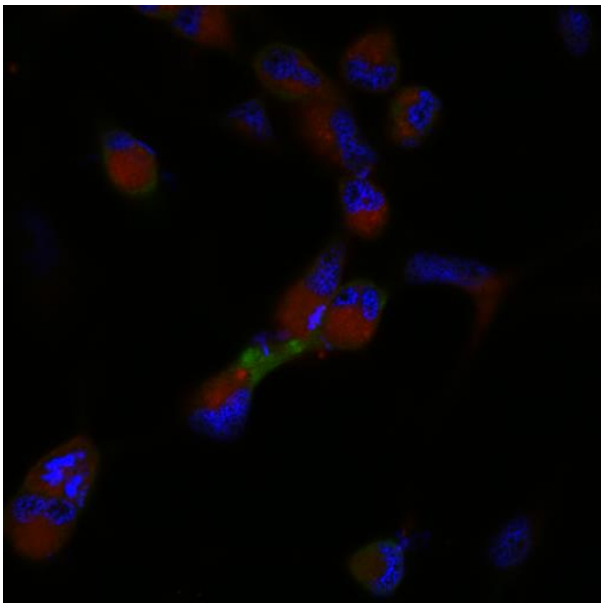

13: Gene/construct: B22R3-N-flag
Isolate: SGPV NOR2019
Staining: Anti-FLAG (488), DAPI (405) and Lysotracker (668)

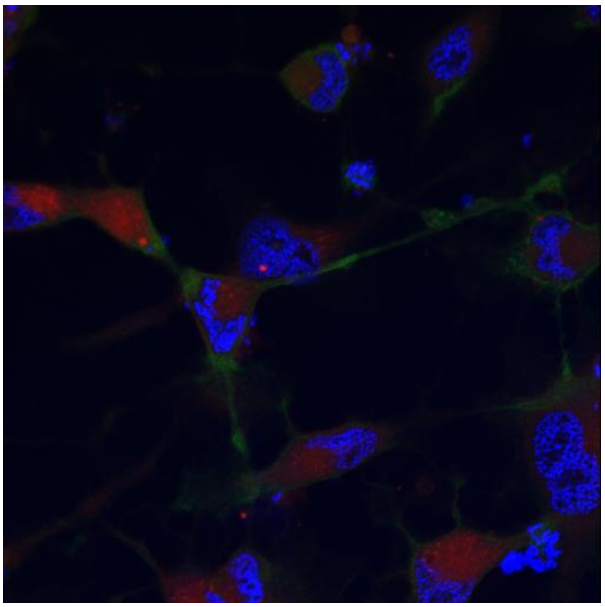

14: Gene/construct: B22R3-N-flag
Isolate: SGPV NOR2019
Staining: Anti-FLAG (488), DAPI (405) and Lysotracker (668)

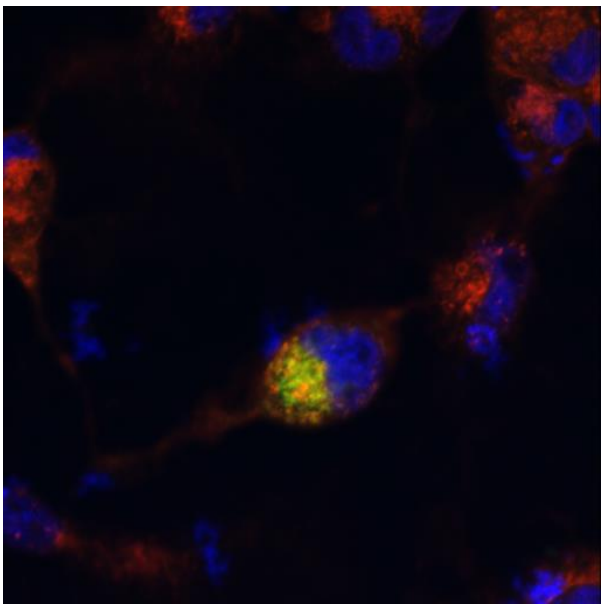

15: Gene/construct: B22R3-C-flag
Isolate: SGPV NOR2009-W
Staining: Anti-FLAG (488), DAPI (405) and WGA (555)

Figure 34: from page 74-77: Findings from the EPC transfection. Every picture is taken with 63x magnification but are somewhat off scale because of image processing. See appendix for details about staining.

The EPC cells transfected with B22R1 seems to have expression mainly in the membrane, while B22R2 seems to be evenly dispersed inside the cells. B22R3-N-FLAG was only detected in a few images (13 and 14 fig. 34) and seems to be located near the plasma membrane. The B22R3-C-FLAG proteins seems to be aggregated in the ER/Golgi. The confocal microscopy results

show that there is no overlap with LysoTracker and anti-FLAG as seen in picture 11 and 12 in figure 34. Picture 3 and 4 from figure 34 display a possible overlay with WGA and anti-FLAG. After looking at all transfected EPC cells, the B22R1 protein appears to be membrane-bound, B22R2 appears to be cytoplasmic, and B22R3 may be in ER/Golgi or the membrane.

4.6 Expression of B22R1-3 proteins in gills of infected fish

RNA samples from gill tissue of salmon presmolts during a natural outbreak of SGPV by Gjessing et al. (2020) (umpublished), was used to detect possible transcripts of B22R. The study was based on four test groups with samples taken at different time points during SGPV infection.

Table 11: Overview of primers for the three SGPV B22R assays. Input describes how much DNA/cDNA used in each analysis.

Genome - gene	**Assay - Fluorophore**	**Input**	**Sequence**
SGPV - B22R1	SYBR green SYBR	5 ng	FP: 5'- ATGCGCACATGTCAGGGTTA -3'
			RP: 5'- AGGGTTACTGGGATCCACGA -3'
SGPV - B22R2	SYBR green SYBR	5 ng	FP: 5'- CGGCACCAGAAACTCCGTAT -3'
			RP: 5'- CAAGATGTGCCAGTGGTGGA -3'
SGPV - B22R3	SYBR green SYBR	5 ng	FP: 5'- CAAGATCTGGCACGGATGGT -3'
			RP: 5'- CTGACCCGAAAGAGCTTGGT -3'
SGPV - D13L*	SYBR green SYBR	5 ng	FP: 5'- GACGGGGCAACTCTTTTCT -3'
			RP: 5'- CACCGTGACCTCGATACGAA -3'

*Positive control: Major capsid protein

The results shown in table 11 indicate that the proteins are expressed in all infected groups. However, it was detected DNA in the RNA isolates, and the results are thus uncertain.

Table 12: Mean Ct-values for each group from the outbreak samples by (Gjessing et al., 2020).

Gene	**M-I B11 during outbreak (Ct mean and range)**	**L-I: B11 one week after (Ct mean and range)**	**E-III: D14 early infection (Ct mean and range)**	**M-II: D24 new tank with outbreak (Ct mean and range)**
B22R1	22,2 (21,3-23,3)	30,3 (29,2-32,4)	37,8 (34,1-40,0)	25,0 (23,4-26,2)
B22R2	22,7 (21,7-23,6)	30,1 (28,2-32,8)	37,7 (34,1-40,0)	24,4 (22,8-25,8)
B22R3	21,0 (20,3-22,3)	28,9 (27,3-31,7)	36,7 (33,2-40,0)	23,6 (22,2-24,7)

Because of the detected DNA in the RNA isolates, the primers were also tested on other samples from a study of experimentally induced SGPV (Thoen et al., 2020) that had been DNase treated. The results are presented in table 13.

Table 13: Mean Ct-values of B22R in two different gill samples from an experimental infection (Thoen et al., 2020).

	Sample	
Gene	L139-gill (Ct)	L141-gill (Ct)
B22R1	20,6 (20,2-21)	21,6 (20-23,3)
B22R2	20,4 (20,3-20,4)	19,9 (19,4-20,3)
B22R3	19,9 (19,7-20,1)	18,9 (18,7-19.1)

To confirm that the primers worked properly, PCR products were analyzed with Bioanalyzer. The products had the expected size. The last qPCR results confirm the presence of B22R1-3 in the gills during an infection.

5.0 Discussion

The main aim of this thesis was to clone and characterize genes from SGPV that resemble the gene B22R in the Variola virus, a gene shown to inhibit immune function. Several crucial steps on the way to enable the visualization and characterization of the genes is being discussed here, as well as the *in silico* tools used to get further insight into protein characteristics. Finally, the relationship between these observations will be discussed, followed by suggested future work.

5.1 Main challenges in cloning large genes like B22R

Large genes can be a challenging to amplify and clone, and all B22R genes are > 3kB (B22R-1 is > 6 kB). Because of this, some adjustments were needed to succeed in the PCR amplification of B22R inserts for cloning. Polymerases with low error rate, suitable for long sequences, were used, and the amplification time was longer than for standard PCR. In particular, it was challenging to amplify the longest gene B22R-1. Since annealing temperature, reagent kit and protocols were changed during the process, one cannot be completely sure what actually led to success at the end. Since both reagent kits are supposed to have comparable quality, it is likely that the lower annealing temperature (60°C to 57°C) made the difference.

Many of the initial cloning experiments failed, and there were often several colonies on the agar plates even though the following colony PCR indicated no insert was present. There should not have been any growth when the cloning reaction was not successful. Colonies on the negative control plate indicated that there may have been some uncut vector left from incomplete vector

linearization. The In-Fusion protocol recommends purifying the linearized plasmid after cutting. Here, the plasmid was only run on a gel to confirm cutting and may have contained some uncut leftovers. If these non-linearized plasmids are transformed into a bacterium, it will be able to grow on an LB plate containing ampicillin. There might also have been some random DNA fragments inserted instead of the B22R target. Unspecific binding of primers during the PCR reaction a possibility, and can give rise to unspecific amplification products.

The presence of the primers for B22R1 was weak during all gel electrophoresis runs, which indicates that they may have been degraded during the PCR reaction. This may be the reason why there was very low amounts of these PCR product compared to the other PCR products. It seemed like the primers became more unstable after repeatedly freezing and thawing.

5.2 Choice of cell lines

To design a study that mimics the naturally occurring infection *in vivo* is the optimal choice to obtain reliable results. SGPV is known to infect epithelial cells of the Atlantic salmon gills (Gjessing et al., 2017b). A search after epithelial cell lines from fish was done in preparation of the transfection experiments, although the availability is limited. The ASG-10 cell line was therefore of huge interest for the present transfection studies, since they are derived from Atlantic salmon gill epithelial cells (Gjessing et al., 2018), but transfection of these cells had never been attempted. The easily transfectable EPC cell line was also included as a control of successful transfection (Fijan et al., 1983). A cell line derived from Rainbow Trout (RT) called RT-Gill could also have been an alternative in the transfection experiments. These cells are more closely related to ASG-10 compared to EPC. However, these cells have been reported to be harder to transfect (Liu et al., 2005) .

5.5 Evaluation of transfection methods and optimization

During the transfection procedures of the EPC and ASG-10 cell lines, an important experience was that the cells needed more time to express the proteins after transfection than cells from mammals. During the first transfections of EPC cells, they were stained the day after transfection. Later, it was discovered that staining would have been more optimal three days after transfection. The optimization figures on page 74-77 displays this difference. According to these images, it seems like expression following transfection with Lipofectamine occurred a bit earlier compared to K2, even though the end results at day 3 were very similar. A flow cytometry analysis could have provided a more accurate result of the transfection optimization of the EPC cell line, but this was not done here.

When transfecting the EPC and ASG-10 cell lines with the B22R constructs, it was decided to incubate the cell culture plates at 15°C. This was done because it is advantageous that the expressed proteins were in an environment that is as near the natural conditions of an SGPV infection as possible. The temperature may affect the folding characteristics and the structure of the proteins. If the proteins are not folded correctly, they might not function properly and produce misleading results or become degraded. It has not been confirmed that the temperature difference between 20°C and 15°C affect the B22R proteins, and it may not play a role either. The temperature may also affect the cellular growth rate and metabolic processes which might slow down at lower temperatures. ASG-10 cells are derived from Atlantic salmon that normally live in environments with temperatures ranging from freezing to over 20°C, with an average significantly lower than the latter. On the other hand, the EPC cells are derived from carp that live at higher temperatures. Hence, optimal growth conditions are different for the two cell lines. However, EPC cells has also been shown to be robust and have a wide temperature growth range (Fijan et al., 1983). To investigate if temperature affects the transfection or growth rate, a range of different temperatures could be included in future transfection optimization.

Different cell densities were tested in the transfection of both cell cultures, and the initial goal was to get cells that did not grow too confluent to thereby get better photos in the microscope. However, this reduced the chance of finding transfected cells since the transfection efficiency was relatively low. The EPC cells had a very high transfection efficiency with the MGFP plasmid, but the efficiency with the B22R constructs was much lower. Plasmid size may have had a large impact on the transfection efficiency as discussed in chapter 5.7.

In every setup with Lipofectamine 2000 or 3000, the medium was changed roughly one day after adding the transfection mixture to the cells, even though the manufacturer states that it should not be necessary. Changing the medium of the cells was done for optimal growth conditions and good morphological appearance. Over time, the cells might be affected by the transfection medium, and for these experiments it was important that the cells appeared as normal as possible when they were about to be examined by a microscope. Figure 28 showed that the EPC cells reacted differently, appearing unaffected when exposed to the K2® reagent, as opposed to the Lipofectamine™ reagent where many cells detached from the plate. The EPC cell line was easily transfected with both reagent kits, but with regards to viability, the K2 transfection system seemed to have a gentler effect on the cells. Cell detachment was also detected on the ASG-10 culture plates but there was no clear difference between cells exposed to the K2 or Lipofectamine 3000 reagents. On a few occasions, the time passed between adding

the K2® Multiplier and the transfection reagents extended beyond the two hours stated by the protocol. This might have influenced the transfection efficiency. It was also tested if the two different culture media L-15 and OPTI-MEM would make a difference on the transfection efficiency, and there was no obvious difference between these media. More experiments must be done to secure the reproducibility of the transfection results. Optimization of the different protocols will make it easier to perform the experiment, probably with shorter time spent.

5.6 Evaluation of staining methods

In the first transfection experiment, cells were stained with 5 µg/mL anti-FLAG antibody and the plate was incubated overnight. Unspecific staining was observed in the fluorescence microscope, so in the rest of the transfection experiments staining was performed with 2 µg/mL and only incubated for one hour. However, this did not seem to solve the problem as a roughly equal amount of unspecific staining was observed in the rest of the transfection experiments. The final transfection of the EPC cell line with the B22R constructs was done with another staining protocol. This protocol included other reagents for fixing and permeabilization. However, some unspecific staining was observed also here in the confocal microscope after using this protocol. The anti-FLAG staining protocol should have been further optimized because of the observed non-specific binding, so that it will be easier to identify transfected cells. This could have been done by testing other reagents to fix and permeabilize the cells.

5.7 Plasmid transfection versus mRNA transfection

Morphological and structural features of cationic lipid-DNA complexes is not dependent of the plasmid DNA length, but gene transfer is less effective with larger plasmids. (Kreiss et al., 1999). This correlates with the results here, where the shortest plasmid containing the B22R2 gene (8471 bp) gave better transfection efficiency in EPC cells compared to the B22R1 (12137 bp) and B22R3 (9362 bp) constructs. The exact mechanism of how lipid-DNA complexes enter the cell is unknown but is thought to occur by endocytosis (Kim and Eberwine, 2010, ThermoFisher). Transfection efficiency of lipofection depends a lot on several factors such as cell membrane conditions, pH in the solution and nucleic acid/reagent ratio (Kim and Eberwine, 2010). These issues will be less important with electroporation as this method is not equally dependent on chemical or biological properties (Kaestner et al., 2015). Transfection by electroporation needs to be further investigated to find out if this method is efficient for transfecting the ASG-10 cells. The Amaxa electroporation program called X-001 gave best

transfection efficiency and least cell death. This result corresponds with literature regarding epithelial cell transfection (Lonza, 2009). Amaxa also offers additional transfection buffers, and it would be interesting to test how they compare to the V solution tested here. A suggestion is to do a new optimization with other solutions in addition to the V solution with only the programs that gave best transfection. A subsequent flow cytometry analysis would reveal the percentage of transfected cells

When transfecting plasmids, they must enter both the cellular and nuclear membranes. Then the host RNA polymerase II must recognize the promoter in the plasmid (in this case CMV promoter) and transcribe the downstream gene of interest. Several of these steps could be affected by the plasmid length. Hornstein et. al suggested that transfection of plasmids does not appear to be affected by cell entry, but endosomal escape, nuclear localization and transcription determines the final transfection efficiency (Hornstein et al., 2016). mRNA transfection of ASG-10 was tested because of the low transfection efficiency with plasmids. This transfection method produced as much as 70% transfected cells. This might be because this method is not dependent on entering the cell nucleus and the mRNA will serve as a template for translation right after entering the cell. With this in mind, mRNA transfection seems to be a much better solution for transfecting ASG-10 cells than plasmid-based transfection, regardless of transfection method. Nucleofection can though not be excluded until the optimization is completed.

Plasmids (dsDNA) are more stable compared to mRNA (ssRNA). mRNA is more prone to degradation, and its survival in the transfected cell will be limited. This study focused on transient transfection and the expressed proteins did not need to be present for a longer period of time. A very good transfection efficiency was not that important either as long as a sufficient number of cells were positive, displaying normal morphology and B22R protein expression. mRNA transfection would be a suitable method in this regard. On the other hand, the *in vitro* transcription done in this study was problematic, especially with the largest gene (B22R1). The *in vitro* transcription could have been affected by several factors, such as human errors, presence of RNases degrading the products, or problems with the Bioanalyzer RNA assay. According to the mMESSAGE mMACHINE® T7 user manual, the kit is designed for transcripts up to 5 kb. B22R1 is 6,7 kb, and this might have affected the length and quality of the transcript for this gene.

5.8 *In silico* interpretations of B22R sequences

It is important to have in mind that many of the *in silico* tools used here are just predictions and it does not mean that these results are true. For instance, the output from TMpred showed options for several models. The B22R1 protein had six possible N-glycosylation sites in the region from about 22 to 459 in the amino acid sequence. According to one TMpred model, this region was predicted to be on the inside of the plasma membrane, meaning that it would not be possible to do N-glycosylations at these sites while this region will be in the cytoplasm, and not in the ER during protein synthesis and sorting. Another TMpred model having about the same scores as the first one, predicted the TM region to be otherwise so that the N-glycosylations would rather be on the outside. Thereby this model was selected. Another thing to have in mind, is that there is a large evolutionary gap between mammals and fish. Although the N-glycosylation motif Asn-X-Ser/Thr seems to be well conserved in eukaryotes, most *in silico* prediction tools are based on human/mammalian systems. Hence, some of the predictions made may not be accurate for fish viruses infecting Atlantic salmon as molecular mechanisms and interactions between the fish host and viruses may be different.

5.8.1 SGPV NOR2009 genome

It was discovered that the gills sequenced for the isolate SGPV NOR2009-W most likely contained more than one SGPV variant (Gulla et al., 2020). This was based on MLVA assay results with double profiles (Gulla et al., 2020). The B22R1 gene had two different DNA sequences extracted from the genome sequencing. Interestingly, the sequence variations observed between the two are located in the conserved B22R motif and may therefore be linked to functional differences between the two. Also, when translating the DNA sequences into amino acid sequences, the difference between the two proteins were small, providing extra support that the two proteins are functional. A further support of a double infection between two SGPV isolates is that the two constructs B22R3-C-FLAG and B22R3-N-FLAG have different DNA sequences. These sequences are theoretically supposed to be identical because they are from the same gene. The extracted B22R1 sequence from the SGPV NOR2009-W genome that was most identical to the cloned B22R1 SGPV NOR2009-W sequence has been used as reference here and included in identity and similarity searches.

5.8.2 Identities and similarities between B22R proteins and SGPV isolates

All three B22R proteins share the B22R family motif and are therefore paralogues. Homologous proteins share similar functions and are descendent from a common ancestor, while

homologous genes in the same species arising from gene duplication are paralogues (Lesk, 2016). The identities between the three paralogues are low (19-26%), and the proteins are likely to have different characteristics and properties. The proteins have a higher similarity (31-37%), meaning that even though the amino acids are different, some share similar physiochemical properties. When comparing the two isolates SGPV NOR2009-W and SGPV NOR2019, the identity and similarity between the protein sequences are high (98-99%). Studies indicate that SGPV infections in wild salmon is often associated with low virulence, while SGPV in farmed salmon is more often associated with acute mortality (Garseth et al., 2018). The virulence differences can be caused by several mechanisms in both the virus and host. The acute mortality in aquaculture may be influenced by several factors such as the environment, stress or the genetic composition of farmed salmon, whereas wild salmon might be less susceptible to infection. These hypotheses should be further investigated. One cannot conclude if these proteins play a part in the differences in virulence between SGPV NOR2009-W and SGPV NOR2019.

5.8.3 Polybasic motifs

A region with several basic amino acids is located after the last hydrophobic TM region for both B22R1 (KSRRRRNRMKALKKS) and B22R3 (CKSKKKN). Okamoto et al. (2013) describes that a polybasic sequence in the C-terminal tail is necessary for cell surface trafficking and is involved in internal cellular trafficking of G-coupled receptors (GPCRs) (Okamoto et al., 2013). Parmar et al. (2014) states that polybasic C-terminal cytoplasmic sequences in integral membrane proteins can mediate ER export or retention, and Golgi export (Parmar et al., 2014). Hence, the polybasic region in B22R1 and 3 may have similar functions. Interestingly, the C-terminus in B22R2 is not located to the cytoplasm, and does not contain a polybasic region, indicating that this protein might possess other functions.

5.8.4 Sequence assembly

After assembling the sequencing contigs from the final plasmids with B22R inserts, and translating the consensus sequence to protein sequence, a stop codon was found in the cloned sequences of B22R1-NOR2019 and B22R3-N-NOR2009-W. This will result in a truncated form of these proteins, and B22R1-NOR2019 will be 1098 aa long (normal 2226 aa) while B22R3-N-NOR2009-W will be 891 aa long (normal 1301 aa). B22R1 has a long gene sequence which increases the probability for a mismatch in the amplified products during PCR. The DNA polymerase in the CloneAmp HiFi PCR Premix has an error rate of 12 misincorporations per 542 580 total nucleotides. The probability of a wrongly incorporated nucleotide in the sequence

will be about 15% for B22R1 and 9 % for B22R3. Other reasons for the stop codons could be an error made in the bacterial cultures, or that they are in fact biologically correct. The latter case does not explain the observed expression of the B22R1 protein in the EPC cells. No EPC or ASG-10 cells transfected with the B22R3-N-NOR2009-W was detected. In this construct, the FLAG-tag is located at the N-terminal of the protein and expression of its putative truncated form should not be affected by the stop codon. However, a protein of wrong length and structure could be degraded in the cell, and therefore not able to visualize.

5.8.5 Signal peptide predictions

The *in silico* predictions of the B22R proteins suggest that all proteins have a signal peptide (SP) in the N-terminus and several N-glycosylation sites on the outside of the plasma membrane (figure 15). The SP predictions indicate that the proteins are destined for the ER and the secretory pathway, and the N-glycosylation further supports the involvement with ER, since N-glycosylation occur inside the ER lumen. The hydrophobicity plots and TM predictions also supports the existence of a SP as they show hydrophobicity and helical structures in the same regions of the proteins. TMpred shows that the proteins have several transmembrane domains indicating that they are multipass membrane proteins. It seems like all the three different genes are still functional because the predicted encoded signal peptide and the C-terminal transmembrane helix are conserved (Gjessing et al., 2017b)

5.8.6 Cellular localization predictions

Cellular localization predictions showed that the probability of presence in the nucleus was very low for all three B22R proteins, and as predicted, neither of the proteins was found in the nucleus during microscopy. However, B22R1 has a predicted NLS, meaning that nuclear localization cannot be excluded. It is a possibility that the protein may be present inside the nucleus for a short period of time, and then go back into the cytoplasm, although the NetNES 1.1 server did not predict any nuclear export signals (NESs) in this protein. The transfection experiments express only one gene from the virus, but in reality, several other proteins will also be expressed by the virus. Some of these proteins may interact with each other, and it is a possibility that the protein is missing another interacting protein partner encoded by the virus that enables B22R1 to enter the nucleus. B22R1 is a large protein, and the probability of the exact combination of amino acids to form an NLS-like sequence will increase. Since the protein has only been detected in the cell membrane and has a low score for nuclear localization the NLS may therefore just be a coincidence.

5.8.7 BLAST search

The BLAST hits cover the region of the B22R family motif, indicating that these regions are conserved and might be important for the protein function. In the BLAST search, B22R1 show similarity with a G-protein-coupled-receptor (GPCR)-like protein from cowpox virus. GPCRs are the largest family of cell-surface receptors and mediate responses to extracellular signals from the environment and from other cells. GPCRs use GTP-binding proteins (G-proteins) to transmit the signals into the cell interior (Alberts et al., 2015). These characteristics indicates that the B22R proteins can have a signaling function, although, according to the TM predictions, B22R1 only have 3 TM regions and not 7 which is the typical GPCR structure. Fowlpox was another hit with BLAST search for B22R1 and 3. Fowlpox also have several homologues of the B22R protein to variola, and these proteins are encoded by the largest genes in the fowlpox genome (Afonso et al., 2000). BLAST search for B22R1 and 3 also show a surface glycoprotein from volepox virus. This also provides support for the N-glycosylation predictions.

5.9 What can B22R localization and in silico studies tell us about protein function?

The transfection experiments indicated that B22R1 may be located to the plasma membrane. This corresponds with other research papers stating that B22R proteins are predicted to be membrane proteins and causing T-cells to be non-responsive to stimuli (Alzhanova et al., 2014). This also correlates with the *in silico* predictions done here: B22R1 has a predicted SP and N-glycosylation sites indicating processing through the ER-Golgi pathway; the predicted TM regions indicates that it is a membrane protein; the polybasic region at the C-terminal end also indicates involvement in the secretory pathway. In the confocal microscope, binding of anti-FLAG to the cell membrane was observed in EPC cells transfected with B22R1-NOR2019 (Figure 34, picture 1 and 2). As discussed earlier, a stop codon was observed in the cloned B22R1-NOR2019 sequence, and the possible intact FLAG-tag contradicts this stop codon. Only the gene sequence before the stop codon will be translated into amino acids, and the C-terminal FLAG-tag would not be translated. This contradiction must be further investigated.

The transfection experiments indicate that B22R2 may be located in the cytoplasm. B22R2 also has a predicted SP and N-glycosylation sites, indicating involvement with the ER-Golgi. The TM predictions contradict the observed cytoplasmic localization of this protein. It should not be excluded that the hydrophobic helices predicted to be TM regions here are instead located inside the protein structure. B22R2 is different from B22R1 and 3 because it does not have the

characteristic basic motif at the C-terminal end. This supports the theory of a cytoplasmic presence of B22R2.

For B22R3, two different constructs were made in the cloning procedure; one where the reporter sequence (FLAG-tag) was placed at the N-terminal end of the gene, and another at the C-terminal end. It is important that the reporter sequence (FLAG-tag) does not disturb the functional properties of the protein, and two different FLAG-locations were therefore tested. The C-terminal FLAG-tag location might disturb the protein folding because of the predicted LL motif in this region. In various membrane proteins and membrane receptors, dileucine motifs are known to act as signals for endocytosis and/or post endocytic sorting (Awwad et al., 2010). The N-terminally placed FLAG-tag can also disrupt the folding of the protein, and most importantly the predicted SP which is crucial for the ER-Golgi path predicted for the protein. According to the transfection results, it might seem like the B22R3-C-FLAG has disturbed the protein function. According to the transfection results, it seems like the protein is aggregating inside the cells. The aggregation may happen because the FLAG-tag has disturbed the functional properties of the protein and it will not be able to fold properly. The dual staining with LysoTracker excludes the possibility of the protein being located to lysosomes since there is no visual overlap of the signals. On the other hand, one cannot say for sure that the proteins have aggregated, and the signal pattern observed may reflect its true localization linked to its functional properties. Also, the observed signal pattern could represent localization in early endosomes or ER/Golgi. Picture 15 from Figure 34 shows that there is some overlap with the anti-FLAG stain and ER/Golgi (WGA) stain indicating that the proteins are being sorted by the host cell. It was time consuming to find cells transfected with a B22R3-N-FLAG construct for both isolates. A few transfected cells were observed, and image 14 from Figure 34 of B22R3-N-NOR2019 indicate that the proteins were located near the plasma membrane. Some weakly stained cells might also have been overlooked, disregarded as background staining.

Further investigations are needed to conclude any location of the B22R proteins.

5.10 Future work

This master thesis work was a long process involving many steps. Further development, improvements or investigations of several steps would be necessary. An investigation on SGPV NOR2019 B22R1 and SGPV NOR2009-W B22R3-N-FLAG must be done to determine if the stop codons are in fact present. Complete sequencing of the B22R2 constructs are needed to be able to align these with the reference sequence. The remaining constructs should be possible to

be reused for transfection, and a new cloning procedure will not be necessary although the sequences should be confirmed by minimum two overlapping sequences from sequencing. The transfection experiments should be repeated to confirm that the experiment and results are reproducible. There are also several other protein related studies that can be done. It would be interesting to analyze the two constructs containing a stop codon in the sequence to find the length of these proteins. Extracting the proteins and analyzing them by gel electrophoresis should reveal their expression and their size. A western blot protocol incubated with anti-FLAG should enable visualization of the proteins. The primers and protocols made for the pPCR experiments of B22R2 and 3 gene expression in infected gills can be used as an assay for detection of these genes in addition to B22R1 in later studies. It would be interesting to investigate B22R's interaction with organelles and other proteins in the cell, as well as the hosts immune cells and T-cells in particular. Transfected cells could be co-incubated with T-cells, to analyze how the proteins potentially influence the T-cells. Being able to grow the virus in cell culture would be a great advantage for future studies. Culturing SGPV in the ASG-10 cell line is an ongoing project but has not yet been successful. Additional dyes staining the other cellular components or compartments can be included when analyzing the transfected cells in a fluorescent or confocal microscope. Markers specific for the cell membrane should prove overlap of signal with the B22R proteins. At present, when it comes to cell staining of Atlantic salmon, the assortment is limited. Today, the only available assay for detecting the B22R proteins in infected gills is by targeting cDNA by PCR. Even though the protein encoding gene is transcribed, it is not an absolute certainty that it will be translated into a protein. An immunohistochemical assay with specific antibodies against the proteins will confirm the presence of the proteins.

Gjessing et. al (submitted manuscript 2020, Frontiers in microbiology) discovered that during SGPVD, several genes involved in mucosal protection was downregulated into the late phase of infection, indicating that the SGPVD could result in impaired mucosal defense (Gjessing et al., 2020). Expression of B22R1 in early infection has been confirmed (Amundsen, 2019). During a study of experimentally induced SGPVD in Atlantic salmon (Thoen et al., 2020), Amundsen (master's thesis) investigated expression of several genes from SGPV and Atlantic salmon. It was not possible to differentiate between the expression of most early, intermediate and late viral genes, except from B22R1 that had a higher expression compared to the other viral genes at day one (Amundsen, 2019). This indicates that B22R1 might play a part in the initial phase of SGPV infection. Interleukin (IL) -22 is a cytokine expressed by T-cells and is

known to induce inflammation and promote wound closure and recovery after damage of epithelial cells. IL-22 is strongly suppressed during early infection of SGPV, indicating that this could be regulated by the virus (Gjessing et al., 2020). B22R proteins has been proven to inactivate T-cells and increase viral virulence (Alzhanova et al., 2014). These observations support the hypothesis that B22R proteins expressed by SGPV inactivates T-cells in early infection, leading to a weakened immune system, and increased viral virulence. The pPCR confirmed that B22R2 and 3 are also being expressed during SGPVD, and it would be interesting to further investigate how they are expressed during a course of infection. Especially if these proteins also have a high early expression as B22R1, and if they could be involved in other viral mechanisms.

6. conclusions

- Cloning of B22R genes from two genetic variants of SGPV into an expression vector was successful
- Transfection optimization of EPC cell lines and ASG-10 cell lines has been done, and plasmid transfection by lipofection seems to be a bad solution for transfecting ASG-10 cells. Further testing of transfection optimization of the ASG-10 cell line with electroporation and preferably mRNA transfection is required.
- *In silico* investigation of the B22R protein sequences provides a better understanding of their structure and properties, as well as information about protein family regions, and identity and similarity to other B22R proteins.
- After studying localizations of the proteins, these hypotheses were made: the B22R1 protein appears to be membrane-bound, B22R2 appears to be cytoplasmic, and B22R3 may be in ER/Golgi or the membrane.
- qPCR of extracted RNA from infected gills proves that all three B22R variants are present during an infection with SGPV.

References

AAT BIOQUEST, I. 2019.

ABBAS, A. K. & LICHTMAN, A. H. 2009. *Basic Immunology Functions and Disorders of the Immune System,* Philadelphia, US, Elsevier.

ADAN, A., ALIZADA, G., KIRAZ, Y., BARAN, Y. & NALBANT, A. 2017. Flow cytometry: basic principles and applications.

AFONSO, C. L., TULMAN, E. R., LU, Z., ZSAK, L., KUTISH, G. F. & ROCK, D. L. 2000. The Genome of Fowlpox Virus. *Journal of Virology,* 74**,** 3815.

AGILENTTECHNOLOGIES 2020. Agilent 2100 Bioanalyzer System. Germany: Agilent Technologies.

ALBERTS, B., JOHNSON, A., LEWIS, J., MORGAN, D., RAFF, M., ROBERTS, K. & WALTER, P. 2015. *Molecular Biology of the Cell,* New York, US, Garland Science.

ALZHANOVA, D., HAMMARLUND, E., REED, J., MEERMEIER, E., RAWLINGS, S., RAY, C. A., EDWARDS, D. M., BIMBER, B., LEGASSE, A., PLANER, S., SPRAGUE, J., AXTHELM, M. K., PICKUP, D. J., LEWINSOHN, D. M., GOLD, M. C., WONG, S. W., SACHA, J. B., SLIFKA, M. K. & FRÜH, K. 2014. T Cell Inactivation by Poxviral B22 Family Proteins Increases Viral Virulence (T Cell Inactivation by Poxviral B22 Proteins). 10**,** e1004123.

AMUNDSEN, M. M. 2019. *Salmon Gill Poxvirus Disease (SGPVD) in Atlantic salmon (salmo salar), development of disease and gene expression in virus and host.* Master's Degree Master's Thesis, Norwegian University of Life Sciences.

AWWAD, H. O., MILLMAN, E. E., ALPIZAR-FOSTER, E., MOORE, R. H. & KNOLL, B. J. 2010. Mutating the dileucine motif of the human β 2-adrenoceptor reduces the high initial rate of receptor phosphorylation by GRK without affecting postendocytic sorting. *European Journal of Pharmacology,* 635**,** 9-15.

BAUER, C. R. 2014. Labeling and Use of Monoclonal Antibodies in Immunofluorescence: Protocols for Cytoskeletal and Nuclear Antigens. *In:* OSSIPOW, V. & FISCHER, N. (eds.) *Monoclonal Antibodies: Methods and Protocols.* Totowa, NJ: Humana Press.

BIONTEX. *Transfection* [Online]. Available: https://www.biontex.com/en/transfection/ [Accessed 2020].

BRENCICOVA, E. & DIEBOLD, S. S. 2013. Nucleic acids and endosomal pattern recognition: how to tell friend from foe? *Frontiers in cellular and infection microbiology,* 3**,** 37-37.

BØRRESEN-DALE, A. L. 2018. Restriksjonsenzymer. *Store medisinske leksikon.*

CANN, A. J. 2001. *Principles of Molecular Virology,* Somerset, UK, Academic Press.

CONDIT, R. C., MOUSSATCHE, N. & TRAKTMAN, P. 2006. In A Nutshell: Structure and Assembly of the Vaccinia Virion. *Advances in Virus Research.* Academic Press.

DEGRÈ, M., HOVIG, B. & ROLLAG, H. 2010. *Medisinsk Mikrobiologi*.

DELL, A., GALADARI, A., SASTRE, F. & HITCHEN, P. 2010. Similarities and Differences in the Glycosylation Mechanisms in Prokaryotes and Eukaryotes. *International Journal of Microbiology,* 2010**,** 148178.

EINHAUER, A. & JUNGBAUER, A. 2001. The FLAG™ peptide, a versatile fusion tag for the purification of recombinant proteins. *Journal of Biochemical and Biophysical Methods,* 49**,** 455-465.

FAUSKE, M. 2019. *Hvor stor er oppdrettsnæringen i Norge?* [Online]. Fiskeridirektoratet. Available: https://www.fiskeridir.no/Akvakultur/Nyheter/2019/0519/Hvor-stor-er-oppdrettsnaeringen-i-Norge [Accessed 08.05.20 2020].

FIJAN, N., SULIMANOVIĆ, D., BEARZOTTI, M., MUZINIĆ, D., ZWILLENBERG, L. O., CHILMONCZYK, S., VAUTHEROT, J. F. & DE KINKELIN, P. 1983. Some

properties of the Epithelioma papulosum cyprini (EPC) cell line from carp cyprinus carpio. *Annales de l'Institut Pasteur / Virologie,* 134**,** 207-220.
FISKERIDIREKTORATET 2019. Statistikk for akvakultur 2018.
GARSETH, Å. H., GJESSING, M. C., MOLDAL, T. & GJEVRE, A. G. 2018. A survey of salmon gill poxvirus (SGPV) in wild salmonids in Norway. *Journal of Fish Diseases,* 41**,** 139-145.
GJESSING, M., CHRISTENSEN, D., MANJI, F., MOHAMMAD, S., PETERSEN, P., SAURE, B., SKJENGEN, C., WELI, S. & DALE, O. 2017a. Salmon gill poxvirus disease in Atlantic salmon fry as recognized by improved immunohistochemistry also demonstrates infected cells in non-respiratory epithelial cells. *Journal of Fish Diseases,* 41.
GJESSING, M., KRASNOV, A., TIMMERHAUS, G., BRUN, S., AFANASYEV, S., DALE, O. B. & DAHLE, M. K. 2020. The Atlantic salmon gill transcriptome response in a natural outbreak of salmon gill pox virus infection reveals new biomarkers of gill pathology and suppression of mucosal defense. Oslo, Ås: The Norwegian Veterinary Institute.
GJESSING, M. C., AAMELFOT, M., BATTS, W. N., BENESTAD, S. L., DALE, O. B., THOEN, E., WELI, S. C. & WINTON, J. R. 2018. Development and characterization of two cell lines from gills of Atlantic salmon.(Research Article). *PLoS ONE,* 13**,** e0191792.
GJESSING, M. C., STEINUM, T., OLSEN, A. B., LIE, K. I., TAVORNPANICH, S., COLQUHOUN, D. J. & GJEVRE, A.-G. 2019. Histopathological investigation of complex gill disease in sea farmed Atlantic salmon. *PLOS ONE,* 14**,** e0222926.
GJESSING, M. C., THOEN, E., TENGS, T., SKOTHEIM, S. A. & DALE, O. B. 2017b. Salmon gill poxvirus, a recently characterized infectious agent of multifactorial gill disease in freshwater- and seawater-reared Atlantic salmon.
GJESSING, M. C., WELI, S. C. & DALE, O. B. 2016. Chapter 7 - Poxviruses of Fish. *In:* KIBENGE, F. S. B. & GODOY, M. G. (eds.) *Aquaculture Virology.* San Diego: Academic Press.
GJESSING, M. C., YUTIN, N., TENGS, T., SENKEVICH, T., KOONIN, E., RØNNING, H. P., ALARCON, M., YLVING, S., LIE, K.-I., SAURE, B., TRAN, L., MOSS, B. & DALE, O. B. 2015. Salmon Gill Poxvirus, the Deepest Representative of the <span class="named-content genus-species" id="named-content-1">Chordopoxvirinae</span&gt. *Journal of Virology,* 89**,** 9348.
GOODWIN, S., J.D, M. & R.W, M. 2016. Coming of age: ten years of next-generation sequencing technologies. *Nature Reviews Genetics,* 17**,** 333.
GULLA, S., TENGS, T., MOHAMMAD, S. N., GJESSING, M., GARSETH, Å. H., SVEINSSON, K., MOLDAL, T., PETERSEN, P. E., TØRUD, B., DALE, O. B. & DAHLE, M. K. 2020. Genotyping of Salmon Gill Poxvirus Reveals One Main Predominant Lineage in Europe, Featuring Fjord- and Fish Farm-Specific Sub-Lineages. *Frontiers in Microbiology,* 11.
HALLER, S. L., PENG, C., MCFADDEN, G. & ROTHENBURG, S. 2014. Poxviruses and the evolution of host range and virulence. *Infection, Genetics and Evolution,* 21**,** 15-40.
HERRERO, A., THOMPSON, K. D., ASHBY, A., RODGER, H. D. & DAGLEISH, M. P. 2018. Complex Gill Disease: an Emerging Syndrome in Farmed Atlantic Salmon (Salmo salar L.). *Journal of Comparative Pathology,* 163**,** 23.
HORNSTEIN, B. D., DANY, R., LIRIO, M. A.-S., MELINDA, A. E. & LYNN, Z. 2016. Effects of Circular DNA Length on Transfection Efficiency by Electroporation into HeLa Cells. *PLoS ONE,* 11**,** e0167537.
JACOBSEN, E. 2019. Elektroforese. *Store norske leksikon.* Norway: Store norske leksikon.

JIA, Y. 2012. Chapter 3 - Real-Time PCR. *In:* CONN, P. M. (ed.) *Methods in Cell Biology.* Academic Press.
KAESTNER, L., SCHOLZ, A. & LIPP, P. 2015. Conceptual and technical aspects of transfection and gene delivery. *Bioorganic & Medicinal Chemistry Letters,* 25**,** 1171-1176.
KIM, T. & EBERWINE, J. 2010. Mammalian cell transfection: the present and the future. *Analytical and Bioanalytical Chemistry,* 397**,** 3173-3178.
KLEPP, O. 2020. *Interferoner* [Online]. NTNU, Trondheim, Norway: Store Medisinske Leksikon. Available: https://sml.snl.no/interferoner [Accessed 20.04.20 2020].
KOPPANG, E. O., KVELLESTAD, A. & FISCHER, U. 2015. 5 - Fish mucosal immunity: gill. *In:* BECK, B. H. & PEATMAN, E. (eds.) *Mucosal Health in Aquaculture.* San Diego: Academic Press.
KREISS, P., MAILHE, P., SCHERMAN, D., PITARD, B., CAMERON, B., RANGARA, R., AGUERRE-CHARRIOL, O., AIRIAU, M. & CROUZET, J. 1999. Plasmid DNA size does not affect the physicochemical properties of lipoplexes but modulates gene transfer efficiency. *Nucleic Acids Research,* 27**,** 3792-3798.
KRYVI, H. & POPPE, T. 2016. *Fiskeanatomi,* Bergen, Oslo, Fagbokforlaget.
LEBLANC, F., DITLECADET, D., ARSENEAU, J.-R., STEEVES, R., BOSTON, L., BOUDREAU, P. & GAGNÉ, N. 2019. Isolation and identification of a novel salmon gill poxvirus variant from Atlantic salmon in Eastern Canada. *Journal of Fish Diseases,* 42**,** 315-318.
LESK, A. M. 2016. *Introduction to protein science : architecture, function, and genomics,* Oxford, Oxford University Press.
LIU, G., MOON, T. W., METCALFE, C. D., LEE, L. E. J. & TRUDEAU, V. L. 2005. A teleost in vitro reporter gene assay to screen for agonists of the peroxisome proliferator-activated receptors. *Environmental Toxicology and Chemistry,* 24**,** 2260-2266.
LODISH, H., BERK, A., ZIPURSKY, S. L., MATSUDARIA, P., BALTIMORE, D. & DARNELL, J. 2000. *Molecular Cell Biology,* New York, W. H. Freeman.
LONZA 2009. Amaxa® Cell Line Nucleofector® Kit T. Germany: Lonza Cologne AG.
MAGNADOTTIR, B. 2010. Immunological Control of Fish Diseases. *Marine Biotechnology,* 12**,** 361-379.
MOUSSATCHE, N. & CONDIT, R. C. 2015. Fine structure of the vaccinia virion determined by controlled degradation and immunolocalization. *Virology,* 475**,** 204-218.
NVI 2019. Fiskehelserapporten. *Fiskehelserapporten***,** 7-8, 10, 12-13,15, 42.
NYLUND, A., WATANABE, K., NYLUND, S., KARLSEN, M., SÆTHER, P. A., ARNESEN, C. E. & KARLSBAKK, E. 2008. Morphogenesis of salmonid gill poxvirus associated with proliferative gill disease in farmed Atlantic salmon (Salmo salar) in Norway. *Archives of Virology,* 153**,** 1299-1309.
OKAMOTO, Y., BERNSTEIN, J. D. & SHIKANO, S. 2013. Role of C-terminal membrane-proximal basic residues in cell surface trafficking of HIV coreceptor GPR15 protein. *The Journal of biological chemistry,* 288**,** 9189-9199.
OLSON, K. R. 2000. Chapter 9 - Respiratory System. *In:* OSTRANDER, G. K. (ed.) *The Laboratory Fish.* London: Academic Press.
PARK, J., THROOP, A. L. & LABAER, J. 2015. Site-specific recombinational cloning using gateway and in-fusion cloning schemes. *Current protocols in molecular biology,* 110**,** 3.20.1-3.20.23.
PARMAR, H. B., BARRY, C. & DUNCAN, R. 2014. Polybasic trafficking signal mediates Golgi export, ER retention or ER export and retrieval based on membrane-proximity.(Report). *PLoS ONE,* 9.

POLYPLUSTRANSFECTION 2019. What is transfection? - Polyplus transfection. *1:36-3:00*. YouTube.
QIAGEN. *Features of QIAGEN CLC Main Workbench* [Online]. Available: https://digitalinsights.qiagen.com/products-overview/discovery-insights-portfolio/analysis-and-visualization/qiagen-clc-main-workbench/ [Accessed 22.04.20 2020].
RAMAN, M. 2015. Cloning without compromise Discover In Fusion! *00.00-17.00 min*. YouTube: Condalab.
RUZGYS, P., JAKUTAVIČIŪTĖ, M., ŠATKAUSKIENĖ, I., ČEPURNIENĖ, K. & ŠATKAUSKAS, S. 2019. Effect of electroporation medium conductivity on exogenous molecule transfer to cells in vitro. *Scientific reports*, 9**,** 1436-1436.
SAND, O., SJAASTAD, Ø. V., HAUG, E., BJÅLIE, J. G. & TOVERUD, K. C. 2012. *Menneskekroppen: Fysiologi og anatomi*, Oslo, Gyldendal Norsk Forlag AS.
SMITH, G. L., BENFIELD, C. T. O., MALUQUER DE MOTES, C., MAZZON, M., EMBER, S. W. J., FERGUSON, B. J. & SUMNER, R. P. 2013. Vaccinia virus immune evasion: mechanisms, virulence and immunogenicity. *The Journal of general virology*, 94**,** 2367-2392.
SOMPAYRAC, L. 2012. *How the Immune System Works*, John Wiley & Sons, Ltd, The Atrium, Southern Gate, Chichester, West Sussex, PO19, UK, Wiley-Blackwell.
SUN, Q.-Y., DING, L.-W., HE, L.-L., SUN, Y.-B., SHAO, J.-L., LUO, M. & XU, Z.-F. 2009. Culture of Escherichia coli in SOC medium improves the cloning efficiency of toxic protein genes. *Analytical Biochemistry*, 394**,** 144-146.
TAKARA BIO, I. E. coli HST08 Premium Competent Cells.
TAKARA BIO, I. 2020. In-Fusion® Cloning mechanism.
TAKARA BIO USA, I. 2016. In-Fusion® HD Cloning Kit User Manual. 1-15.
TESGERA, T., HUAIJIE, J., CHEN, G., XIANG, F., HE, X., WANG, X. & JING, Z. 2019. Methodical Review on Poxvirus Replication, Genes Responsible for the Development of Infection and Host Immune Response Against the Disease. *Archives of Microbiology & Immunology*, 03.
THERMOFISHER. *How Cationic Lipid Mediated Transfection Works* [Online]. Thermo Fisher Scientific. Available: https://www.thermofisher.com/no/en/home/references/gibco-cell-culture-basics/transfection-basics/gene-delivery-technologies/cationic-lipid-mediated-delivery/how-cationic-lipid-mediated-transfection-works.html [Accessed 12.04.20 2020].
THERMOFISHER 2015a. Anza™ Restriction Enzyme Cloning System. 23.
THERMOFISHER 2015b. PureLink™ HiPure Plasmid DNA Purification Kits. 18-22.
THERMOFISHERSCIENTIFIC 2009. NanoDrop 2000 User Manual. USA.
THOEN, E., TARTOR, H., AMUNDSEN, M., DALE, O. B., SVEINSSON, K., RØNNING, H. P., GRØNNEBERG, E., DAHLE, M. K. & GJESSING, M. C. 2020. First record of experimentally induced salmon gill poxvirus disease (SGPVD) in Atlantic salmon (Salmo salar L.). *Veterinary Research*, 51**,** 63.
VIRALZONE Poxvirus Replication Cycle. Swiss Institute of Bioinformatics.
VIRALZONE 2014. Poxviridae Virion. Swiss Institute of Bioinformatics.
VØLLESTAD, A. 2019. *Laks* [Online]. Store norske leksikon. Available: https://snl.no/laks [Accessed 04.05.20 2020].
WATSON, J. D., BAKER, T. A., BELL, S. P., GANN, A., LEVINE, M. & LOSICK, R. 2014. *Molecular Biology of the Gene*, The United States of America.
WENNEVIK, V. & HANSEN, T. 2019. *Tema: Laks* [Online]. Havforskningsinstituttet. Available: https://www.hi.no/hi/temasider/arter/laks [Accessed 04.05.20 2020].

WINTON, J., BATTS, W., DEKINKELIN, P., LEBERRE, M., BREMONT, M. & FIJAN, N. 2010. Current lineages of the epithelioma papulosum cyprini (EPC) cell line are contaminated with fathead minnow, Pimephales promelas, cells. *Journal of fish diseases,* 33**,** 701-704.

YU, X., GENG, W., ZHAO, H., WANG, G., ZHAO, Y., ZHU, Z. & GENG, X. 2017. Using a Commonly Down-Regulated Cytomegalovirus (CMV) Promoter for High-Level Expression of Ectopic Gene in a Human B Lymphoma Cell Line. *Medical science monitor : international medical journal of experimental and clinical research,* 23**,** 5943-5950.

Appendix

1.0 Cloning

1.1 Linearization of plasmid

Materials:

- Vector: pcDNA™3.1(+), 0,5 µg/µL
- Anza™ Restriction Enzyme Cloning System
- Nuclease Free Water
- Add the reagents in the order indicated in table 1.

Table 1: Linearization protocol based on the user guide "Anza™ Restriction Enzyme Cloning System".

Restriction digestion protocol	
Reagent	*Volume (µL)*
Nuclease-Free Water	Up to final required volume
Anza™ 10X buffer	2
pcDNA 3.1 vector	(0,2-1 µg)
Anza™ 16 (HindIII enzyme)	1
Final volume	**20**

1. Incubate at 37 °C for 15 minutes.

1.2 Gel electrophoresis

Protocols are based on the available manuals at the Norwegian Veterinary Institutes databases.

Materials used:

- Agarose, universal, pecGOLD, VWR. Product code: 443666A.
- 1X TBE buffer
- GelRed™ from Biotium. Cat.: 41003
- GeneRuler 1 kb DNA Ladder. Cat.: SM0313
- 6X DNA Loading dye. Cat.: R0611

- Gel tray and comb
- Gel caster
- Electrophoresis chamber with electrodes
- Power pack
- UV Transilluminator
- ChemiDoc XRS by BioRad

Manual (small gel):

- Put 0,5 g agarose powder + 50 mL TBE 1x buffer in a reagent bottle
- Microwave until powder is fully solved
- Let cool for a few minutes
- Add 5 µL GelRed and mix
- Prepare a gel tray with a fitting comb in a gel caster
- Pour the gel mix into the gel tray and let be until solidified
- Prepare the samples: Total volume will be 6 µL. Add 1-5 µL with sample and add water as required to make up final volume. Add 1 µL of loading dye (1/6 of total volume). The ladder is ready to use.
- Put the gel in an electrophoresis chamber filled with 1x TBE
- Add the samples and 2 µL ladder (database protocol says 5 µL ladder, but resulted in a "smear" at the gel) into the respective wells
- Close the lid and put the electrodes in a power pack, and put on a voltage at about 100 (mV??)
- Follow the color from the loading dye in the samples and stop the reaction when they have travelled about 2/3 through the gel.
- Examine the gel either with a UV Transilluminator or take a picture of the gel with a ChemiDoc XRS.

1.3 B22R Insert PCR

This protocol is based on the CloneAmp™ HiFi PCR Premix Protocol from TaKaRa Bio. https://www.takarabio.com/products/pcr/pcr-master-mixes/high-fidelity/cloneamp-hifi-pcr-premix.

Materials:

- ClonTech (TaKaRa): CloneAmp™ HiFi PCR Premix
- Nuclease Free Water
- Fragment primers: See table x. Stock solutions; 100 µM. Diluted, ready to use; 5 µM
- Thermo cycler
- Isolates/templates: NOR2009-W (21,8 ng/µL) and 2019-04-287/F2 (25 ng/µL), negative control from same infection experiment 2019 (2,5 ng/µL).

1. Add all the reagents in table 2 into a test tube/directly into respective wells in a PCR strip.

Table 2: reaction mix for the CloneAmp HiFi PCR.

CloneAmp™ HiFi PCR		
Reagent	*Volume (µL)*	*Final Conc.*
HiFi Premix	10	1X
F-primer	2	0,2-0,3 µM
R-primer	2	0,2-0,3 µM
Template	4	< 100 ng
H2O	2	
Total	20	

2. Mix briefly by tapping the bottom of the tube and do a short spin.
3. Set up a thermal cycler with the following program:

Temperature	Time	Step
98°C	30 sec	Preheat
98°C	10 sec	34 cycles
55°C	15 sec	
72°C	1 min (5 sec/kb)	
72°C	5 min	Elongation
4°C	∞	

1.4 Colony-PCR

Materials:

- LB broth with 50 mg/L ampicillin
- Phusion High-Fidelity PCR Master Mix, Thermo Scientific
- Nuclease Free Water
- 1 µL bacterial suspension

Table 3: Reaction mix for colony-PCR

Colony-PCR		
Components	Volume µL	Final conc.
2X Phusion Master Mix	10	
F-primer (B22R1/T7)	1	
R-primer (BHG)	1	0,5 µM
Template	1	0,5 µM
Nuclease Free Water	7	
Total	20	

Temperature	Time	step
94°C	3 min	Preheat
94°C	45 sec	34 cycles
55°C	30 sec	
72°C	3 min	
72°C	10 min	Elongation
4°C	∞	

2.0 Flow cytometry

Protocol for preparation of cells from a 48 well plate:

1. Remove medium and wash cells with 500 µL PBS
2. Add 100 µL TrypLE and incubate until cells are detached and in solution (incubation time depends on cell type).

3. Add 400 µL complete growth medium and transfer each sample to an Eppendorf tube
4. Sentrifuge at 500 g for 10 minutes at 4 °C
5. Gently remove the supernatant, and let about 50 µL be left in the tube to ensure no cells are removed
6. Resuspend in 150 µL PBS and transfer each sample to a flow tube
7. Add 2 µL Propidium Iodide (concentration: 1 mg/mL)
8. Put samples on ice until analysis

3.0 Immunochemical staining

The first protocol includes a staining procedure for visualization of cells by a fluorescence microscope. Cytofix/Cytoperm™ Kit (Cat. No. 554714) from BD has been used to fix and permeabilize the cells in this protocol. The 10X Perm/wash buffer was diluted to 1X.

3.1 Protocol for staining cells from a 48 well plate with Anti-FLAG:

1. Wash the cells carefully 2-3 times with 500 µL PBS
2. Fix cells with 200 µL Cytofix/cytoperm solution from in 30 min.
3. Wash cells 2-3 times with 500 µL PBS
4. Add 1X Perm/wash buffer and incubate for 15 min.
5. Add 100 µL Anti-FLAG (2 µg/mL in Perm/wash) and incubate 1 hour
6. Wash the cells 2-3 times with 500 µL PBS. Add DAPI directly into the wells filled with PBS in the last wash (0,01 µg/µL) and incubate for 5 min.

3.2 Staining protocols to prepare cells for confocal microscopy:

Anti-FLAG, DAPI and Lysotracker:

- Allow the Lysotracker reagent to reach room temperature, then spin down the tube
- Dilute 0,5 µL supernatant in 10 mL L-15 medium (50 nM)
- Remove medium from culture plates and add 400 µL diluted Lysotracker. Let incubate for 30 min. Use fluorescent microscope to see if any staining is appearing.

- Wash the cells carefully 2 times with 500 µL PBS. Let incubate for 5 min for each wash step.
- Fix cells with 4% PFA for 30 min
- Wash the cells carefully 2 times with 500 µL PBS. Let incubate for 5 min for each wash step.
- Permeabilize/block in 400 µL 3% BSA/PBS/0,05 saponin for 30 min at room temperature.
- Add 300 µL Anti-FLAG dissolved in 1% BSA/PBS/0,05 saponin and incubate dark, in room temperature for one hour.
- Wash the cells carefully 2 times with 500 µL PBS. Let incubate for 5 min for each wash step. Include DAPI (1:1000) in the last was step.
- Wash one time with 500 µL water and let air-dry.
- Mount cover slides with mounting medium on microscope slides (NB: cell side down against the microscope slide)
- Let dry flat, dark in room temperature overnight.

Anti-FLAG, DAPI and Phalloidin:

- Remove medium from culture plates and wash the cells carefully 2 times with 500 µL PBS. Let incubate for 5 min for each wash step.
- Fix cells with 4% PFA for 30 min
- Wash the cells carefully 2 times with 500 µL PBS. Let incubate for 5 min for each wash step.
- Permeabilize/block in 400 µL 3% BSA/PBS/0,05 saponin for 30 min at room temperature.
- Add 300 µL Anti-FLAG dissolved in 1% BSA/PBS/0,05 saponin and incubate dark, in room temperature for one hour.
- Dilute Phalloidin: 5 µL stock + 195 µL 1%/BSA/PBS (1:40)
- Add 300 µL Phalloidin and let incubate for 20 min dark and in room temperature

- Wash the cells carefully 2 times with 500 µL PBS. Let incubate for 5 min for each wash step. Include DAPI (1:1000) in the last was step.
- Wash the cells carefully one time with 500 µL water and let air-dry.
- Mount cover slides with mounting medium on microscope slides (NB: cell side down against the microscope slide)
- Let dry flat, dark in room temperature overnight.

Anti-FLAG, DAPI and WGA:

- Remove medium from culture plates and wash the cells carefully 2 times with 500 µL PBS. Let incubate for 5 min for each wash step.
- Fix cells with 4% PFA for 30 min
- Wash the cells carefully 2 times with 500 µL PBS. Let incubate for 5 min for each wash step.
- Permeabilize/block in 400 µL 3% BSA/PBS/0,05 saponin for 30 min at room temperature.
- Add 300 µL Anti-FLAG dissolved in 1% BSA/PBS/0,05 saponin and incubate dark, in room temperature for one hour.
- Wash the cells carefully 2 times with 500 µL PBS. Let incubate for 5 min for each wash step.
- Dilute WGA to 10 µL/mL
- Add diluted WGA to the cells and incubate dark, in room temperature for one hour.
- Wash the cells carefully 2 times with 500 µL PBS. Let incubate for 5 min for each wash step. Include DAPI (1:1000) in the last was step.
- Wash one time with 500 µL water and let air-dry.
- Mount cover slides with mounting medium on microscope slides (NB: cell side down against the microscope slide)
- Let dry flat, dark in room temperature overnight.

4.0 Cell culturing and transfection

4.1 Cell splitting

Cell splitting of a 75 cm^2 flask protocol:

1. Remove medium
2. Add 10 mL PBS (Ca^{+}/Mg^{2+} free) to wash the cells. Remove.
3. Add 2 mL TrypLE
4. Incubate at room temperature for 2-7 minutes (depending on cell line)
5. Knockm the bottle gently to detach the cells
6. Add 5-10 mL complete growth medium

4.2 Transfection

4.2.1 EPC transfection setups and Flow Cytometry results

Table 4: Plate setup for transfection of EPC using the METAFECTENE and K2 reagent kits.

		150 000 cells/cm^2		*250 000 cells/cm^2*					
		1	**2**	**3**	**4**	**5**	**6**	**7**	**8**
K2	**A**	0,3 µg phMGFP	0,3 µg pGFP	0,3 µg phMGFP	0,3 µg pGFP				
METAF.	**B**	0,2 µg phMGFP	0,2 µg pGFP	0,2 µg phMGFP	0,2 µg pGFP				
	C			neg K2	neg METAF.				
	D								
	E								
	F								

2,5 µLK2® Multiplier in each K2 well

1,2 µL K2® transfection reagent in each K2 well

1 µL METAFECTENE® in each METAFECTENE well

Table 5: Flow Cytometry results from transfection of EPC using the METAFECTENE and K2 reagent kits. The well names refer to table 4.

Well	% transfected cells (M3 gate)
A1	6,25
A2	6,42
A3	9,77
A4	7,64
B1	0,51
B2	0,11
B3	0,68
B4	0,05

Table 6: Plate setup for transfection of EPC with the K2 transfection kit and all the different constructs.

250 000 cells/cm²

		1	2	3	4	5	6	7	8
K2	**A**	0,3 µg* pGFP	NC +Ab-stain.						
K2	**B**	B22R1-19	B22R1-W						
K2	**C**	B22R2-19	B22R2-W						
K2	**D**	B22R3-C-19	B22R3-C-W						
K2	**E**	B22R3-N-19	B22R3N-W						
K2	**F**	NC ÷ Ab-stain.							

* 0,3 ng DNA in all wells

2,5 µLK2® Multiplier in each well

1,2 µL K2® transfection reagent in each well

Table 7: Plate setup for K2, Lipofectamine 2000 and Lipofectamine 3000 optimization of EPC.

Cell density (cells/well):		*5 000*			*10 000*			*20 000*				*40 000*	
Reagent:		**1**	**2**	**3**	**4**	**5**	**6**	**7**	**8**	**9**	**10**	**11**	**12**
K2	**A**				0,15 µg 0,3 µL	0,15 µg 0,45 µL	0,15 µg 0,6 µL	0,15 µg 0,3 µL	0,15 µg 0,45 µL	0,15 µg 0,6 µL	0,15 µg 0,3 µL	0,15 µg 0,45 µL	**0,15 µg 0,6 µL**
Lipof. 2000	**B**				0,2 µg 0,1 µL	0,2 µg 1,5 µL	0,2 µg 2 µL	0,2 µg 0,1 µL	0,2 µg 1,5 µL	0,2 µg 2 µL	0,2 µg 0,1 µL	0,2 µg 1,5 µL	0,2 µg 2 µL
Lipof. 3000	**C**				0,2 µg 0,15 µL	0,2 µg 0,3 µL	0,2 µg 0,5 µL	0,2 µg 0,15µL	0,2 µg 0,3 µL	0,2 µg 0,5 µL	0,2 µg 0,15 µL	0,2 µg 0,3 µL	0,2 µg 0,5 µL
NC	**D**												
K2	**E**				0,15 µg 0,3 µL	0,15 µg 0,45 µL	0,15 µg 0,6 µL	0,15 µg 0,3 µL	0,15 µg 0,45 µL	0,15 µg 0,6 µL	0,15 µg 0,3 µL	0,15 µg 0,45 µL	**0,15 µg 0,6 µL**
Lipof. 2000	**F**				0,2 µg 0,1 µL	0,2 µg 1,5 µL	0,2 µg 2 µL	0,2 µg 0,1 µL	0,2 µg 1,5 µL	0,2 µg 2 µL	0,2 µg 0,1 µL	0,2 µg 1,5 µL	0,2 µg 2 µL
Lipof. 3000	**G**				0,2 µg 0,15 µL	0,2 µg 0,3 µL	0,2 µg 0,5 µL	0,2 µg 0,15µL	0,2 µg 0,3 µL	0,2 µg 0,5 µL	0,2 µg 0,15 µL	**0,2 µg 0,3 µL**	0,2 µg 0,5 µL
NC	**H**												

*Blue: Opti-MEM

*White: L-15

*100 µL of cell suspension in each well

Table 8: plate setup for transfection of EPC with the eight constructs with K2® Transfection System and Lipofectamine™ 3000 Reagent

Reagent:	*Samples:*	*phMGFP*	*B22R1-19*	*B22R2-19*	*B22R3C-19*	*B22R3N-19*	*B22R1-W*	*B22R2-W*	*B22R3C-W*	*B22R3N-W*	*neg*			*Cell density (cells/well):*
		1	**2**	**3**	**4**	**5**	**6**	**7**	**8**	**9**	**10**	**11**	**12**	
K2	**A**	0,15 µg DNA 0,6 µL reagent	0,15 µg 0,6 µL	0,15 µg 0,6 µL	0,15 µg 0,6 µL	0,15 µg 0,6 µL	0,15 µg 0,6 µL	0,15 µg 0,6 µL	0,15 µg 0,6 µL	0,15 µg 0,6 µL	0 µg 0,6 µL	Ab ÷		*30 000*
Lipof. 3000	**B**	0,2 µg DNA 0,3 µL reagent	0,2 µg 0,3 µL	0,2 µg 0,3 µL	0,2 µg 0,3 µL	0,2 µg 0,3 µL	0,2 µg 0,3 µL	0,2 µg 0,3 µL	0,2 µg 0,3 µL	0,2 µg 0,3 µL	0 µg 0,3 µL			*30 000*
K2	**C**	0,15 µg DNA 0,6 µL reagent	0,15 µg 0,6 µL	0,15 µg 0,6 µL	0,15 µg 0,6 µL	0,15 µg 0,6 µL	0,15 µg 0,6 µL	0,15 µg 0,6 µL	0,15 µg 0,6 µL	0,15 µg 0,6 µL	0 µg 0,6 µL			*30 000*
Lipof. 3000	**D**	0,2 µg DNA 0,3 µL reagent	0,2 µg 0,3 µL	0,2 µg 0,3 µL	0,2 µg 0,3 µL	0,2 µg 0,3 µL	0,2 µg 0,3 µL	0,2 µg 0,3 µL	0,2 µg 0,3 µL	0,2 µg 0,3 µL	0 µg 0,3 µL			*30 000*
	E													
	F													
	G													
	H													

Table 9: setup for transfection of EPC with Lipofectamine™ 3000 and 8 constructs to be used for confocal microscopy.

Plate 1						
	1	**2**	**3**	**4**	**5**	**6**
A	B22R1-19	B22R1-W	B22R1-19	B22R1-W	**MGFP**	
B	B22R2-19	B22R2-W	B22R2-19	B22R2-W	**NC**	
C	B22R3-C-19	B22R3-C-W	B22R3-C-19	B22R3-C-W		
D	B22R3-N-19	B22R3-N-W	B22R3-N-19	B22R3-N-W		
Plate 2						
	1	2	3	4	5	6
A	B22R1-19	B22R1-W				
B	B22R2-19	B22R2-W				
C	B22R3-C-19	B22R3-C-W				
D	B22R3-N-19	B22R3-N-W				

Light blue: Anti-flag, DAPI and Phalloidin

White: Anti-flag, DAPI and WGA

Dark blue: Anti-flag, DAPI and Lysotracker

2.2.2 ASG-10 transfection setups and Flow Cytometry results

Table 10: Plate setup for transfection of ASG-10 using the METAFECTENE and K2 reagent kits.

METAFECTENE		
Well 1	*Well 2*	*Well 3*
? tror ikke vi tok noe oppi her	30 µL serum-free medium, 1µL METAFECTENE	0,2 µg DNA, 30 µL serum- free medium, 1µL METAFECTENE
K2		
Well 4	*Well 5*	*Well 6*
30 µL serum-free medium, 1.2 µL K2 reagent	0,3 µg DNA, 30µL serum-free medium, 1.2 µL K2 reagent	0,6 µg DNA, 30 µL serum-free medium, 1.2µL K2 reagent

Table 11: Plate setup of transfection optimization of ASG-10 with K2® Transfection System. The best result seen in the microscope is highlighted with a green color.

		1	**2**	**3**	**4**	**5**	**6**	**7**	**8**
2,5 µl K2® Multiplier in each well	**A**	0,2 1:2	0,3 1:2	~~0,4~~ ~~1:2~~	0,2 1:3	0,3 1:3	~~0,4~~ ~~1:3~~		
	B	0,2 1:4	0,3 1:4	~~0,4~~ ~~1:4~~	0,2 1:5	0,3 1:5	~~0,4~~ ~~1:5~~		
5 µl K2® Multiplier in each well	**C**	0,2 1:2	0,3 1:2	~~0,4~~ ~~1:2~~	0,2 1:3	0,3 1:3	~~0,4~~ ~~1:3~~		
	D	0,2 1:4	0,3 1:4	~~0,4~~ ~~1:4~~	0,2 1:5	**0,3** **1:5**	~~0,4~~ ~~1:5~~		
	E								
	F								

Table 12: Flow Cytometry results from transfection optimization of ASG-10 with K2® Transfection System. The well names refer to table 11.

Well	% transfected cells (M3 gate)	Well	% transfected cells (M3 gate)
A1	0,05	C1	0,06
A2	0,04	C2	0,07
A4	0,03	C4	0,03
A5	0,03	C5	0,03
B1	0,06	D1	0,04
B2	0,02	D2	0,05
B4	0,06	D4	0,03
B5	0,04	D5	0,04

Table 13: Testing transfection of two constructs and further optimization of ASG-10 with the K2® transfection reagent kit

		1	**2**	**3**	**4**	**5**	**6**	**7**	**8**
phMGFP	A	0,3 µg 1:5 µg/µL	0,4 1:5	0,3 1:5	0,4 1:5	0,3 1:5			
pGFP	B	0,3 1:5	0,4 1:5	0,3 1:5	0,4 1:5	0,3 1:5			
B22R2-19	C	0,3 1:5	0,4 1:5	0,3 1:5	0,4 1:5	0,3 1:5			
B22R2-W	D	0,3 1:5	0,4 1:5	0,3 1:5	0,4 1:5	0,3 1:5			
NC	E	(Ab neg)	(Neg-neg)						
	F								

5 µL multiplier in every well (-NC).

Column 1-2: 132 000 cm^2 cells/well

Column: 3-4: 66 000 cm^2 cells/well

Column 5: 44 000 cm^2 cells/wel

Table 14: Setup of the transfection optimization of ASG-10 with K2® Transfection system and Lipofetamine™ 3000 reagent kit. Wells with Opti-MEM are blue. phMGFP plasmid and GFP mRNA was used.

Cells/well		*70 000*	*70 000*	*60 000*	*60 000*	*45 000*	*45 000*	*30 000*	*30 000*	*20 000*	*20 000*	*10 000*	*10 000*
		1	**2**	**3**	**4**	**5**	**6**	**7**	**8**	**9**	**10**	**11**	**12**
K2	**A**	0,15 µg DNA 1 µL reagent	0,15 µg 0,6 µL	0,15 µg 1 µL	0,15 µg 0,6 µL	0,15 µg 1 µL	0,15 µg 0,6 µL	0,15 µg 1 µL	0,15 µg 0,6 µL	0,15 µg 1 µL	0,15 µg 0,6 µL	0,15 µg 1 µL	0,15 µg 0,6 µL
Lipof. 3000	**B**	0,2 µg DNA 0,3 µL reagent	0,2 µg 0,5 µL	0,2 µg 0,3 µL	0,2 µg 0,5 µL	0,2 µg 0,3 µL	0,2 µg 0,5 µL	0,2 µg 0,3 µL	0,2 µg 0,5 µL	0,2 µg 0,3 µL	0,2 µg 0,5 µL	0,2 µg 0,3 µL	0,2 µg 0,5 µL
K2	**C**	0,15 µg DNA 1 µL reagent	0,15 µg 0,6 µL	0,15 µg 1 µL	0,15 µg 0,6 µL	0,15 µg 1 µL	0,15 µg 0,6 µL	0,15 µg 1 µL	0,15 µg 0,6 µL	0,15 µg 1 µL	0,15 µg 0,6 µL	0,15 µg 1 µL	0,15 µg 0,6 µL
Lipof. 3000	**D**	0,2 µg DNA 0,3 µL reagent	0,2 µg 0,5 µL	0,2 µg 0,3 µL	0,2 µg 0,5 µL	0,2 µg 0,3 µL	0,2 µg 0,5 µL	0,2 µg 0,3 µL	0,2 µg 0,5 µL	0,2 µg 0,3 µL	0,2 µg 0,5 µL	0,2 µg 0,3 µL	0,2 µg 0,5 µL
mRNA	**E**	0.1 µg mRNA 0,3 µL reagent		0,1 µg 0,3 µL		0,1 µg 0,3 µL		0,1 µg 0,3 µL		0,1 µg 0,3 µL		0,1 µg 0,3 µL	
neg	**F**												
	G												
	H												

Table 15: Flow Cytometry results from transfection optimization of ASG-10 with K2® Transfection System, Lipofectamine 3000 and mRNA transfection. The well names refer to table 14.

Well	% Transfected cells (M3 gate)	Well	% Transfected cells (M3 gate)	Well	% Transfected cells (M3 gate)	Well	% Transfected cells (M3 gate)
A1	0	B1	0,65	D1	0,22	E1	71,67
A2	0,07	B2	1,3	D2	0,74	E3	73,19
A3	0,07	B3	0,87	D3	0,37	E5	44,93
A4	0,08	B4	1,3	D4	0,8	E7	55,6
A5	0,06	B5	0,94	D5	0,26	E9	74,1
A6	0,12	B6	1,3	D6	0,82	E11	94,13
A7	0,05	B7	0,8	D7	0,63		
A8	0	B8	1,96	D8	1,27		
A9	0,03	B9	1,2	D9	1,21		
A10	0	B10	2,64	D10	1,87		
A11	0	B11	0,88	D11	0,52		
A12	0	B12	1,99	D12	1,47		

Table 16: setup of transfection of ASG-10 with the 8 constructs using Lipofectamine™ 3000.

Samples:	phMGFP	B22R1-19	B22R2-19	B22R3C-19	B22R3N-19	B22R1-villf.	B22R2-villf.	B22R3C-villf.	B22R3N-villf.	neg		Cells/well
	1	2	3	4	5	6	7	8	9	10	11	12	
A	0,2 µg DNA 0,5 µL reagent	0,2 µg 0,5 µL	0,2 µg 0,5 µL	0,2 µg 0,5 µL	0,2 µg 0,5 µL	0,2 µg 0,5 µL	0,2 µg 0,5 µL	0,2 µg 0,5 µL	0,2 µg 0,5 µL	0 µg 0,5 µL			30 000
B													30 000
C	0,2 µg DNA 0,5 µL reagent	0,2 µg 0,5 µL	0,2 µg 0,5 µL	0,2 µg 0,5 µL	0,2 µg 0,5 µL	0,2 µg 0,5 µL	0,2 µg 0,5 µL	0,2 µg 0,5 µL	0,2 µg 0,5 µL	0 µg 0,5 µL			45 000
D													45 000
E													
F													
G													
H													

5.0 Bioinformatical predictions

5.1 Secondary structure predictions

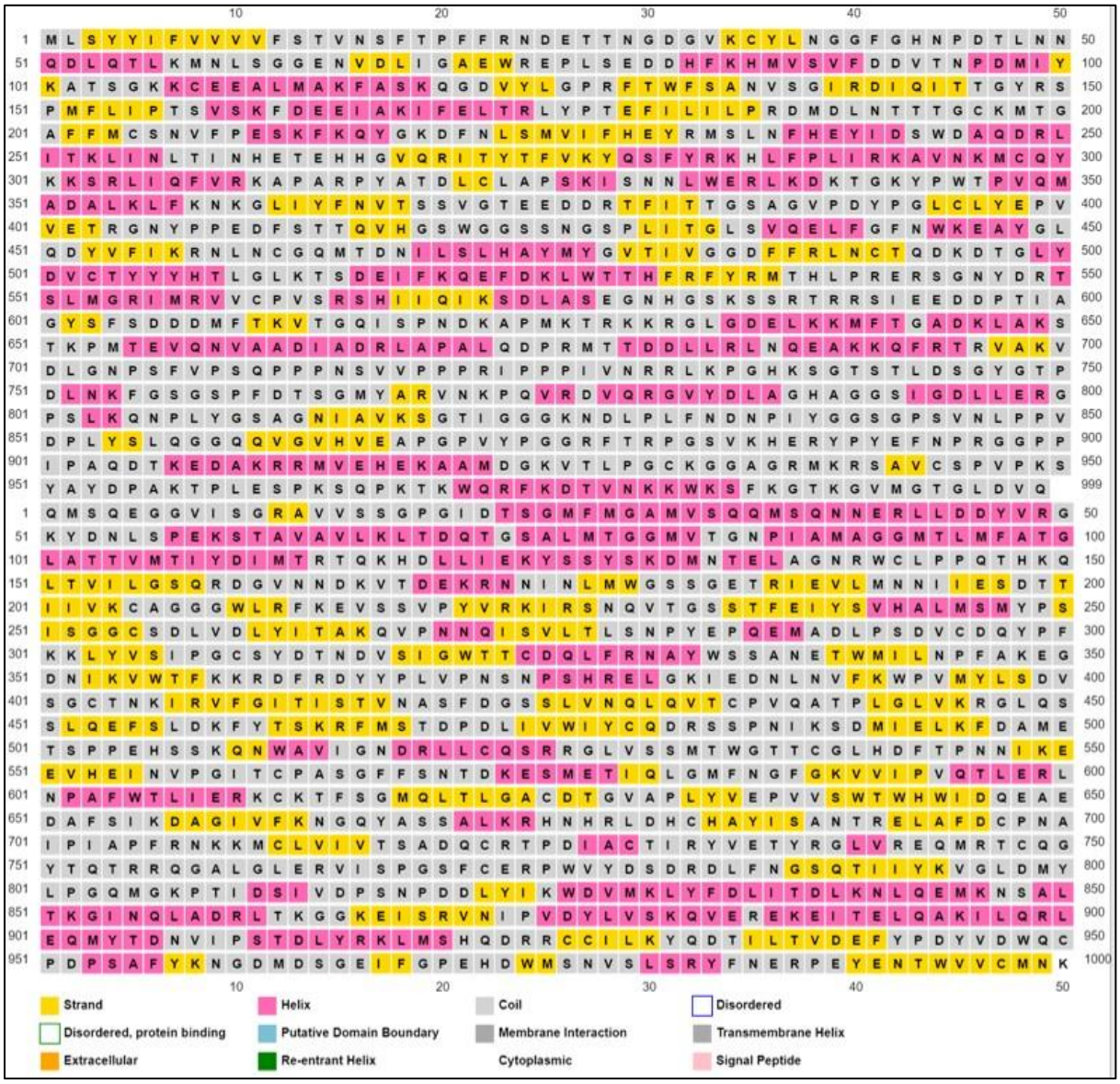

Figure 1: Secondary structure prediction of B22R1 SGPV NOR2012

Figure 2: Secondary structure prediction of B22R2 SGPV NOR2012

Figure 3: Secondary structure prediction of B22R2 SGPV NOR2012

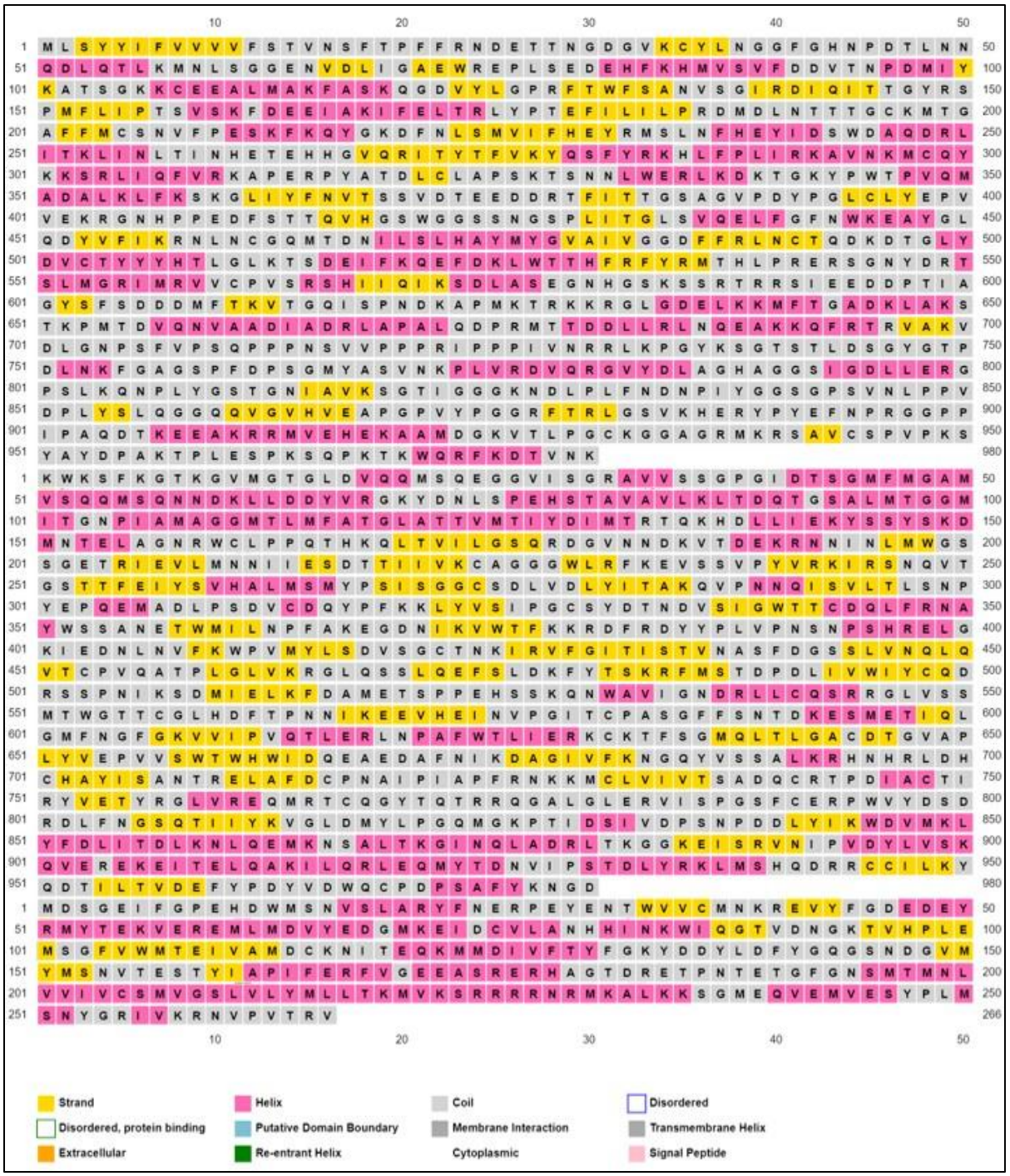

Figure 4: Secondary structure prediction of B22R1 SGPV NOR2009-W

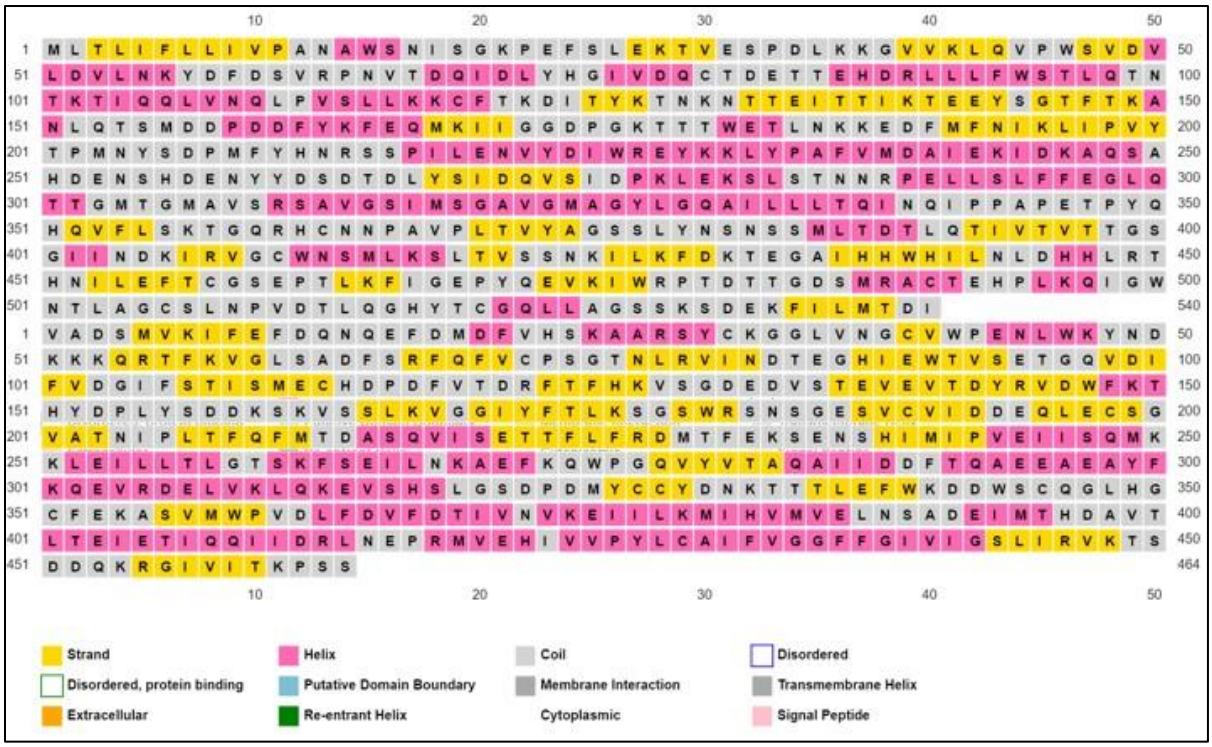

Figure 5: Secondary structure prediction of B22R2 SGPV NOR2009-W

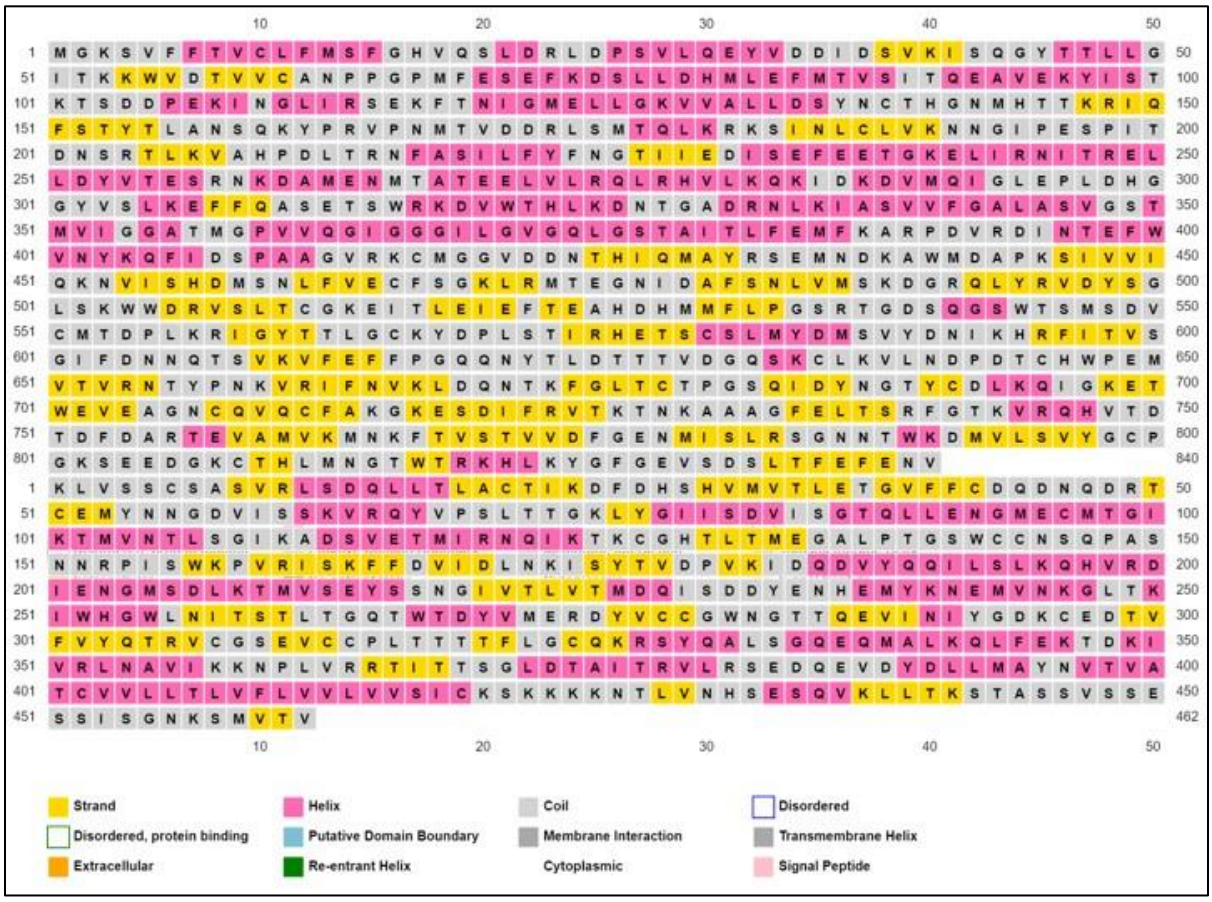

Figure 6: Secondary structure prediction of B22R3 SGPV NOR2009-W

5.2 Hydrophobicity plots

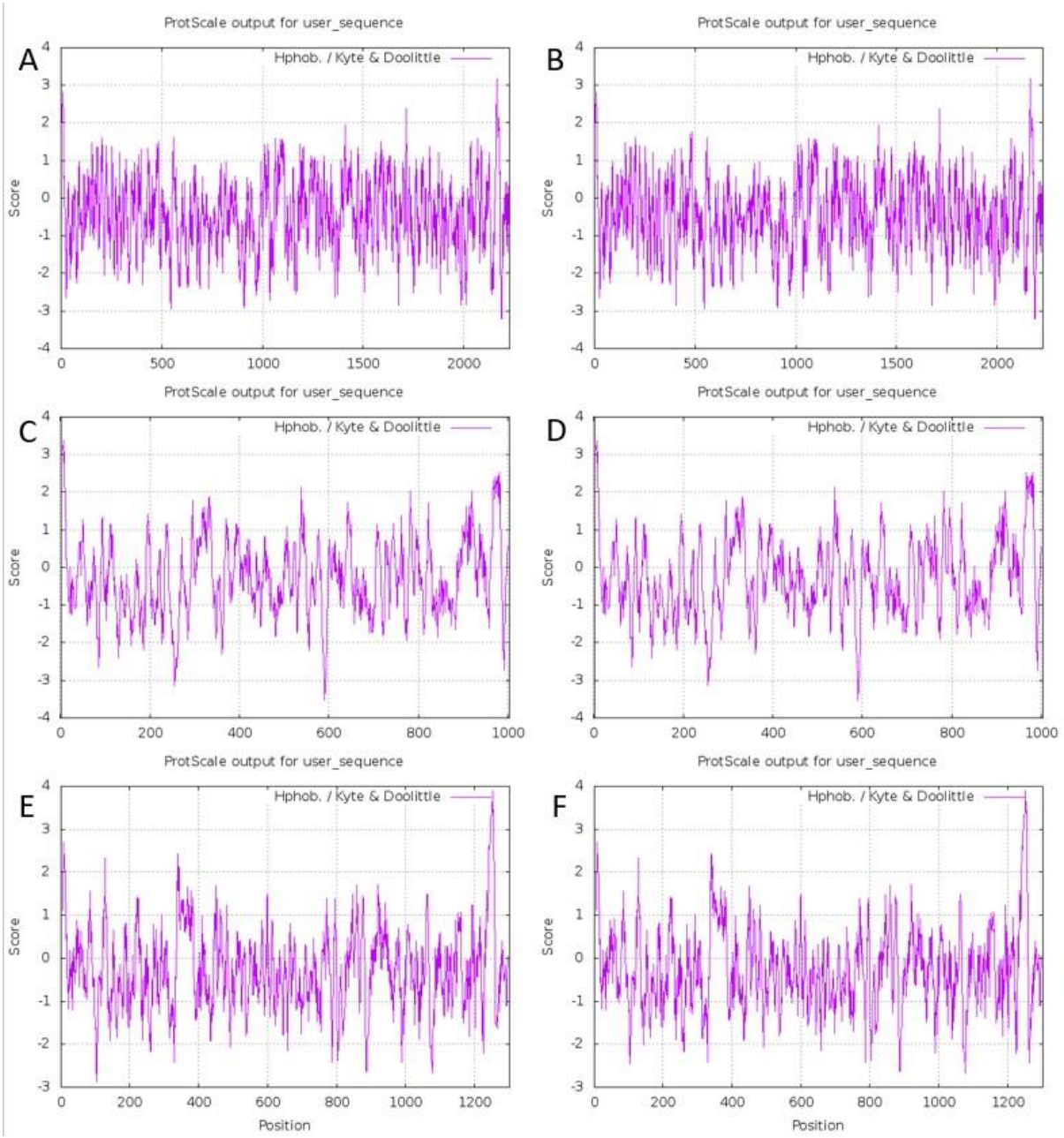

Figure 7: Kyte & Doolittle Hydrophobicity plots for the two reference sequences. **A:** B22R1 SGPV NOR2012, **B:** B22R1 SGPV NOR2009-W, **C:** B22R2 SGPV NOR2012, **D:** B22R2 SGPV NOR2009-W, **E:** B22R3 SGPV NOR2012, **F:** B22R3 SGPV NOR2009-W

6.0 Expression of B22R1-3 in gills of infected fish

Table x: First plate setup for the qPCR of cDNA from gills of infected fish. All samples are cDNA, except from well I22-P22, that was intended to be materials directly from the samples before cDNA synthesis, but was not included and therefore set up with a new PCR reaction.

	1	2	3	4	5	6	7	8	9	10	11	12	13	14	15	16	17	18	19	20	21	22	23	24
A	1	9	20	29	37	45		1	9	20	29	37	45		1	9	20	29	37	45		13		
B	1	9	20	29	37	45		1	9	20	29	37	45		1	9	20	29	37	45		13		
C	2	10	22	30	38	46		2	10	22	30	38	46		2	10	22	30	38	46		14		
D	2	10	22	30	38	46		2	10	22	30	38	46		2	10	22	30	38	46		14		
E	3	13	23	31	39	47		3	13	23	31	39	47		3	13	23	31	39	47		16		
F	3	13	23	31	39	47		3	13	23	31	39	47		3	13	23	31	39	47		16		
G	4	14	24	32	40	48		4	14	24	32	40	48		4	14	24	32	40	48		17		
H	4	14	24	32	40	48		4	14	24	32	40	48		4	14	24	32	40	48		17		
I	5	16	25	33	41	NC		5	16	25	33	41	NC		5	16	25	33	41	NC		~~13~~		
J	5	16	25	33	41	NC		5	16	25	33	41	NC		5	16	25	33	41	NC		~~13~~		
K	6	17	26	34	42			6	17	26	34	42			6	17	26	34	42			~~14~~		
L	6	17	26	34	42			6	17	26	34	42			6	17	26	34	42			~~14~~		
M	7	18	27	35	43			7	18	27	35	43			7	18	27	35	43			~~16~~		
N	7	18	27	35	43			7	18	27	35	43			7	18	27	35	43			~~16~~		
O	8	19	28	36	44			8	19	28	36	44			8	19	28	36	44			~~17~~		
P	8	19	28	36	44			8	19	28	36	44			8	19	28	36	44			~~17~~		

Primers: B22R1 B22R2 B22R3 D13L

Table x: Second plate setup for qPCR of cDNA from gills of infected fish, including material from the original samples.

	D13L	B22R1	B22R2	B22R3	D13L	B22R1	B22R2	B22R3	NC			
	1	**2**	**3**	**4**	**5**	**6**	**7**	**8**	**9**	**10**	**11**	**12**
A	13	13	13	13	13	13	13	13	D13L NEG			
B	13	13	13	13	13	13	13	13	D13L NEG			
C	14	14	14	14	14	14	14	14	B22R1 NEG			
D	14	14	14	14	14	14	14	14	B22R1 NEG			
E	16	16	16	16	16	16	16	16	B22R2 NEG			
F	16	16	16	16	16	16	16	16	B22R2 NEG			
G	17	17	17	17	17	17	17	17	B22R3 NEG			
H	17	17	17	17	17	17	17	17	B22R3 NEG			

cDNA

RNA (original sample)

Norges miljø- og biovitenskapelige universitet
Noregs miljø- og biovitskapelege universitet
Norwegian University of Life Sciences

Postboks 5003
NO-1432 Ås
Norway